University of Southern Queensland

Statistical Downscaling of Precipitation Projections in Southeast Queensland Catchments

A Thesis submitted by

Adam Blazak

For the Award of

Masters of Science (Research)

2012

Abstract

Southeast Queensland has experienced a reduction in annual rainfall over the last 40 years of about 200mm and evidence is emerging that links global warming to declines in sub-tropical rainfall. Population growth in the same region has remained above the national average since 1986 and level 5 water restrictions where enforced as dam levels dropped to 16.7% in 2007. Dam levels for the region returned to full capacity by the end of 2010 due to several consistent years of rainfall and runoff. However, regional water supply managers still require information of future rainfall, more specifically if there will be a continuation of the observed long term drying trend.

One of the tools that can assist the water supply industry in managing future water needs are Global Climate Models (GCM's). These deliver projections of future rainfall but on a scale that is unable to resolve regional physical processes as well as other features that determine local rainfall, such as topography and land surface composition. For example, the catchments of Upper Brisbane and Stanley in Southeast Queensland are located adjacent to one another. Despite their proximity, average annual rainfall substantially varies from 840mm at one station in the Upper Brisbane catchment to 1700mm at one location in the Stanley catchment. GCM's with spatial resolutions of several hundred kilometres are unable to supply regional rainfall information at a usable scale for policy makers.

Downscaling methods are employed to refine GCM's scale to a regional level. Statistical downscaling by linear regression of projected climate predictor variables on a monthly basis is used in this thesis to conduct an analysis of future rainfall at three stations in Southeast Queensland.

Statistical downscaling models provided average monthly rainfall for Peachester of 144.7mm/month, which is a good match for the observed average total of 142.8mm/month. Improvements are made over the rainfall totals derived from GCM data at the nearest grid point of 75.7mm/month. This location plays an important role in receiving the majority of the region's rainfall and providing a significant portion to the regions dams. Average rainfall at the other two locations of Mount Brisbane and Crow's Nest were adequately described by the GCM output at the nearest grid point and were not improved upon by implementing the statistical downscaling techniques. The use of specific humidity in the climate models proved an unstable climatic predictor variable which created overestimations. Both GCM and statistical downscaled models project rainfall in the region to remain relatively constant over the next 30 years with only a small decrease in average annual rainfall of 4 to 5%.

Declaration

I certify that the ideas, experimental work, results, analyses and conclusions reported in this dissertation are entirely my own effort, except where otherwise acknowledged. I also certify that the work is original and has not been previously submitted for any other award, except where otherwise acknowledged.

..... Date:

Signature of Candidate

Adam Blazak

ENDORSEMENT

..... Date:

Signature of Supervisor

A/Prof. Joachim Ribbe

Contents

List of Figures vi
List of Tables viii
Acknowledgements ix
Chapter 1: Research issues 1
1.1 Introduction 1
1.2 Theory behind this research 7
1.3 Aims and Objectives 9
1.4 Outline of thesis 10
Chapter 2: Background Literature 11
2.1 Introduction 11
2.1.1 The Climate of Australia 11
2.1.2 The Climate of Southeast Queensland 19
2.1.3 Rainfall Trends of Southeast Queensland 22
2.1.4 Southeast Queensland Dam Catchments 23
2.2 Research problem 29
2.2.1 Precipitation Projections 29
2.3 Current methodologies 31
2.3.1 Global Climate Models 31
2.3.2 Downscaling Methods 33
2.3.3 Statistical Downscaling 35
2.4 Conclusions 40
Chapter 3: Data and Methodology 41
3.1 Introduction 42
3.2 Data Sources 43
3.3 Transformed Data 44
3.4 Missing Data 46
3.5 Research procedures 46
3.5.1 Time Frame 46
3.5.2 Site Selection 47
3.5.3 Predictor Selection 48
3.5.4 Regression Analysis 52
3.5.5 GCM Selection 53

3.5.6 Precipitation Simulations 56
3.5.7 Precipitation Projections 56
Chapter 4: Results 58
4.1 Introduction 58
4.2 20th Century Rainfall simulations 59
4.2.1 Testing Statistical Models with NCEP Data 60
4.2.2 Testing GCM Data with Observations 68
4.2.3 Testing Statistical Models with GCM Data 71
4.3 Rainfall Projections 86
4.3.1 Rainfall Projections (2010 -2040) 87
4.3.2 Long Term Rainfall Projections 92
Chapter 5: Discussion and Conclusion 97
5.1 Introduction 97
5.2 Discussion 97
5.3 Conclusion 101
5.3.1 How does the data answer the original research question? 102
5.4 Implications for policy or practice 103
5.4.1 How does the data contribute to the field of study? 104
5.5 Limitations 104
5.6 Further research 105
References 108
Appendix A: Monthly Climatic Predictors 120
Appendix B: Statistical Models used to calculate Monthly rainfall 124
Appendix C: Shifts in Lat/Lon values from NCEP to GCM's 126
Appendix D: 20th Century GCM Rainfall Simulations 129
Appendix E: Projected Changes in Climate Predictor Variables 147

List of Figures

Figure 1.1	Australian Annual Rainfall Trends (1950 – 2010)	3
Figure 1.2	Australian Population Distribution	4
Figure 2.1	Climate Zones of Australia	12
Figure 2.2	Average Annual Australian Rainfall Map	12
Figure 2.3	Australian Climate Drivers	14
Figure 2.4	Winter East Coast Lows	21
Figure 2.5	Australian Annual Rainfall Trends (1900 – 2010)	23
Figure 2.6	Southeast Queensland Catchments	25
Figure 2.7	Accumulated Rainfall Deficit west of Brisbane (2001 – 2007) & (1898 – 1903)	26
Figure 2.8	Southeast Queensland Dam Levels (2001 – 2007)	27
Figure 2.9	Southeast Queensland Dam Levels (1994 – 2011)	28
Figure 2.10	IPCC Rainfall Projections for Queensland	30
Figure 3.1	Grid Point Locations for NCEP Climatic Predictors	51
Figure 4.1	Observed and Simulated Rainfall at Crow's Nest (1948 – 2000)	61
Figure 4.2	Observed and Simulated Rainfall at Mount Brisbane (1948 – 2000)	64
Figure 4.3	Observed and Simulated Rainfall at Peachester (1948 – 2000)	66
Figure 4.4	Comparison of Observed Average Rainfall with GCM rainfall and Statistical Downscaled Model using MIROC – medres	72
Figure 4.5	Comparison of Observed Average Rainfall with GCM rainfall and Statistical Downscaled Model using GFDL Mk2.1	74

Figure 4.6	Comparison of Observed Average Rainfall with GCM rainfall and Statistical Downscaled Model using GISS – er	77
Figure 4.7	Comparison of Observed Average Rainfall with GCM rainfall and Statistical Downscaled Model using CCCMA – t63	79
Figure 4.8	Comparison of Observed Average Rainfall with GCM rainfall and Statistical Downscaled Model using CNRM – cm3	81
Figure 4.9	Comparison of Observed Average Rainfall with GCM rainfall and Statistical Downscaled Model using CSIRO Mk3.5	84
Figure 4.10	Projected Crow's Nest Rainfall (2010 – 2040)	87
Figure 4.11	Projected Mount Brisbane Rainfall (2010 – 2040)	88
Figure 4.12	Projected Peachester Rainfall (2010 – 2040)	89
Figure 4.13	Projected GCM's Rainfall at the Nearest Grid Point	91

List of Tables

Table 3.1	Characteristics of GCM's used in Regression Analysis	55
Table 4.1	R^2 correlations between Observed and GCM Rainfall (1950 – 2000)	69
Table 4.2	Mean and Standard Deviations of Observed and GCM Rainfall	69
Table 4.3	Projected Monthly Rainfall at Crow's Nest (2010 – 2100)	93
Table 4.4	Projected Monthly Rainfall at Mount Brisbane (2010 – 2100)	94
Table 4.5	Projected Monthly Rainfall at Peachester (2010 – 2100)	95

Acknowledgements

The completion of this thesis is due to the help and patience of my supervisor A/Prof. Joachim Ribbe, with the support of the Australian Centre for Sustainable Catchments. Thanks also to my beautiful wife Lina and our precious daughter Peri for all the sacrifices you made in providing me with time to complete my work.

Chapter 1: Research issues

1.1 Introduction

Much of the success of human civilisation can be credited to the use of fossils fuels. It has provided a relatively cheap form of energy to supply our heating, electricity and transport needs and powers our farms and industry. The rapid growth of the human population since the 1800's using this 'cheap' form of energy has not come without some cost though. The emissions produced have increased atmospheric greenhouse gas (GHG) levels above naturally occurring concentrations, tipping the Earth's energy balance in favour of trapping heat in the climate system (Pittock, 2009).

Greenhouse gases including water vapour, carbon dioxide, methane, nitrous oxide and halocarbons (CFC's) are an essential part of the climate system because they absorb heat radiated by the Earth back into space. Without them, this heat energy would be lost and the temperature of the Earth would drop to a level that would be too low to sustain life as we know it. However, the naturally occurring concentration of these gases in the atmosphere creates a climate system where, on average, outgoing heat is equivalent to the amount of heat that enters, thereby keeping the Earth's temperature in relative stasis (Raupach & Fraser, 2011). Despite these gases only making up a very small proportion of the overall gases in the atmosphere, their

influence on the entire system is amplified because of the efficiency with which they trap heat combined with the fine balance of the Earth's climate system. Human introduced GHG's may only be a small fraction of the total GHG naturally produced each year, but this small addition increases atmospheric global greenhouse gas concentrations and impacts on the global climate (IPCC, 2007).

The 2007 Intergovernmental Panel for Climate Change (IPCC) 4th Assessment Report (IPCC, 2007) states that the observed increase in global temperatures since the mid 20th century is *very likely* due to the observed increase in anthropogenic GHG concentrations. Future changes to the climate may already be inevitable, and adaptation practices need to be devised in order to continue to provide society with the essentials such as food, water, housing and health care (CSIRO-BoM, 2007).

The social and economic consequences of climate change have been assessed recently in reports by Stern (2006) in the United Kingdom and by Garnaut (2008) and Garnaut (2011) in Australia. The Garnaut report of 2008, documents the possible impacts of increased temperatures on the Australian environment, primary industries, human health, settlement and infrastructure and what mitigation strategies need to be implemented to reduce the impact of climate change. The economic cost and benefit of

mitigation strategies are revised in the updates 2011 report. Weitzman (2009) investigates the complex topic of determining if the cost of mitigation exceeds associated economic benefits.

One way in which the climate system has begun to change over recent decades is atmospheric circulations and rainfall distributions have trended away from the historical average towards a generally wetter world (Alexander et al., 2006). Spatial distribution of rainfall is also influenced in climate change models with an increase in annual rainfall at the high latitudes and a decrease in the sub-tropical latitudes (Meehl et al., 2007; Zhang et al., 2007). In Australia the trend in rainfall from the Bureau of Meteorology (BoM) over the last 40 years has been towards wetter conditions in the northwest and drier conditions in the east, southeast and southwest of the country (Fig. 1.1).

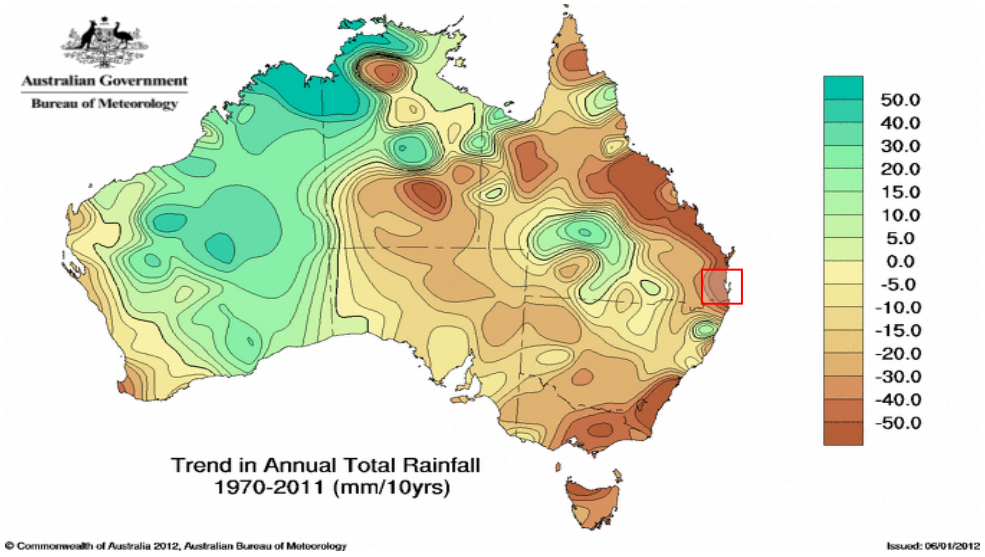

Figure 1.1: Australian Annual Rainfall trends, from 1970-2011. Southeast Queensland (Region of study) highlighted by red box. Source: BoM, 2011.

According to the Australian Bureau of Statistics (ABS) census of 2006, most of Australia's population is concentrated on the eastern seaboard (Figure 1.2), the same region that has experienced a significant reduction in precipitation over the last 40 years and no study has investigated the cause of this strong drying trend (Nicholls, 2006). Freshwater supplied from rainfall and runoff into dams did not meet the increasing demand and by the start of 2008 water restrictions were imposed in many regions. Future projections of increased periods of drought, higher temperatures and evaporation in the region will decrease the ability of our current systems to continue to provide an adequate supply under climate change scenarios (BoM-QCCCE, 2011).

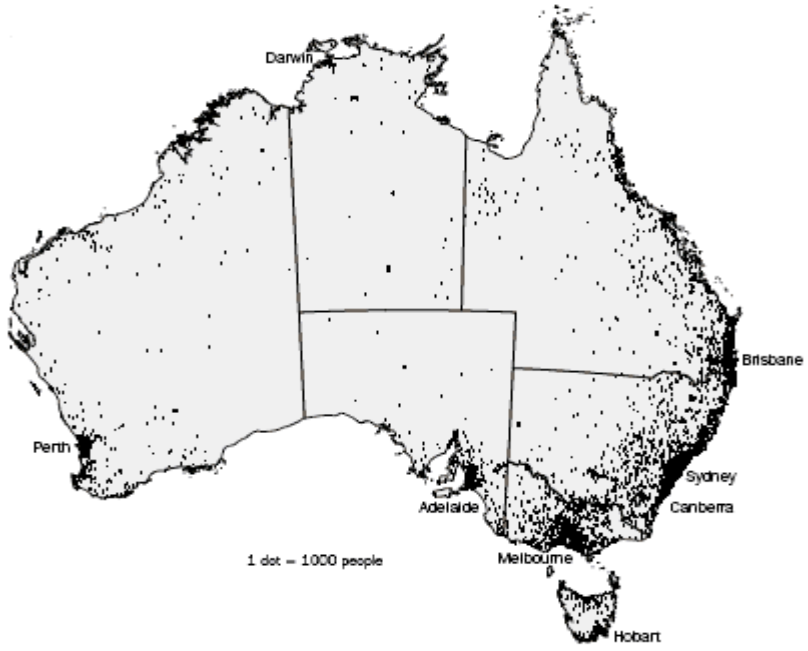

Figure 1.2: Australia's Population Distribution as at the 2006 Census. Source: ABS, 2006

Australia's water resources in general have high vulnerability to climate change scenarios (Preston and Jones, 2006; Cheiw & McMahon, 2002; Timbal & Jones, 2008). Alternative water sources such as recycled sewage, groundwater and desalination are being investigated as possible resources in order to supplement the dwindling supplies from rainfall and run-off (Kaspura, 2007). Household water demands in Brisbane, Sydney, Melbourne and Perth can be met by combining dam supplies with water sourced from rooftop stormwater (Coombes & Barry, 2007). Some new housing developments now take water management issues more seriously, with different drainage systems to separate sewage from grey water which can be reused in the garden or to flush toilets (McAlister et al., 2004).

Rainfall in Southeast Queensland rainfall has varied significantly over recent decades typically subjected to periods of drought broken up by episodes of extreme rainfall events. Receiving 'average' rainfall totals in the region has become unusual with excursions from these totals becoming the norm. Managing water resources in the region is made more difficult as the region also undergoes one of the country's highest growths in population (Pacific Southwest Strategy Group, 2007). The period from 2001 to 2007 was one of marked low rainfall and the region's water resources barely managed to cope, dam levels dropped below 20% (SEQWater, 2011). With water on the verge of running out, the state government quickly implemented a water management plan linking 12 dams, at some considerable cost. In 2011, with

dams overflowing, water consumers are still paying the high cost for the rapid implementation of the water grid that is said to 'drought proof' the region.

Decision makers not only have to deal with inconsistent annual rainfall but complicating the issue further is how climate change may impact on future rainfall events. The last 40 years has seen a marked reduction in average annual rainfall, though over a 100 year period the annual reduction is less significant (BoM, 2011). The question still remains whether the dry period of the last 40 years is typical of the region, and 40 years is not long enough to detect multi-decade cycles, or is the reduction in rainfall, in fact a precursor to future climatic conditions.

To assist in determining future rainfall patterns, scientists employ the help of global climate models (GCM's) to simulate atmospheric conditions of the future. Climate models are more accurate at simulating large scale climatic parameters like air pressure and wind direction, but precipitation is more difficult as it can vary significantly within climate model grid points.

The grid points of a GCM are the positions on the globe where the projections are made. They are spaced out around the planet, hundreds of

kilometres apart, with actual distances between points varying between models from 200 to 400km. 'Raw' GCM output lacks required spatial resolution to represent local features such as topography, land cover and water courses which can influence rainfall. Basing long term water management decisions using 'raw' climate model output, makes it difficult to know what actions, if any, should be taken to work towards a more sustainable use of the region's water resources. Downscaling of this data is being employed to provide improved projections of future rainfall on a scale that is useful for the management of smaller regions.

1.2 Theory behind this research

To make precipitation projections from climate models more useful, downscaling methods can be applied to the climate model output. Downscaling is a process that takes climate model output and increases the resolution of the data to a more regional basis, up to 5km² in some cases or can provide information at a specific location.

Downscaling methods can be broken up into dynamical and statistical techniques. Dynamical downscaling involves nesting a regional climate model inside GCM grid points, and is forced at the edge of its domain by Global Climate Model simulations with boundary conditions provided by Global Climate Model simulations. With the ability to simulate atmospheric

physics at a higher resolution it gives a more accurate representation of climatic processes on a regional scale.

Statistical downscaling uses statistical probability to link observed regional rainfall with large scale climatic parameters. One method produces mathematical equations or statistical models that estimate rainfall based on other climate variables. This process assumes that future atmospheric composition and chemistry will produce rainfall in a similar fashion to previous atmospheric conditions. It is more simplistic than dynamical downscaling but requires a lot less computer power and programming.

The statistical models produced by these methods contain both independent and dependent variables. In the case of this thesis the independent variables are the large scale climatic conditions, or predictors. The dependent variable, or predictand, is rainfall.

This statistical downscaling method will be used to test if the extreme drying trend of Southeast Queensland over the last 40 years will continue over the coming decades under climate change scenarios. Statistical downscaling is more useful in regions with consistent annual rainfall than regions that experience large variations from year to year. This is one downfall of using this method and to help overcome this issue the results are broken down into monthly values to capture climatic variation that may occur within seasons.

1.3 Aims and Objectives

The initial motivation for this study was the dire situation that faced southeast Queensland water resources at the end of 2006. After six years of below average rainfall combined with the pressures of supplying an increasing population, water resources fell to record lows and serious consideration was given to alternative water sources. How long would the drought continue for? How will our water resources cope if this recent dry period is the beginning of future conditions under climate change scenarios? Planning for future growth in the region will benefit from improved precipitation projections and this can be provided by implementing statistical downscaling techniques to improve the resolution of CGM output.

The objective of this study is to statistically downscale GCM projection data over Southeast Queensland (Figure 1.1) to provide an improved estimate of future rainfall in two Southeast Queensland catchments and determine if the recent drying trend will continue into the coming decades. It aims to do this by linking observed monthly rainfall at the stations of Crow's Nest, Mount Brisbane and Peachester with climatic predictors, such as air pressure and wind direction, from around the region via a linear regression analysis.

1.4 Outline of thesis

The topics discussed above will be covered more deeply in future chapters. In chapter 2 the current knowledge will be investigated via a literature review on the work. This will demonstrate a gap in our understanding of future rainfall trends in Southeast Queensland and chapter 3 will detail the data collection and the methodology used to derive the rainfall projections. The results from that research will be presented in chapter 4 which will provide both results and an interpretation. The implications of these results to current knowledge and a conclusion will be included in Chapter 5.

Chapter 2: Background Literature

2.1 Introduction

This literature review documents current information on the Australian climate and that of Southeast Queensland. Recent Australian rainfall trends are investigated as is the reduction of Southeast Queensland rainfall that led to unprecedented low dam levels for the region. Rainfall projections from Global Climate Models (GCM) are examined and the possibility of improving the spatial resolution of these projections using downscaling methods to provide information that is useful on a regional scale. Different downscaling methods will be examined to determine an appropriate method to improve rainfall projections for Southeast Queensland.

2.1.1 The Climate of Australia

Australia is a large landmass but the inhospitable climate renders most of the area uninhabitable for large communities. Under the Koppean climate classification system, 70% of the country is under either desert or grassland (Figure 2.1). These regions have infertile soils and erratic rainfall making it difficult, if not impossible, to settle. (CSIRO BoM, 2007)

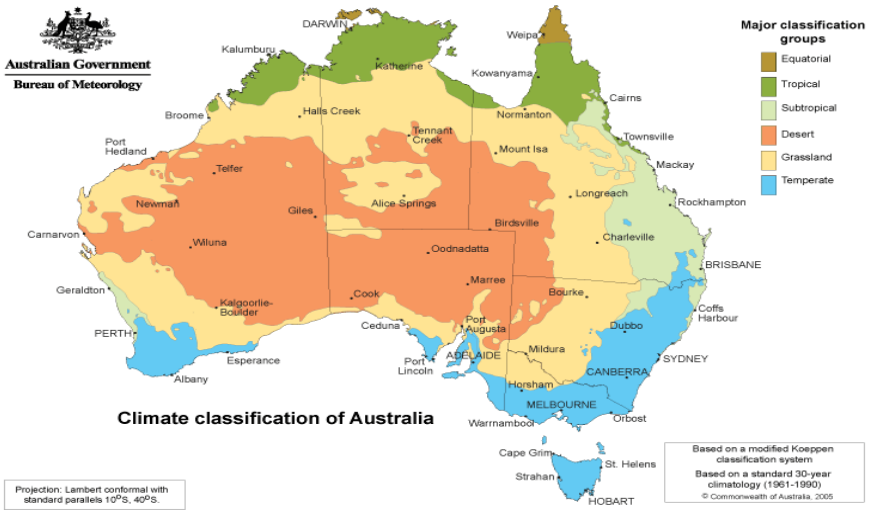

Figure 2.1: The Climate zones of Australia (1961 – 1990) based on a modified Koeppen classification system. Source: BoM, 2011

It is no coincidence that the country's population is concentrated around the eastern coastline (Figure 1.2) where the climate is moderated by moist air; receives the majority of the rainfall (Figure 2.2) and contains fertile soils for food production.

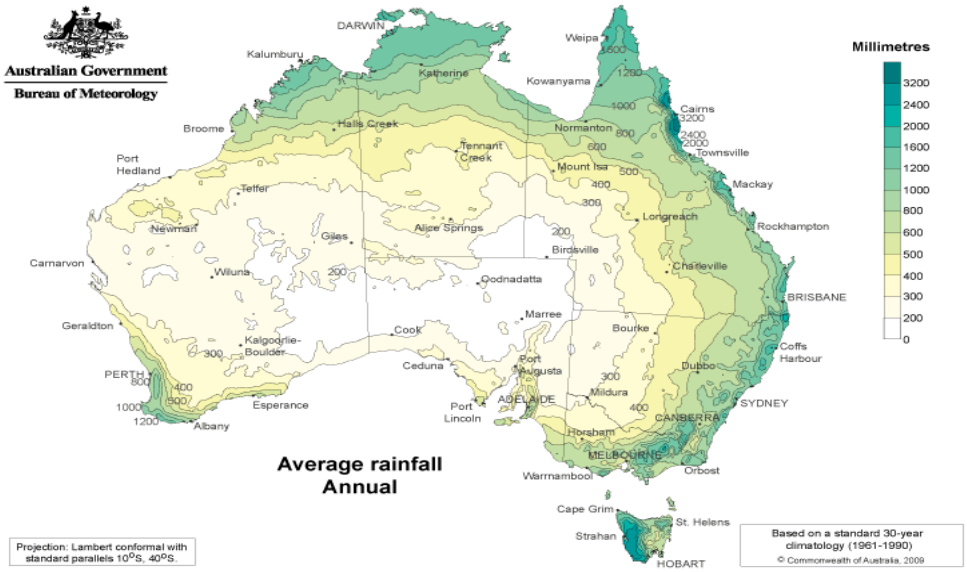

Figure 2.2: Average annual rainfall of Australia (1961 – 1990) coincides with the areas of largest concentration of population Source: BoM 2011

Figure 2.2 displays the average annual rainfall for Australia over the period 1961 to 1990. The majority of the country receives less than 500mm/year, leading to the creation of desert and grassland conditions covering 70% of the country as shown in Figure 2.1. The population of Australia is distributed (Figure 1.2) in the areas that receive above 800mm/year, i.e. entire eastern coastline and south-western tip. The north of the country receives ample rainfall to support large communities, but is also subject to high temperatures and humidity with possible cyclonic conditions during summer.

The large landmass of Australia is subject to various natural climatic drivers influencing different regions throughout the year. Different regions can also be impacted in different ways by the same climate driver (Risbey et al., 2009). These multiple influences also interact with one another to create a rainfall climatology which can vary not only from year to year but also decade to decade (Meinke et al., 2005). This can make it difficult to separate natural variability from that being imposed by climate change.

Figure 2.3 (BoM, 2011) features the major climate drivers and synoptic systems that influence the Australian climate. The drivers featured in this section include the El Niño Southern Oscillation (ENSO), Interdecadal Pacific

Oscillation (IPO), Indian Ocean Dipole (IOD), Sub-tropical Ridge (STR), trough systems and the Southern Annular Mode (SAM).

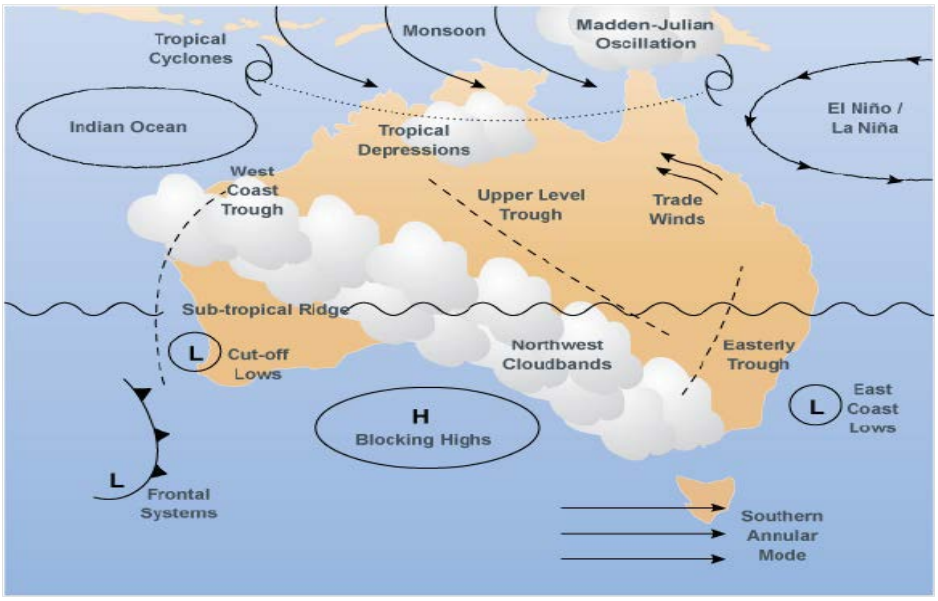

Figure 2.3: A diagram of the Australian Climate Drivers. Source: BOM 2011.

The El Nino Southern Oscillation (ENSO) refers to the oscillation of warm sea surface temperatures from the western equatorial Pacific across to the east (Ropelewski & Halpert, 1987). The naturally occurring 'Pacific Warm Pool' located in the western Pacific creates convection in the atmosphere over the region. Conversely, in the central and Eastern Pacific, relatively cooler surface waters create a region of sinking air which then travels back toward the low pressure area in the west. This surface flow towards the west and upper level flow towards the east, referred to as the Walker Circulation or 'Trade Winds', are strengthened or weakened depending on the temperature differential between the two regions. When the temperature differential is less pronounced, under El Niño conditions, the flow is weakened and less

moist air is directed towards the eastern Australian coastline, consequently, less rainfall is likely (Allan et al., 1996; Wang & Hendon, 2007). When the natural state is amplified by anomalous warm water in the western Pacific, a La Niña event, the Walker Circulation is strengthened and wetter conditions over eastern Australia prevail.

The relative position of the warm pool of water in the equatorial Pacific creates ENSO events with different impacts on the climate. The ENSO Modoki Index refers to a warm pool of water located in a more central equatorial Pacific region (Ashok & Yamagata, 2009), an anomaly that has shown to influence seasonal Australian rainfall (Ashok et al. 2009; Taschetto & England 2009; Langford et al., 2011)

The Southern Oscillation Index (SOI) can provide a measure of the relative strength of the El Niño or La Niña event. The index is derived from average monthly air pressure differences between Darwin and Tahiti and is connected to seasonal rainfall variations. This connection can be further refined by dividing the SOI values for two sequential months up into phases. These phases then have the ability to predict rainfall for the coming months not only over Australia but also over entire planet (Stone et al. 1996).

The Interdecadal Pacific Oscillation (IPO) is a temperature differential across the Northern Pacific Ocean. Despite being in a different hemisphere, the affects are still felt in Australia due to the ability of the phenomenon to strengthen or weaken the ENSO signal (Chiew and Leahy 2003, Micevski et al. 2006, Speer 2008).

The temperature differential across the Indian Ocean, referred to as the Indian Ocean Dipole (IOD), influences Australian rainfall over the north, west and south of the country. This driver has trended towards more positive phases since the 1950's and this may have contributed to drier conditions in southern Australia during winter (Cai et al. 2009).

The Sub-tropical Ridge is an area of down welling air at the southern extremity of the Hadley Cell. The area of high pressure stretches across the latitudes of approximately 30° to 40°. This ridge is made up of high pressure systems that have the ability to "block" oncoming storm fronts that can deliver significant quantities of rainfall throughout the warmer months.

Studies have been carried out to determine whether this atmospheric system has been making a pole ward shift. Gibson (1992) found a pole ward shift in the position of the Ridge created by global warming. Increased convection at

the equator brought about by global warming affects the Hadley Cell circulation which alters where the down welling component of the Cell occurs. Later, Thresher (2002) found natural decadal variation in the Sub-tropical Ridge and this was later back by Drosdowsky (2005) who found no statistically significant shift. More recently Williams and Stone (2009) did find evidence of a pole ward trend in the ridge's position.

Trough Systems are semi-permanent depressions in the upper atmosphere causing instability and subsequent rain during the warmer months of the year. The heat of the day deepens the trough and creates rain and storms to the east of its position. The position of the upper level trough can influence the amount of rainfall received by surface frontal systems and also are involved in the creation of cut-off lows (BoM 2011, Dowdy et al. 2011).

Cut-Off Lows are low pressure systems forming at sea level adjacent to the coastline. East coast lows refer to these systems forming adjacent to the East coast of Australia. They are an important rain producing synoptic feature on the coastal Australian climate (Hopkins and Holland 1997, Speer 2008).

The Madden Julian Oscillation (MJO) operates over the warmer months on a 20 to 40 day cycle and describes moist air travelling from the eastern Indian

Ocean in a south-easterly direction across Australia. This moist air penetrates into Australia and impacts on rainfall over the country. (Donald et al. 2006)

The Southern Annular Mode is large scale atmospheric circulations to the south of Australia and over Antarctica. The primary influence on Australian weather is through the impact it has on the position of the extra-tropical cyclones (low pressure systems at mid to high latitudes) and cold fronts (Meneghini et al. 2007) which impacts on temperatures and precipitation in Australia (Hendon et al., 2007). SAM is also linked to ocean currents around Australia which can have influence on rainfall. (Gillet et al. 2006, DNRW 2007)

As mentioned at the start of this section, the interaction between the numerous climate drivers creates climate variability that can occur over months, season, years and decades (Power et al. 1999a, White et al. 2003, Meinke et al. 2005). This variability makes it difficult to distinguish if the recent dry periods experienced in Australia are the caused by natural climate variability or have been imposed by human induced climate change. Hunt (2009) found droughts of 8 years or more are part of the natural Australian climate cycle at three different regions in Australia.

The impact of climate change on the climatic drivers influencing Australian rainfall has begun to leave its mark on the Australian rainfall regime. Australian rainfall, on average, is trending towards more extreme events and away from periodic rainfall (Smith 2004, Alexander et al. 2007). Over the past decades the significant winter drying trend experienced in Southwest Western Australia has been partly attributed to an increase in greenhouse gas concentration (Hope et al 2006, Christensen et al. 2007, Cai et al. 2009). This drying trend may also be extending over to Southeast Australia as well (Murphy and Timbal 2008, Hope et al. 2009). The increase in annual rainfall over the Northwest of the country may also be due to man made sources, with activity in Southeast Asia increasing atmospheric aerosols in the region (Nicholls 2006). The same review noted that no study had investigated the cause of the strong drying trend over the East of the continent, and this was a region of economic importance because of large population base.

2.1.2 The Climate of Southeast Queensland

Southeast Queensland is located on the eastern seaboard of Australia at latitude 27°S. It typically experiences warm wet summers [30°C, 110mm/month] and mild dry winters [19°C, 40mm/month] (BoM 2011). The majority of the significant rainfall events in the region come from tropical depressions or monsoonal trough systems (Wilson et al. 2010), but can also be subjected to high intensity rainfall events. The impact of the Australian

climate phenomenon on Southeast Queensland at different times of the year will be discussed in this section.

SOI can be linked to decadal variations in Southeast Queensland with a correlation coefficient of greater than 0.4 (Power et al. 1999b) is also linked to runoff in Northern NSW and Southern QLD (Cheiw & McMahon 2003).

The IPO strengthens the SOI signal, making the SOI a more reliable indicator for ensuing rains in the Southeast Queensland region. Anecdotally the dams of Southeast Queensland began to fill (as will be shown in Figure 2.9) at a similar time as the IPO switched from positive to negative in September 2007.

The position of the Subtropical Ridge during spring and summer months impacts on rainfall in Southeast Queensland (Williams and Stone, 2009). The further poleward the subtropical ridge is positioned in the warmer months is statistically correlated with higher rainfall for that period.

The inland trough interacts with Southeast Queensland rainfall over the summer months. The position of the trough can result in several consecutive

days of afternoon rain and thunderstorms, an important component of annual rainfall for the region (Queensland Farmers Federation, 2008).

Cut-off Lows are a critical source of rainfall for the catchments east of the Great Dividing Range (Dowdy et al. 2011), which includes the catchments of Southeast Queensland. They provide significant rainfall events through-out the year, primarily from March to October (Queensland Farmers Federation, 2008) and can be an important water source through the cooler months, as shown in Figure 2.4.

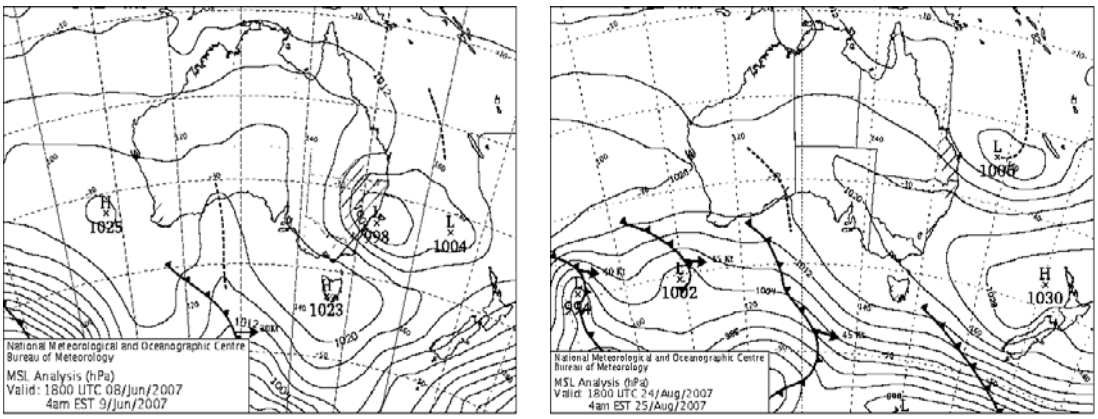

Figure 2.4: Two Winter Rainfall Events for Southeast Queensland produced by East Coast Lows on 8th June and 24th August 2007. Source: BoM 2011.

The influence of the Madden Julian Oscillation (MJO) on rainfall in Southeast Queensland is to enhance rainfall as the circulation anomaly passes over the region in to western Pacific Ocean, where it proceeds to suppress rainfall for the region (Donald et al. 2006).

Despite the fact that both the Indian Ocean Dipole (IOD) and Southern Annular Mode (SAM) are large climate drivers that impact on the majority of Australian rainfall, their impact on the Southeast Queensland Region is only minor (Cai et al. 2009, Meneghini 2007).

2.1.3 Rainfall Trends of Southeast Queensland

Australian Bureau of Meteorology (BoM) rainfall trends maps from 1970 to 2011 show a reduction in average annual rainfall in the east of the continent of up to 50mm/year every decade (Figure 2.5). According to these rainfall trend maps, southeast Queensland catchments are located in one of the worst affected regions, experiencing a reduction in annual rainfall over the last 40 years of approximately 200mm. However this statistic may be biased by long term cycles in regional rainfall; the second half of the 20th century was wetter than the first and the 110 year average shows a smaller reduction in annual rainfall of less than 50mm (Fig. 2.5). Australia has a large amount of natural climate variability, which may occur over long time scales, making it difficult to attribute recent drying trends to anthropogenic global warming (BoM 2011). This makes the task of planning future water resources very difficult and highlights the need for improved precipitation projections.

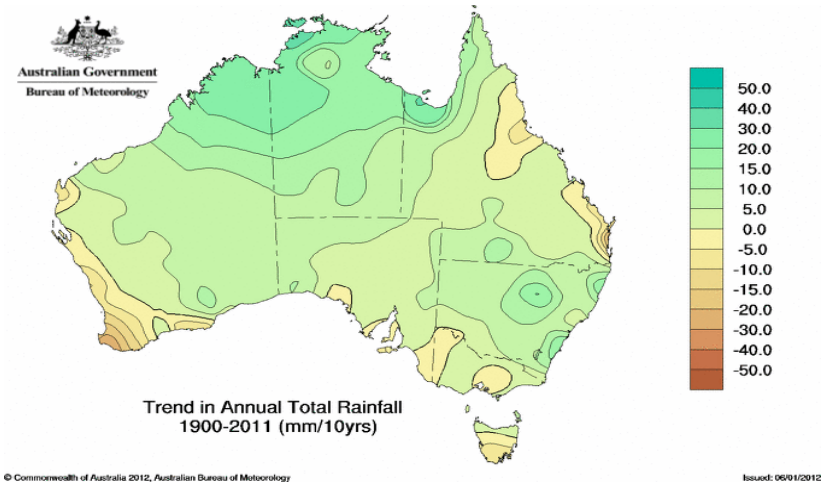

Figure 2.5: Australian Annual Rainfall trends, from 1900-2011. Source: BoM 2011.

Discerning whether the recent drying trend over Southeast Queensland is merely a natural part of the regions climate variability or the beginnings of human induced climate change is still unproven one way or the other. Increased greenhouse gas concentrations in the atmosphere have raised temperatures which strengthens the severity of naturally occurring prolonged dry periods (Nicholls 2004), contributing to making the 2001 - 2007 drought one of the worst on record.

2.1.4 Southeast Queensland Dam Catchments

Twenty-three dams contribute to southeast Queensland's water supply. Since 2008 twelve of these dams are now linked to assist in securing a reliable water supply for the region into the future (SEQWater 2011). The regions dams provide freshwater to Brisbane, Ipswich, Logan, Gold Coast and west

to Esk, Gatton, Laidley, Kilcoy and Nanango servicing a population of about 3 million (ABS 2010). Tarong North and Swanbank power stations also derive their water needs from the same supply.

The two largest dams providing water to southeast Queensland are the Wivenhoe Dam (1,165,238 ML capacity), fed by the Upper Brisbane catchment and Somerset Dam (379, 849 ML capacity) fed by the Stanley catchment (Fig. 2.6). Somerset Dam was constructed in 1959 specifically for the purpose of water storage and collects runoff from an area of about 1,340km². Wivenhoe, completed in 1984, has the largest catchment of 7,020km² and was constructed for both water storage and flood mitigation purposes (SEQWater, 2011). These two dams alone contribute to approximately 70% of the total water storage volume for all the 23 dams in the region (1,545,087/2,220,181Ml).

The Upper Brisbane and Stanley catchments are located to the northwest of Brisbane in southeast Queensland between the D'Aguilar and Great Dividing Ranges (Figure 2.6). These ranges create topographical features that influence rainfall in the region. To the east, the D'Aguilar range provides a small rain shadow effect from the adjacent coastline, but in return it captures rain from storm systems moving in from the southwest. This creates an imbalance in rainfall received over the two catchments with the upper reaches of the

Stanley Catchment receiving more. Most of the area within the catchments is under agricultural production because of the fertile soils and gentle terrain.

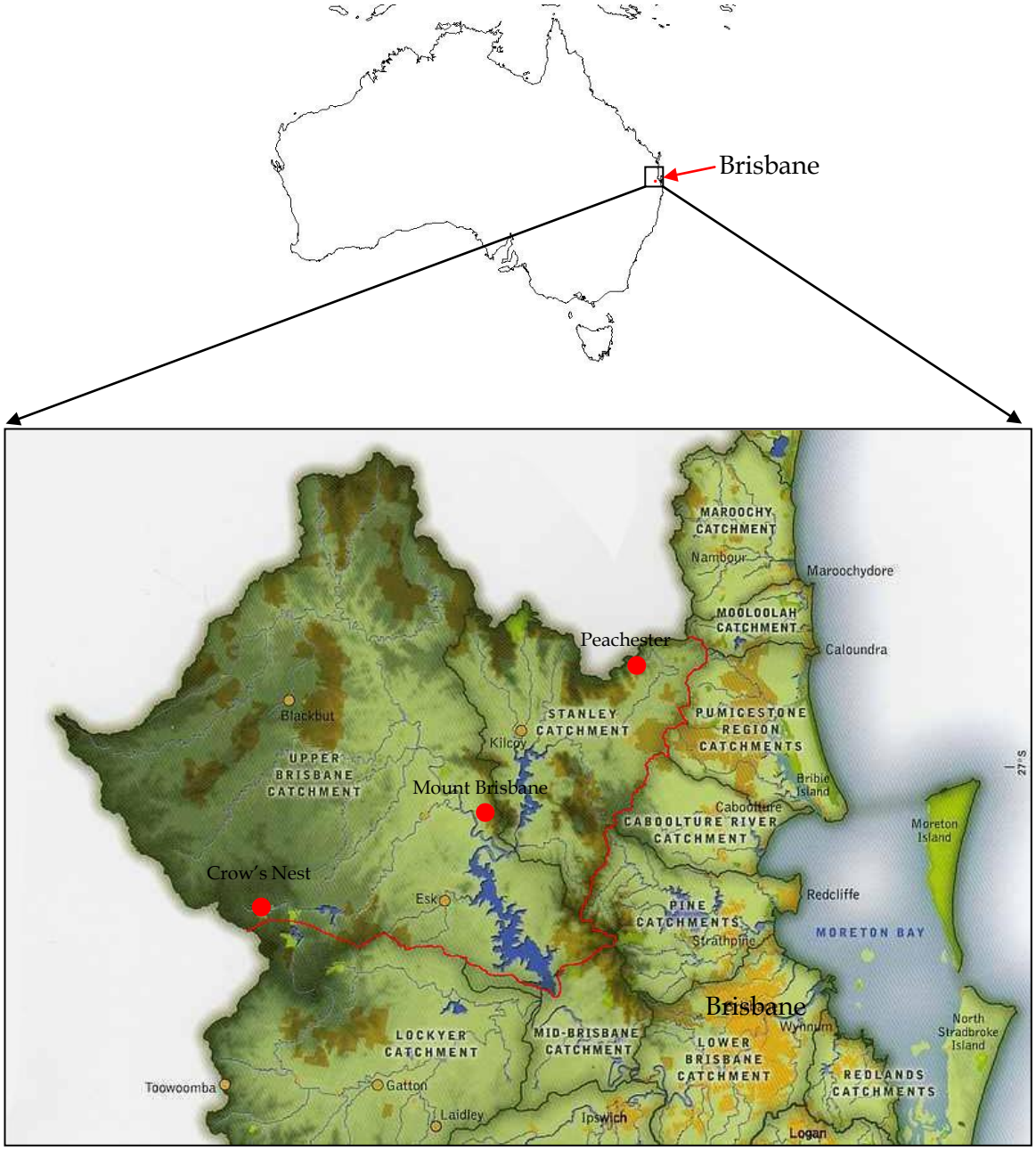

Figure 2.6: The Upper Brisbane Catchment feeds into Wivenhoe Dam and the Stanley Catchment feeds into Somerset Dam, which, in turn, also feeds into the Wivenhoe Dam. Three stations that will be the focus of this research have been included (Crow's Nest, Mount Brisbane and Peachester). Source: Southeast Queensland Healthy Waterways, 2008.

The Stanley catchment provides the majority of water despite being only one fifth of the size of the Upper Brisbane catchment. This shows the effect that topography and distance from the coastline has on regional precipitation. So, despite being situated next to each other, the Upper Brisbane and Stanley catchments can regularly experience different rainfall events. Annual rainfall averages for Peachester in the Stanley catchment is 1707.1mm, compared to 844mm for Crow's Nest in the Upper Brisbane catchment (BoM, 2011). These variations in rainfall are not evident in the coarse CGM resolution and can be made more apparent using downscaling techniques.

The recent drought (2001 – 2007) had a strong impact on the catchments. The drought can be considered the worst on record for the region, even worse than the Federation Drought (1898 – 1903) when comparing rainfall deficit (Fig 2.7) (Department of Natural Resources and Water (DNRW), 2007).

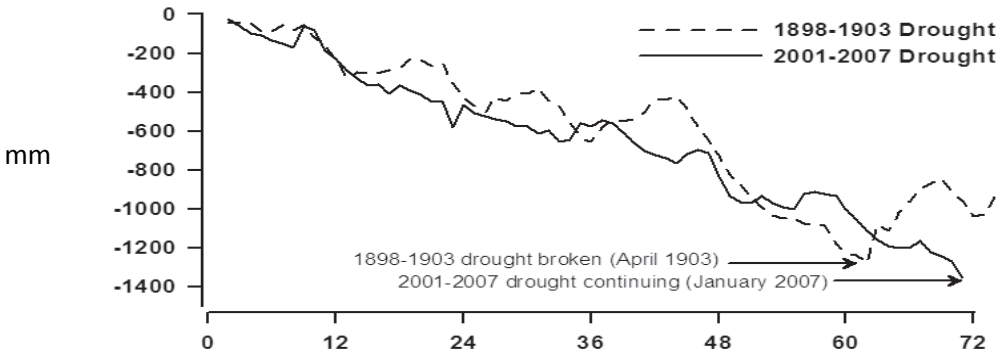

Figure 2.7: Comparison of the accumulated rainfall deficit in the catchment area to the west of Brisbane during the current drought (from April 2001 to January 2007) with the previous worst drought (from April 1898 to April 1903). (Source: DNRW 2007)

In the seven years from 2001 to 2007 dam water storage levels in southeast Queensland decreased from 100% to less than 20% (Fig. 2.8) (SEQWater, 2011). Level 5 water restrictions were brought in for the first time and the situation became dire. With no reprieve in sight, the question could be asked as to whether this was the first signs of climate change in the region and was also the impetus for this research.

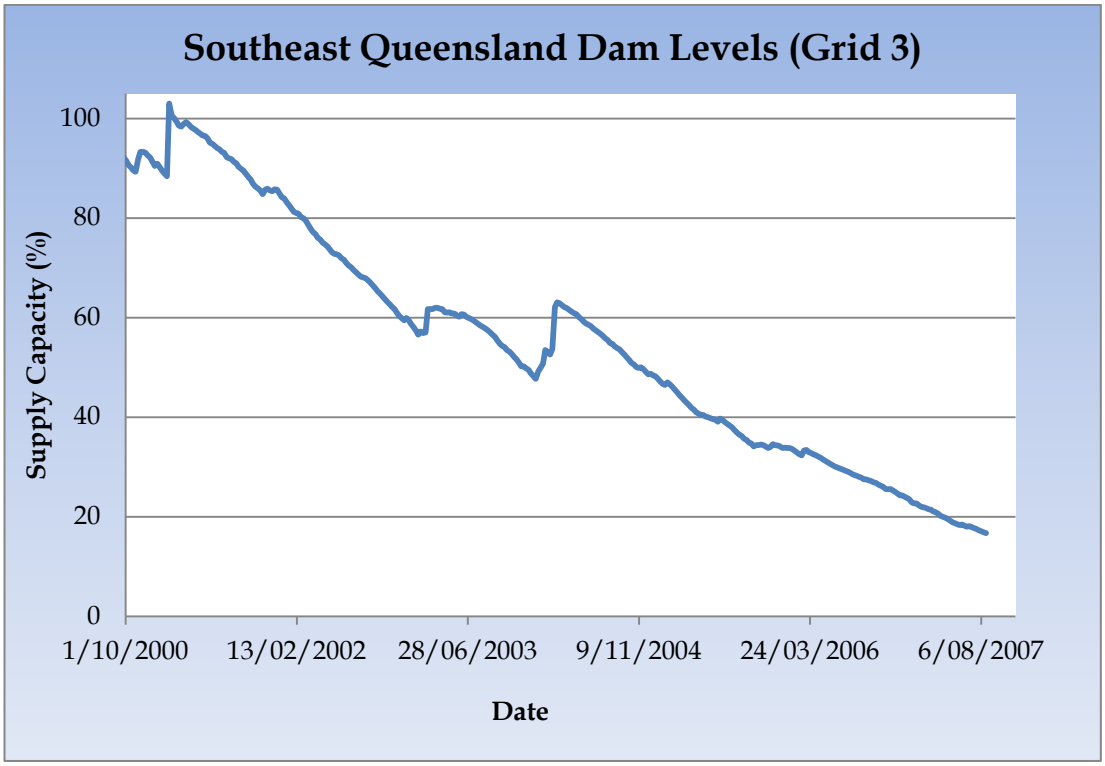

Figure 2.8: The decrease in Southeast Queensland Grid Three Dam Levels which includes Wivenhoe and Somerset Dams between 2001 and 2007. The scale on the left is percentage of full capacity. Source: SEQWater 2011.

The La Nina event of 2007/08 delivered torrential rain to the region with flooding in Sunshine Coast, Gold Coast and Northern NSW though the majority of this rain missed the Upper Brisbane and Stanley catchments. By

the end of 2008 dam levels were back up over 45% and continued to rise through 2009 to reach over 75%. However, some localities in southeast Queensland, such as Toowoomba, still remained in a dire situation with combined dam totals below 10% at the end of 2009 (SEQWater, 2011).

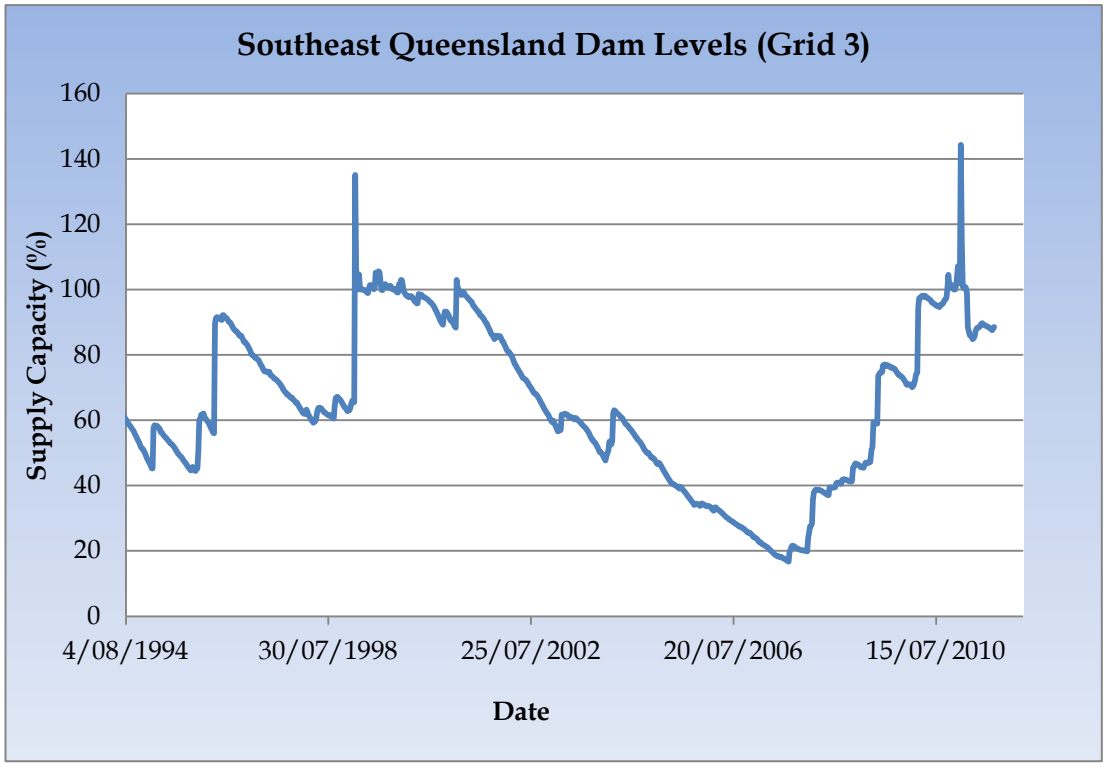

Figure 2.9: Southeast Queensland Grid Three dam levels from 1994 to 2011, shows recovery of dam level after 2007. Source: SEQWater 2011.

Figure 2.9 shows water being released from Wivenhoe Dam in October of 2010, the first time in ten years (SEQwater, 2011). The region went on to experience severe flooding in January 2011, which cost numerous lives in a terrible flash flood in Toowoomba and the Lockyer Valley. This event did return the regions dams to full supply but at a heavy cost to the community. In addition to the loss of life, many thousands of houses were inundated in Brisbane and Ipswich as the ensuing flood waters travelled downstream. The

Lockyer Creek and the Bremer River both experienced record flooding and the flood mitigation capacity of the Wivenhoe Dam was exceeded all at the same time.

2.2 Research problem

Severe drought followed by severe flood has taken its toll on the community. Projections of future rainfall events need to be assessed to find what is in store for the future of the region. The projections of future events vary and this will be briefly discussed in the following section.

2.2.1 Precipitation Projections

Global Climate Models (GCM's) are used to project future climatic conditions. Current projections for Australia suggest rainfall intensity will increase, due to the projections of a decrease in the number of rain days but the overall average rainfall is to remain relatively constant (CSIRO-BoM, 2007). Current rainfall projections for Queensland from coarse resolution GCM's under a greenhouse gas enriched environment show 80% projecting little or no change. The remaining 20% are divided between less rainfall and more rainfall (Walsh et al., 2004; CSIRO-BOM, 2007) (Fig. 2.10).

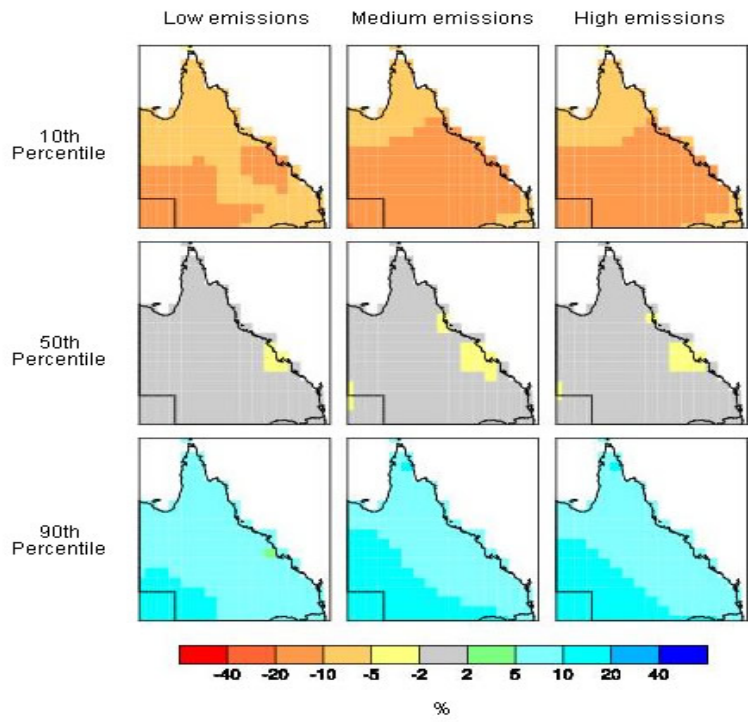

Figure 2.10: IPCC models of percentage change in annual Queensland rainfall by 2030 under 3 different emission scenarios. 10% of the models (10th percentile) suggest drier conditions can be expected, whilst another 10% (90th percentile) project an increase in annual rainfall. (Source: CSIRO-BoM 2007)

Water resources are expected to be detrimentally affected in the future by longer droughts and increased evaporation (CSIRO-BoM, 2007). Rainfall in Southeast Queensland is projected to decrease by about 5% with a 6% increase in evaporation. At this rate, the region will suffer a shortfall in water supply of between 97,000 and 308,000 Ml/year by 2050 depending on population growth, adaptation measures and the overall impact of climate change (BoM-QCCCE, 2011).

Further impacting on the future Southeast Queensland climate are studies showing that there will be a drying trend in the subtropics under a greenhouse gas enriched environment, so this recent drying trend may indeed be indicative of what is to come as suggested by model projections (Meehl et al., 2007; Held, 2006; Zhang et al., 2007).

2.3 Current methodologies

As shown in the section above, the variation between GCM's in rainfall projections demonstrates the difficulty involved in recreating the complex nature of precipitation. This difficulty is made even more extreme when making rainfall projections on a regional scale. This section investigates the different methods that can be employed to assist in regional rainfall simulations and projections.

2.3.1 Global Climate Models

Global climate models (GCM's) simulate the Earth's climate system by dividing it up into a three dimensional grid and applying mathematical equations to solve the basic laws of physics, fluid motion and chemistry. The size or resolution of the grid differs between models but is on an approximate scale of 250km x 250km. The IPCC used output from 31 GCM's

in its recent assessment report on the state of the climate (IPCC, 2007) and these results are drawn from contributions made from climate organisations around the world to the Coupled Model Intercomparison Project (CMIP3).

Some atmospheric components are too complex or too small to be physically resolved by the low resolution (approx. 60,000km^2) of the CGM's, e.g. topography, clouds, storm fronts. The physical processes that drive these components need to be parameterised and are represented in GCM's using simplified models. Different parameterisations between different models can result in variations in output. Despite the disagreements between models, GCM's are still our best tool for simulating and projecting the climate system.

The ability of a model to accurately simulate observed climatic conditions in a certain region can be measured statistically and is referred to as the model's "skill". There are many different measures of skill; each involves comparing simulations and forecasts with the corresponding observed value (Wilks, 2006). The simplest method of calculating skill, using only a correlation coefficient, does not take bias into account. Other methods involve mean square error (MSE) and the relevant correct and incorrect forecasts of climatic projections (Murphy & Epstein, 1989). Skill also varies between models for different locations and different times of the year. Models with the highest

level of skill at simulating observed conditions are assumed to have a better ability of making realistic projections.

Many climatic components are involved in producing the correct atmospheric conditions that result in rainfall events. Atmospheric circulations are driven by interactions between the ocean, atmosphere, cryosphere, biosphere and local landscape. The inherent complexity and randomness of the atmospheric circulation make it difficult for coarse resolution GCM data to accurately simulate regional rainfall and for some applications the data requires downscaling methods to increase the resolution.

2.3.2 Downscaling Methods

Downscaling involves processes that increase the resolution of GCM output to resolve important sub-grid details that have a significant impact on local climate variables. Resolution of most GCM data grids are typically on a scale of approximately 60,000km² (250km x 250km), but can be as much as 160,000km². This is problematic when using GCM data to determine projected rainfall for individual catchments which are in the order of 1000's of km². Downscaling of the low resolution GCM output is essential when applying climate projections to regional management issues.

Dynamical and Statistical techniques are the two primary methods used for downscaling data from coarse resolution models. Dynamical downscaling involves nesting a high resolution Regional Climate Model (RCM) in a coarse resolution GCM (Murphy, 1999; Leung et al., 2004). The nested model uses boundary conditions obtained from GCM's as input and makes calculations from that data to determine climatic conditions within the region over which the RGM is situated. This technique requires a high level of computer power and prowess. Statistical downscaling involves statistically representing desired fields from course resolution GCM data. Both dynamical and statistical downscaling methods have advantages and disadvantages with studies carried out to compare the two different processes to highlight the various positives and negatives of each (Wilby et al., 2004; Fowler et al., 2007; Murphy, 1999).

Statistical downscaling is more economical, less computer intensive and can be more easily transferred between regions, and different statistical rules need to be built up for each region. Site specific information is also able to be provided, which can be useful in climate change impact studies (Wilby et al., 2004). It does, however, require a large amount of accurate data to begin with, an appropriate choice of predictors and the assumption that the relationship between these predictors and the predictand will remain the same in the future. Dynamical downscaling is much more computer intensive, has a limited number of scenario ensembles and is strongly

affected by boundary conditions, but does produce fine resolution information based on physically consistent processes (Fowler et al., 2007).

Dynamical downscaling is more effective at simulating rainfall in regions with summer dominated rainfall than statistical methods because of its ability to capture mesoscale structure in the climate responsible for summer convective rainfall (Murphy, 1999). Statistical downscaling is effective at capturing temperature variations but requires regions with consistent weather patterns to simulate rainfall. Seasonal rainfall variability can also be captured by statistical downscaling methods where there is a strong link between rainfall and climatic predictors at specific times of the year as with Southwest Western Australia (Timbal, 2004; Charles et al., 2004) and South Australia (Timbal & Jones, 2008).

2.3.3 Statistical Downscaling

There are numerous types of statistical downscaling methods most of which essentially link large scale climatic conditions to local scale variables. These climatic predictors do not vary significantly on a regional scale and are better simulated in the coarse GCM resolution. Rainfall projections for specific locations can be improved by correlating rainfall with climatic predictors, assuming that future atmospheric conditions produce similar rainfall events

and that no new influences on regional rainfall develop. Though this assumption may be flawed in the long term as atmospheric composition become altered in ways never seen before, so future conditions may not follow what has happened previously (Milly et al., 2008). However, robust selection of climate predictors with a physical basis for driving local predictands, such as rainfall, can provide projections comparable to dynamical model projections (Timbal et al., 2008)

The main statistical downscaling techniques can be divided into the three groups: weather classification schemes, regression models and weather generators (Wilby et al., 2004). Each method has their relative strengths and weaknesses.

Weather classification or weather typing schemes group days into similar synoptic events and relates those with local conditions such as temperature and precipitation. In Australia this system has been used to investigate a reduction in winter rainfall in southeast Australia (Timbal & Jones, 2008), rainfall decline in southwest Western Australia (Hope et al., 2006) and the reduction in rainfall extremes on the east coast (Speer, 2008).

Winter rainfalls in areas of Victoria and South Australia have experienced declines from the long term average since 1977. These observed reductions in rainfall were linked to changes in large scale atmospheric components of mean sea level pressure (MSLP) and precipitable water using weather classification methods. Future projections using five models under climate change scenarios found that this trend may continue, more so in late winter and early spring. This is expected to impact on Melbourne's water supply as runoff will decrease at a faster rate than rainfall (Timbal & Jones, 2008).

Since the late 1970's, the southwest of Western Australia has also undergone a significant reduction in winter rainfall. This has been attributed to an increase in high pressure systems over the continent and a reduction in the amount of troughs associated with wet conditions. The study used a self-organising map of 20 different synoptic types to make its conclusions (Hope et al., 2006).

An investigation into decreased extreme rainfall events in eastern New South Wales since 1977 divides rain bearing systems into four different types; inland low pressure and trough systems and coastal low pressure and trough systems. The study found a general increase in MSLP off the eastern Australian coastline was responsible for the number of low pressure systems developing in the region and delivering rain. Links are also made with the

timing of this reduction in rainfall to a change to IPO 'warm phase' (Speer, 2008).

Regression models link local climate variables with large scale atmospheric forcing by the use of a regression analysis. This method produces a statistical equation which can incorporate one or several large scale climatic predictor to estimate the local scale variable. Regression models are simple to apply and have been used worldwide to produce both temperature and precipitation simulations and projections.

It was mentioned earlier that it is possible for adjacent catchments to receive different quantities of rain. A location's proximity to the coastline and mountain ranges has a significant effect on annual precipitation. Statistical relationships exist between topography and precipitation patterns. Slope, orientation, elevation and exposure all influence localised rainfall (Basist et al., 1994). Atmospheric variables and terrain characteristics can also be incorporated to downscale NCEP (National Centre for Environmental Prediction) data to make correlations with precipitation on a regional scale (Kyriakidis et al., 2001).

Different predictors are also more effective at different locations and for different times of year. Numerous predictors were tested and a combination of mean sea level pressure (MSLP) and preciptable water (PWTR) best simulated observed rainfall events in southwest Western Australia (Timbal, 2004). MSLP has a close association with rainfall variation of southern Australia (Li & Smith, 2009).

One regression study over eastern Canada identified correlations between observed temperature and rainfall values obtained from specific weather stations with the climatic predictors mean sea level pressure (MSLP), humidity, geopotential height and airflows (Hessami et al., 2008).

Weather generators use stochastic models based on a gamma distribution for rainfall amounts and a Markov chain for transition probabilities between states. They are able to generate daily and sub-daily information and produce a long series of data which can capture extreme events. Weather generators have been used to investigate precipitation in both the U.K and Canada.

The Streamflow of the Thames in the U.K. was investigated using Stastical DownScaling Model (SDSM) which incorporates both a stochastic weather

generator and regression based downscaling methods. The flows were projected to decrease mainly due to an increase in potential evaporation which has the possibility of impacting on the region's water supply (Diaz-Nieto & Wilby, 2005).

A Canadian study evaluated the ability of two stochastic weather generators to reproduce daily climate scenarios at three stations across the country to determine their suitability for climate change impact studies. The weather generator with 2nd order transition probabilities was more able to simulate wet/dry spell periods, and hence define monthly rainfall (Qian et al., 2005).

2.4 Conclusions

There is a need for water resources in Southeast Queensland to be better managed in the future to prevent dams dropping to seriously low levels again still provide flood mitigation. Both Australia's and Southeast Queensland water resources are highly vulnerable to climate change scenarios (Preston & Jones, 2006). Increased temperatures, higher evaporation and longer droughts reduce stream flow more significantly than reductions in rainfall. Having reliable and robust rainfall projections are important when planning water resource management strategies that will adapt to changes in the regions rainfall regime. Statistical downscaling

methods will be used to increase the resolution of GCM output to provide rainfall projections on a regional scale for southeast Queensland. Whilst dynamical downscaling methods do provide more robust rainfall simulations, the expertise and computer power required for these methods is beyond the scope of this analysis.

Chapter 3: Data and Methodology

3.1 Introduction

The statistical downscaling technique of linking rainfall to climate predictor's by utilising linear regression will be used in this study. Linear regression is used with some efficacy for seasonal simulations in regions where rainfall is dictated primarily by one or two climatic variables, as occurs for winter rainfall in Mediterranean climates such as the climate of Southwest Western Australia (Charles et al., 2004). Applying this method to simulate rainfall in the sub-tropics is a simplistic method of expressing the numerous vectors through which rainfall is received in such areas. Rainfall will be linked with climatic predictors on a monthly basis. This is hoped to enhance the ability of this method to detect both annual and intra-seasonal variations in rainfall climate drivers for the region.

The steps involved are:

1. Correlate National Centre for Environmental Prediction (NCEP) predictor variables from around the region with observed rainfall for each month at the three selected stations.
2. The NCEP predictor variables with highest correlation coefficients for each month are linked to observed rainfall totals via linear regression to produce a statistical model. Each station will then have its own site specific statistical model for each month of the year.

3. Use NCEP predictor variables in the statistical models to test the models ability to recreate observed monthly rainfall totals.
4. Use GCM values for the predictor variables in the statistical models to find the efficacy of the models to recreate long term rainfall averages.
5. Use projected GCM values for the predictor variables in the statistical models to make 30 year rainfall projections at the three selected sites.

3.2 Data Sources

Monthly rainfall data for the stations used in the study were obtained from the Australian Bureau of Meteorology (www.bom.gov.au). Forty weather stations in the region were analysed to find the most complete rainfall records. The stations of Crow's Nest, Mount Brisbane and Peachester (see Figure 2.6) were selected because they have some of the most complete records and are representative of the region.

Climatic predictor data were obtained from the National Centre for Environmental Prediction (NCEP) / National Centre for Atmospheric Research NCAR Reanalysis Project. The predictors tested were geopotential height, precipitable water, relative and specific humidity, and zonal and meridional wind speed.

The projected values for the selected climatic predictors come from the six Global Climate Models in section 3.3.5. Their data was obtained from the World Climate Research Programme – Climate Model Intercomparison Project (WCRP – CMIP3) multi-model dataset archive at Program for Climate Model Diagnosis and Intercomparison (PCMDI) website.

3.3 Transformed Data

Linear regression analysis requires data that is normally distributed and monthly rainfall totals do not comply with this format. A log transformation of monthly rainfall data was undertaken to create a normal distribution.

The statistical models developed used NCEP data with specific humidity values given in the form of gm/m^3. However, GCM specific humidity output is given as standardised values which cause problems if these values are inserted into the statistical models. The distributions of the GCM specific humidity values from 1948 to 2000 are adjusted using a linear transformation so they resemble the NCEP distributions over the same period.

The linear transformation takes the mean and standard deviation of the NCEP and GCM values of specific humidity data and calculates a linear equation ($Y=aX + b$) that was applied to the GCM values and changes them

into data (GCM′) on the same scale (with rounding error) as the NCEP data from which the statistical models are derived. The format is as follows:

$$a = \sigma(GCM) / \sigma(NCEP)$$

$$b = \overline{GCM} - (a \,.\, \overline{NCEP})$$

$$GCM' = a \,.\, GCM + b$$

σ (GCM) – Standard deviation of the GCM values

σ (NCEP) - Standard deviation of NCEP values

$\overline{GCM}$ - Mean of GCM values

$\overline{NCEP}$ - Mean of NCEP values

GCM′ - Transformed GCM value

GCM - Original GCM value

This transformed list of GCM values for specific humidity (GCM′) was used in the statistical models to provide 20th Century rainfall simulations and make 21st Century projections.

3.4 Missing Data

In the event that rainfall was not recorded for one or more days of a particular month then the entire month is excluded from the Bureau of Meteorology records. The rainfall for the missing day is included in daily rainfall records the following day as an accumulated value. Monthly Rainfall data found to be missing were amended by accessing daily rainfall values and manually calculating monthly rainfall using the accumulated values. The amended values were then compared to the nearby stations to check no erroneous values were entered.

3.5 Research procedures

The following section describes the details of the data and research procedures used in the thesis to produce and apply the statistical models for rainfall projections.

3.5.1 Time Frame

Regression analysis of rainfall benefits from using the longest reliable time series possible (Fowler et al., 2007). This can be problematic as the more historic the records become, the less reliable climate predictor records can be. NCEP/NCAR climate predictor data begins at 1948 and continues through to

2000. This will be the same start and finish times over which the correlations and regression analysis were made in this thesis. Finishing in 2000 also coincides with the end of the 20th Century simulations provided by the GCM's, though this time frame will miss the 2000 – 2006 drought it is more used as a calibration period.

3.5.2 Site Selection

Applying statistical downscaling methods to precipitation requires high quality rainfall records to produce accurate simulations (Fowler et al., 2007). The calibration of the downscaling models is dependent upon a reliable relationship between climate predictor variables and observed rainfall. Inaccuracies in rainfall data will be magnified in rainfall simulations produced by statistical models that fail to completely grasp the link between predictor variables and regional rainfall. The Upper Brisbane and Stanley catchments shown in Figure 2.6 have approximately 40 weather stations reporting to the Bureau of Meteorology. Monthly rainfall records were investigated to determine which stations had the most complete rainfall records and also represented eastern, central and western locations within the catchments. Three stations were selected that fit those two criteria; those of Crow's Nest, Mount Brisbane and Peachester (Figure 2.6).

Creating a point value analysis rather than a pattern or gradient field is less informative but still provides some details on the ability to simulate rainfall in the region using multi-variate linear regression on monthly data. The statistical models provided assume independence between sites and thus can assist in verifying that the predictor variables selected are appropriate.

3.5.3 Predictor Selection

The method used to simulate precipitation relies on finding large scale predictors that have a strong association with observed rainfall. Rainfall in the region is driven by numerous phenomena at different times of the year. The monsoonal trough and cut-off low's can be detected in GCM output with wind direction and geopotential height, which is a measure of air pressure. The ENSO signature can be found in the wind direction and general water content of the atmosphere. Predictor selection will also be aided by previous studies by Charles et al. (2004), Kyriakidis et al. (2001) and Timbal and Jones (2008) using regression analyses. Six climatic predictor variables are chosen for this study. They are Precipitable water, Geopotential Height, Relative Humidity, Specific Humidity, Zonal wind speed and Meridional wind speed.

Precipitable (Prw) water is a measure in kg/m^2 of how much water is in a column of the atmosphere stretching from the ground up. Geopotential

Height (Z) measures in m the height of a specified pressure level above the surface of the Earth. For the purpose of this research the specified pressure level will follow the Z abbreviation, e.g. Z850 is the height in meters of the 850hPa pressure level above the ground. As air pressure increases over a region, the value of geopotential height also increases.

Relative Humidity (RH) is a percentage measure of how saturated the atmosphere is with water vapour. At 100%, the atmosphere can absorb no more water vapour at that temperature and pressure. The pressure level will follow the RH abbreviation. This also applies to Specific Humidity (q), which is a measure of how many grams of water are in 1kg of atmosphere, i.e. g/kg. Examples of a relative and specific humidity value that may follow in this thesis are RH400 (relative humidity at the 400hPa level) and q600 (specific humidity at the 600hPa level).

Zonal wind speed (u) is a measure in m/s of the wind speed in the west to east direction (westerly wind). A negative value of zonal wind speed denotes a flow in the opposite direction i.e. an easterly flow from east to west. Again for the purpose of this research, zonal wind speeds are taken at nine different levels in the atmosphere from 850hPa up to 10hPa, and the level follows the u abbreviation, e.g. u850 is zonal wind at the 850hPa level.

Meridional wind (v) is also measured in m/s, but this time a southerly flow is measured, i.e. wind travelling from south to north. Air pressure level at which the wind speed is taken again follows the zonal wind speed levels and the same abbreviation applies.

These selected predictors were correlated with monthly rainfall records at each station to determine which predictor(s) had the highest correlation with rainfall totals for each month of the year (Appendix A). The values of these coefficients of determination vary for each month from values as low as 0.47 up to 0.76 at a 95% level of significance. All values included in the regression analyses had the highest correlation for that month of all predictors tested.

The spread of the predictors covers the region from 20°S and 145°E to 32.5°S and 160°E at a spacing of 2.5° longitude and latitude (Figure 3.1), and were taken at eight levels and 42 locations using the predictors. The location of the catchment is approximately in the middle of the spread at 27.5°S 152°E. Predictors exhibiting highest correlation with rainfall are then used in linear backward stepwise regression to produce statistical models that simulate rainfall.

Backward stepwise regression starts with all the selected variables and removes one at a time to find which combination provides an equation that

best simulates the predictand, in this case monthly rainfall. This method is best used with a small number of predictors that have undergone a pre-selection process, such as identifying which predictor is most highly correlation with monthly rainfall, and it is unknown which variables need to be used in the statistical equation. Other statistical methods including forwards stepwise regression and forced entry are not employed in this analysis because they require a large number of variables with unknown relevance for the former and a complete set of variables with known relevance for the latter.

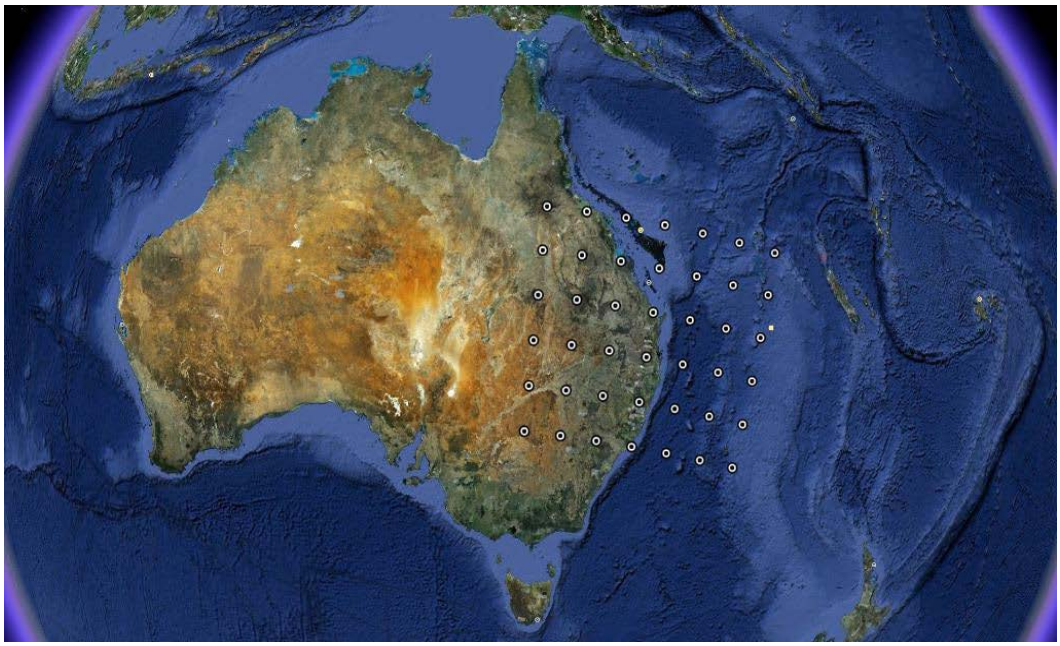

Figure 3.1: Grid Point locations where NCEP climate predictors were taken and correlated with observed monthly rainfalls. Source: Google Earth 2011

3.5.4 Regression Analysis

Each monthly set of predictors and rainfall observations was used in a backward stepwise regression analysis in the statistical program "R" version 2.11.1 (2010). The output is an equation that estimates monthly rainfall through the value of the large scale climatic predictor variables. The resulting equation is the statistical model and is of the form:

$$\text{Monthly Rainfall [mm]} = \alpha_1 \times CP_1 + \alpha_2 \times CP_2 + \ldots + \alpha_n \times CP_n + \text{constant}$$

α – coefficient of variable
CP – Climate Predictor variable
Constant – the y intercept of the regression line

Each month has a different number of climate predictor variables depending on the relative influence the regression model assigns between each variable and monthly rainfall. Too many climate predictor variables in the regression analysis will confuse the regression analysis and the coefficient of the variable will not display the correct sign of that variable's impact on rainfall. For instance, if geopotential height is selected as a component of a statistical model and its coefficient has a positive indice then this would be incorrect as a negative relationship exists between geopotential height and rainfall, i.e. as geopotential height decreases rainfall should increase. It should be noted the short lived intense rainfall events may be unable to be replicated by using

this method as climate predictors averaged over a month may not indicate an extreme occurred.

To ensure the coefficients in the statistical models developed are of the correct nature, each were checked with the corresponding predictor variable to make sure it displays the correct influence on rainfall. The full list of statistical models for each month at the three stations can be found in Appendix B. The following example is provided to more clearly explain the point:

January rainfall for Crow's Nest = 28.33977 - 0.01758.Z850 + 0.04212.RH850

The Z value (Geopotential Height) has a negative coefficient (-0.01758) and this is correct as the Z value increases, one would expect rainfall to be reduced. The same follows for the RH (Relative Humidity) variable which has a positive coefficient (+0.04212) and this holds as rainfall will be more prevalent with more moisture in the atmosphere.

3.5.5 GCM Selection

Numerous models were employed to produce an ensemble of projections, which increases the confidence in the output. Model selection was assisted Suppiah et al. (2007) and by the author's previous unpublished work carried

out at the Queensland Centre for Climate Change Excellence that measured the ability of 31 climate models to simulate regional Australian rainfall. The selected models are listed below with characteristics highlighted in Table 3.1;

Center National de Recherches Meteorologiques - (CNRM - cm3)

Commonwealth Scientific and Industrial Research Organisation - (CSIRO Mk3.5)

Goddard Institute for Space Studies - (GISS - er)

Geophysical Fluid Dynamics Laboratory - (GFDL Mk2.1)

Centre for Climate System Research - (MIROC - medres)

Canadian Centre for Climate Modelling and Analysis - (CCCMA - t63)

Suppiah et al. (2007) found the CNRM – cm3, CSIRO, GFDL Mk2.1 and the MIROC – medres models were among the best performing GCM's to reproduce Australian average 1961 – 1990 patterns of temperature, rainfall and mean sea level pressure. In the authors previous unpublished research at QCCCE, the models CCCMA – t63 and GISS – er also performed well at simulating rainfall averages in Queensland.

Table 3.1: Table of Global Climate Models (GCM's) used to extract climate predictor data from that will be incorporated into the statistical models. Resolution is in degrees latitude and longitude, number of atmospheric layers, years over which data is produced and the number of external forcings used in GCM besides atmosphere, ocean, sea ice and prescribed land/vegetated surface. Source: Adapted from Suppiah et al. 2007.

Model (Country of Origin)	Resolution	Atmospheric Levels	Data	External Forcings
CCCMA – t63 (Canadian)	2.8 x 2.8	31	1850 – 2100	Na
CNRM – cm3 (French)	2.8 x 2.8	45	1860 -2099	4
CSIRO mk 3.5 (Australian)	1.9 x 1.9	18	1871 – 2100	3
GISS – er (U.S.A)	4.0 x 5.0	15	1880 – 2100	11
GFDL mk 2.1 (U.S.A)	2.5 x 2.0	24	1861 – 2100	8
MIROC – medres (Japanese)	2.8 x 2.8	20	1850 – 2100	10

External forcing applied in the GCM calculations include well-mixed GHGs, ozone, sulfate (direct), sulfate (indirect), black carbon, organic carbon, mineral dust, sea salt, land use, solar irradiance and volcanic aerosol. While the GISS – er model has the lowest resolution of all GCM's it does use the greatest number of external forcing of the selected model which assists in the ability to replicate real world results as will be shown in the results section 4.2.2.

The grid points of each GCM differ from the NCEP coordinate system and are taken at the nearest point to the NCEP data. The full list of changes in coordinates is tabled in Appendix C.

3.5.6 Precipitation Simulations

To check the accuracy of the statistical models that are developed, NCEP values for the climate predictors were inserted back into the models and the monthly rainfall values obtained were compared with the observed values from 1948 to 2000 in section 4.2.1. This process was then repeated with the GCM simulated values for the climate predictors over the same period and the results were again compared with the observed values. This assisted with attributing a level of confidence with each model, and how much value can be placed on their projections of 21st century precipitation in section 4.2.

3.5.7 Precipitation Projections

Precipitation projections were made by inserting 21st century projected climate predictor values into the statistical models developed by the regression analysis. This output was used to construct long term means for each station to provide an indication of whether drying trends will continue by looking at projected rainfall over the next 30 years (Section 4.3). A snapshot at 30 year intervals of average monthly rainfall over the next 90 years was also made in section 4.3.2 using the GCM's. The statistical models used in these long term projections were the ones that perform best at

recreating average monthly rainfall for the second half of the 20th Century (section 4.2.3).

Chapter 4: Results

4.1 Introduction

The main objective of this study is to investigate if the recent drying trend Southeast Queensland over the last 40 years will continue into the coming decades. The statistical downscaling method selected is a relatively simple process to try and explain the complex systems described in chapter 2 that are involved in the production of subtropical rainfall that occurs over southeast Queensland. The hope is that the methodology will capture any significant changes in atmospheric dynamics. The statistical rainfall models was first checked for their ability to simulate month to month rainfall using the original NCEP data as input in order to verify the equations were capable of simulating rainfall in the region. These equations then had GCM data used as input and long term means were compared to observed rainfall from the three stations. Models whose downscaled data performs best at simulating observed rainfall can then be focused on for more realistic projections.

The results from this research are presented in section 4.2 which shows the ability of the regression models to simulate observed rainfall totals at the three stations. Observed and simulated monthly rainfall totals using NCEP climate predictor data were graphed for the period 1948 to 2000 and coefficient of determination values are provided. Section 4.3 then uses climate predictor values from the six chosen GCM's as input for the statistical

models and provides long term rainfall averages. These long term averages were compared with averages taken from the GCM monthly rainfall totals at the nearest grid point and rainfall averages provided by observed data derived from selected weather stations. Projected climate predictor values were inserted into the statistical models and the subsequent annual monthly rainfall projections are presented in section 4.4.

4.2 20th Century Rainfall simulations

The statistical models (Appendix B) were produced by linking NCEP values for climate predictors with rainfall from the three stations. The month to month values for the NCEP predictors were reinserted back into the equations to test their ability of producing rainfall values that accurately simulate observations.

20th Century GCM values for climatic predictor variables were then used as input into the equations. These values were unable to match month to month NCEP values, but models that can emulate the distributions of these values will have the ability to provide an accurate example of long term rainfall. It is hoped that these simulations will be an improvement over the GCM rainfall simulations at the nearest grid point.

4.2.1 Testing Statistical Models with NCEP Data

In this section, monthly rainfall totals derived using climatic predictors in the statistical models were compared with the observed rainfall at the stations of Crow's Nest, Mount Brisbane and Peachester. The statistical models were produced through a regression analysis between NCEP climatic predictors and monthly rainfall totals. These NCEP climatic predictor values were then reinserted back into the statistical models to test the relationship between the monthly rainfall values obtained from the models and real life observations.

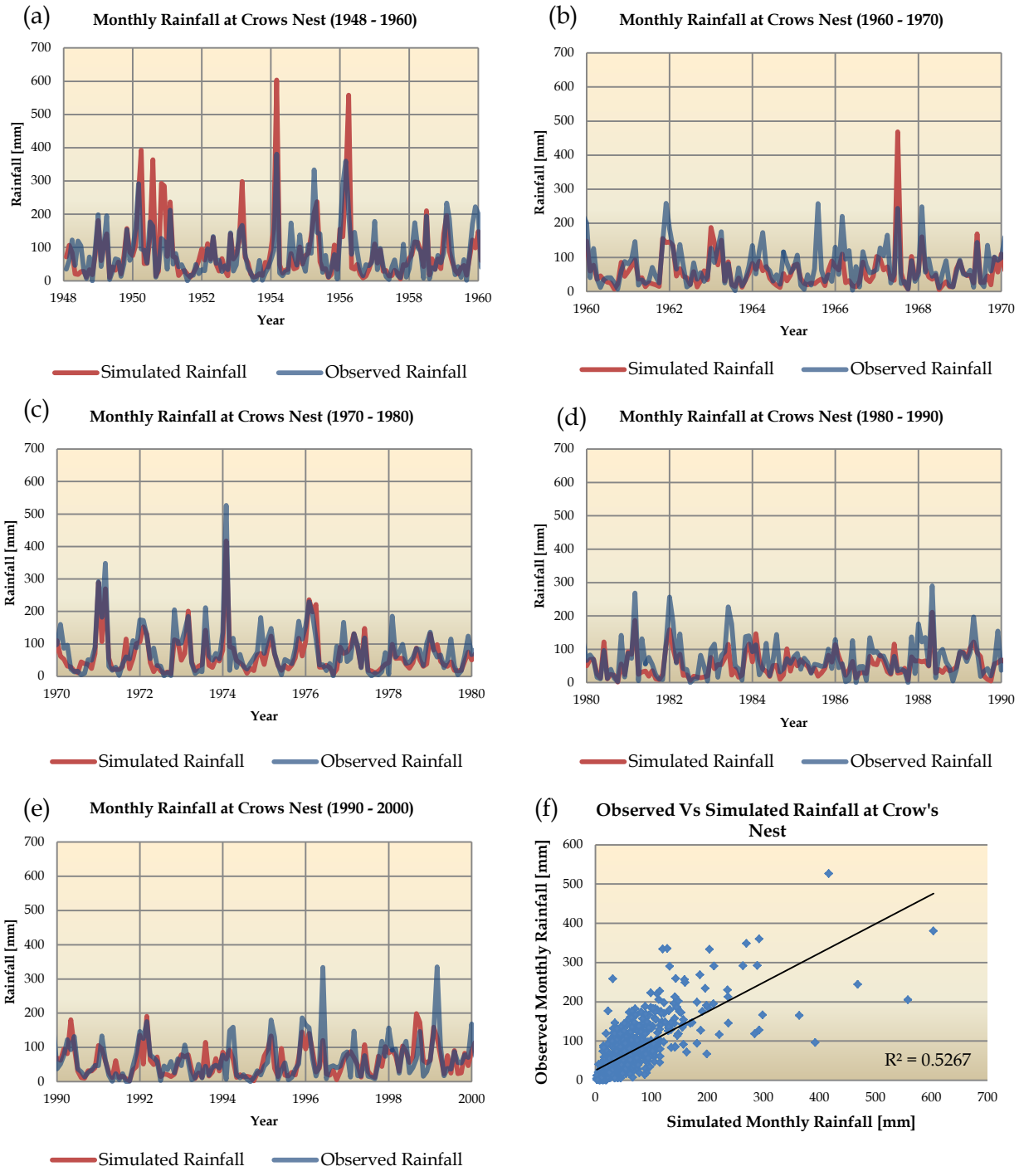

Figure 4.1: Comparison of Observed rainfall [mm] [blue] at Crow's Nest for the periods (a) 1948 – 1960, (b) 1960 - 1970, (c) 1970 – 1980, (d) 1980 – 1990 and (e) 1990 – 2000 with data derived from the statistical downscaled models [red]. Coefficient of Determination for the two sets of data provided in (f).

In Figure 4.1(a) the period from 1950 to 1956 was marked by high monthly rainfalls at Crow's Nest in the years 1950, 1951, 1954, 1955 and 1956. The rainfall totals from the statistical downscaled model simulations overestimated the amounts in the years 1950, 1954 and 1956. Monthly rainfall was also overestimated in 1953 despite the fact that this year experienced only average rainfall. In general, there is a strong spread with high rainfall amounts.

The heavy winter rainfall event in August 1965 (Figure 4.1(b)) was not picked up in the monthly climate predictors and the simulation underestimated the rainfall total for that month by over 200mm. There was also a large overestimation by the model in the winter (June) 1967 by a similar margin of around 220mm.

Figure 4.1(c) shows the ability of the models to capture the heavy rainfall events of both 1971 and 1974. Marginal misses of around 100mm were found in 1975 and 1978, otherwise the models proved to be an effective means of simulating rainfall over the period 1970 to 1980.

The period 1980 to 1990 (Figure 4.1(d)) is characterised by a general underestimation of rainfall totals by the statistical models. Of note was the high rainfall in May and June of 1983 which the models were not able to detect, but they did go some way in picking up the higher than normal total

in 1988. However, this was then followed by an inability to recreate the 1989 and 1990 totals.

The models made an overestimation in late winter (August) of 1993 and missed the 1996 and 1999 events by around 200mm (Figure 4.1(e)).

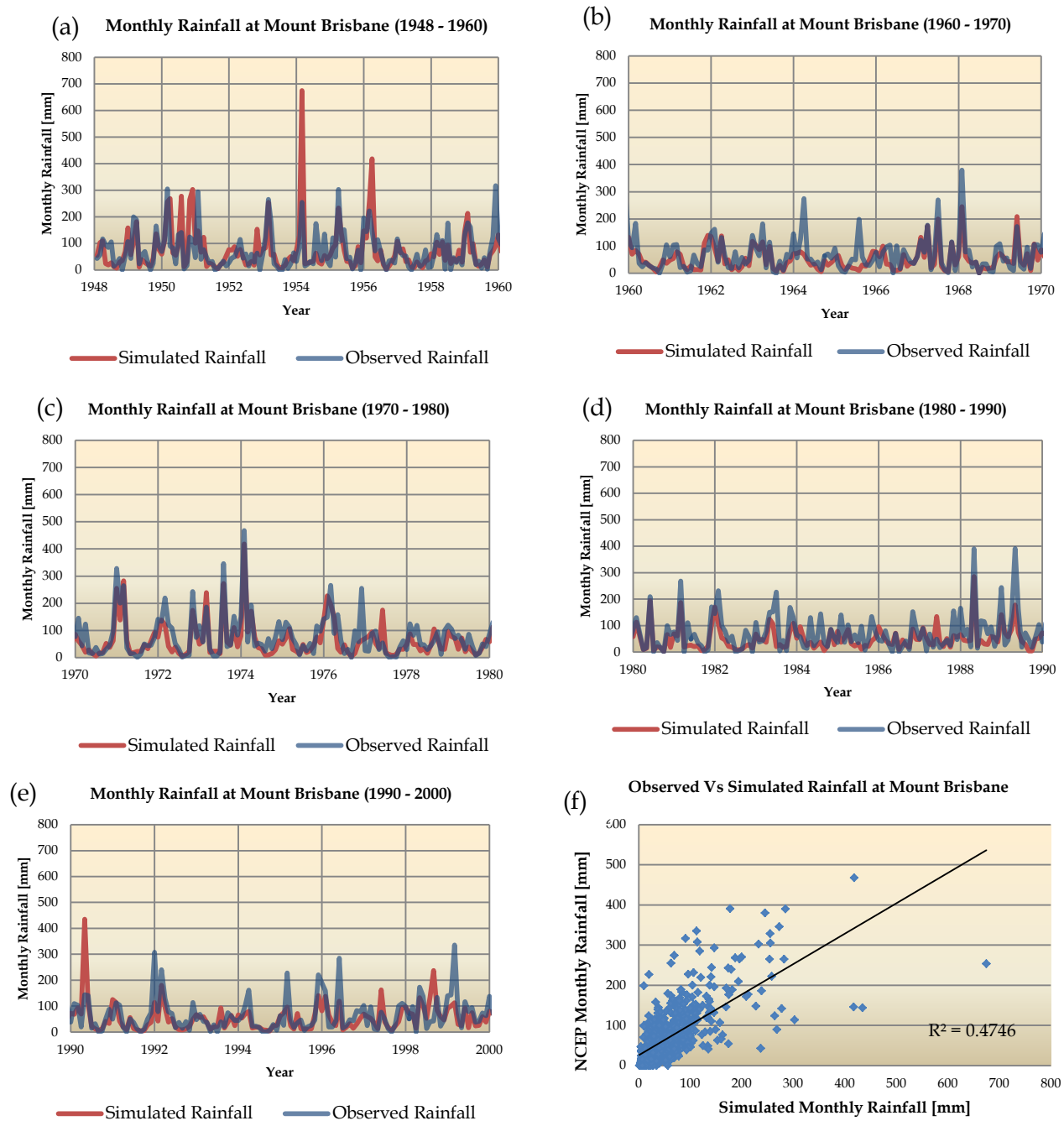

Figure 4.2: Comparison of Observed rainfall [mm] [blue] at Mount Brisbane for the periods (a) 1948 – 1960, (b) 1960 - 1970, (c) 1970 – 1980, (d) 1980 – 1990 and (e) 1990 – 2000 with data derived from the statistical downscaled models [red]. Coefficient of Determination for the two sets of data provided in (f).

Figure 4.2(a) shows the statistical models captured 2 of the 3 heavy rainfall events in 1950 and 1951 at Mount Brisbane. There is a strong over estimation in 1954 by about 400mm and again in 1956 by a margin of 200mm. Again, there is a strong spread with high rainfall amounts.

In Figure 4.2(b) the high rainfall observed in 1964 was not matched in the models, nor was the winter (August) event in 1965. Despite the model not matching the exact total in 1968 the observed and simulated totals were both at a peak in that same month over the period 1960 to 1970.

The high rainfall in 1971, 1974 and to a lesser extent in 1973 are simulated by the models in Figure 4.2(c). The December total in 1976 is under estimated by the model by just less than 200mm and in May of 1977 by over 100mm.

The graph in Figure 4.2(d) shows again as in Figure 4.1(d) that rainfall simulations for the period 1980 to 1990 are consistently below observed values. There is a slight overestimation in the winter (June) of 1987 and an underestimation for the 1988 and more so for the 1989 high rainfall events.

Figure 4.2(e) shows a strong overestimation by the models for the monthly total in May of 1990. The models then go on to miss the high winter totals in May of 1995 and June 1996. There is also a significant miss in March of 1999 by over 200mm.

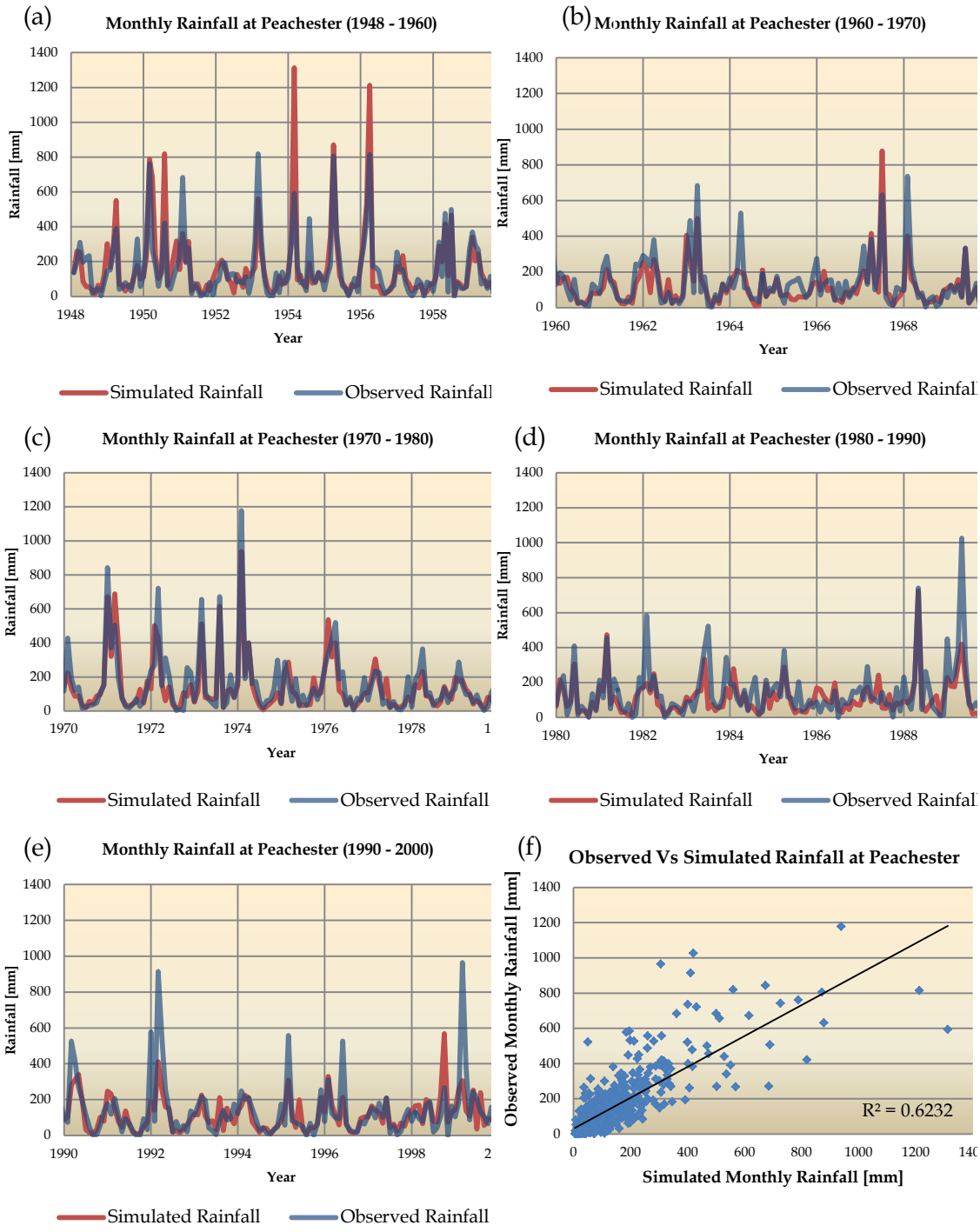

Figure 4.3: Comparison of Observed rainfall [mm] [blue] at Peachester for the periods (a) 1948 – 1960, (b) 1960 - 1970, (c) 1970 – 1980, (d) 1980 – 1990 and (e) 1990 – 2000 with data derived from the statistical downscaled models [red]. Coefficient of Determination for the two sets of data provided in (f).

Figure 4.3(a) displays the observed and simulated rainfall totals for Peachester from 1948 to 1960. It shows the high rainfall experienced in March 1950 was matched by the model but then went on to overestimate the April rainfall for the same year. As with Figures 4.1(a) and 4.2(a) there is a strong overestimation in March of 1954, this time by a margin of 700mm. The model was able to capture the 1955 event and less so for the 1956 event, though this was an overshoot by 400mm. The model was able to accurately simulate the period from 1958 to 1959.

The period from 1960 to 1970 is presented in Figure 4.3(b) and shows the model made a significant miss of the rainfall totals received in the summer of 1964. The model goes on to overestimate rainfall in 1967 and underestimate the 1968 totals.

There is a good match between the model and observations between 1970 and 1976 (Figure 4.3(c)). Of note is the close relationship between the totals for the 1971, 1973 and 1974 high rainfall. The 1972 event is underestimated by around 200mm but there is still a noticeable response from the climate predictors for that event.

The high rainfall total observed in 1981 is matched in the models but there is a strong miss for the 600mm total in 1982 with the models providing total of 200mm. The period of low rainfall from 1986 to 1988 did translate into the

simulated rainfall, though the exact tracking was off, the averages between the two totals for that phase are similar. There is a very good match for the high 1988 total but then a strong miss for the 1989 event with the simulation giving a total 600mm less than the observed 1000mm.

Overall, the models displayed modest values for coefficient of determination but the values are an improvement over values obtained directly from GCM output at the nearest grid point (Appendix D). Peachester has the highest coefficient of determination value of 0.6232 (Figure 4.3(f)) and Mount Brisbane the lowest with an R^2 value of 0.4746 (Figure 4.2(f)). The outlier value of 1954 of 400mm contributed some of the Mount Brisbane value being the lowest, as would the strong clumping of correlations. Crow's Nest coefficient of determination value of 0.5267 (Figure 4.1(f)) also would have suffered from the models strongly overestimating monthly rainfall on at least 5 occasions.

4.2.2 Testing GCM Data with Observations

Values for monthly rainfall obtained from GCM's at the grid point nearest the locations of interest for this study are compared to observations from those stations. The full series of graphs can be found in Appendix D, results of which have been summarised below in Tables 4.1 and 4.2.

Table 4.1: R^2 values for the correlation between observed rainfall (1950 to 2000) at Crow's Nest, Mount Brisbane and Peachester and values derived directly from the 6 chosen climate models at the nearest grid point.

GCM	Crow's Nest	Mount Brisbane	Peachester
CCCMA – t63	0.00003	0.00002	0.00004
CNRM – cm3	0.1186	0.0878	0.0807
CSIRO – mk 3.5	0.0892	0.0763	0.1013
GISS – er	0.0995	0.0682	0.0530
GFDL – mk 2.1	0.0142	0.0100	0.0120
MIROC - medres	0.0375	0.0305	0.0360

Table 4.2: Mean and standard deviation [mm/month] of rainfall over the period 1950 to 2000 for Crow's Nest, Mount Brisbane and Peachester, and from rainfall values derived from the 6 chosen models at the nearest grid point.

GCM	Mean	Standard Deviation
Crow's Nest	73.14	64.85
Mount Brisbane	70.22	67.80
Peachester	145.62	156.53
CCCMA – t63	49.65	45.61
CNRM – cm3	76.03	71.22
CSIRO – mk 3.5	58.86	65.38
GISS – er	94.31	76.97
GFDL – mk 2.1	50.55	52.15
MIROC - medres	74.10	57.93

The R^2 values obtained in Figures 4.1 (f), 4.2(f) and 4.3(f) of between 0.4746 and 0.6232 are a strong improvement in the value of the coefficient of determination obtained from comparing observed rainfall totals with those derived from GCM 20th century simulated values at the nearest grid point (Table 4.1). This is not to discount the viability of GCM simulated rainfall totals, as they have some ability to approximate rainfall distributions with means and standard deviations approaching those observed at the designated grid point (Table 4.2). However, the ability for GCM models to produce real world temporal and spatial variations on a month to month and regional basis is far too complex for current computer systems and models to reproduce. This is made more evident in a region where rainfall variability produces values for standard deviation higher than mean rainfall as seen in Table 4.2 at Peachester. This fact makes it difficult to make direct comparisons between GCM and observed rainfall totals but nevertheless the results show an improved reproduction over the exact GCM month to month totals. Peachester monthly totals are also unable to be replicated by the GCM output as totals at this specific site are not representative of the region as a whole.

The statistical models produced in this research are one method to fill the gap that exists between raw GCM output and regional precipitation simulations. The following section will provide rainfall simulations derived from the statistical downscaling methods over the last half of the 20th century

and compare the values to those derived directly from GCM output and to observed monthly rainfall totals.

4.2.3 Testing Statistical Models with GCM Data

In section 4.2.1 the climate models were tested using monthly NCEP climate predictor values. This section goes on to use GCM 20th Century values for climate predictors as input for the statistical models to find what improvement, if any, these models have over the raw CGM rainfall simulations at the nearest grid point. As shown in Tables 4.1, GCM's are unable to reproduce exact month to month climate predictor values but a better able to provide an approximation of mean and standard deviation (Table 4.2). To allow for this, the 20th Century rainfall simulations derived from GCM data are presented as long term means. The following graphs show observed long term (20 year) rainfall at each station, the long term GCM rainfall value at the nearest grid point and the values derived from the statistical models using GCM climate predictor values from the six chosen models.

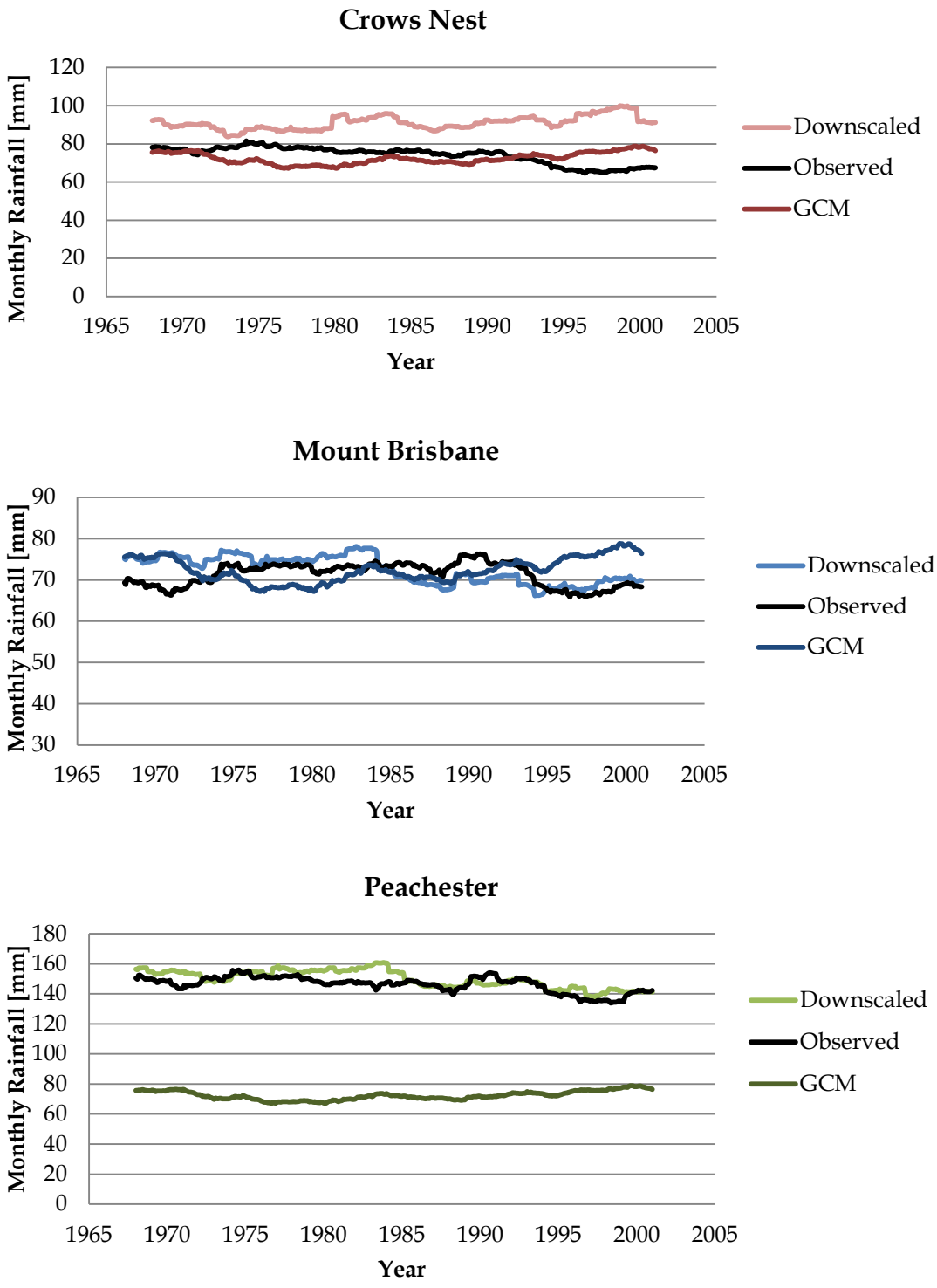

Figure 4.4: A comparison of GCM monthly rainfall [mm] simulations at the nearest grid point, data obtained from downscaling GCM output and observed rainfall. The simulations are 20 year running means taken at Crow's Nest, Mount Brisbane and Peachester. The GCM used is the **MIROC – medres** model from Japan.

Figure 4.4 shows precipitation in [mm] for three locations, i.e. Crow's Nest, Mount Brisbane and Peachester for the period 1965 to 2000. It is comparison between data statistically downscaled, those observed at the actual location, and those directly obtained from the GCM at the nearest grid point.

Observed rainfall averages range from 70 mm to 80mm at Crow's Nest and Mount Brisbane and 140 to 150 mm/month for Peachester. The first two stations are matched by simulated values at the nearest grid point derived from the MIROC – medres GCM which also range from approximately 70 to 80mm/month. Downscaled values at Crow's Nest are between 85 and 100mm/month which overestimates observed values by 5 to 20mm/month. Values from the statistical models for Mount Brisbane are on par with both the observed rainfall totals and the GCM data at the nearest grid point.

The statistical downscaling methods prove to be an effective means of simulating long term rainfall averages at Peachester. The models provided monthly rainfall totals of between 140 to 160mm/month which closely tracked the observed long term means. These results are a significant improvement over monthly GCM rainfall totals from the nearest grid point, which underestimated rainfall by approximately 80mm/month. This improvement is an example of how the statistical downscaling methods in this research can provide useful climate information on a regional scale.

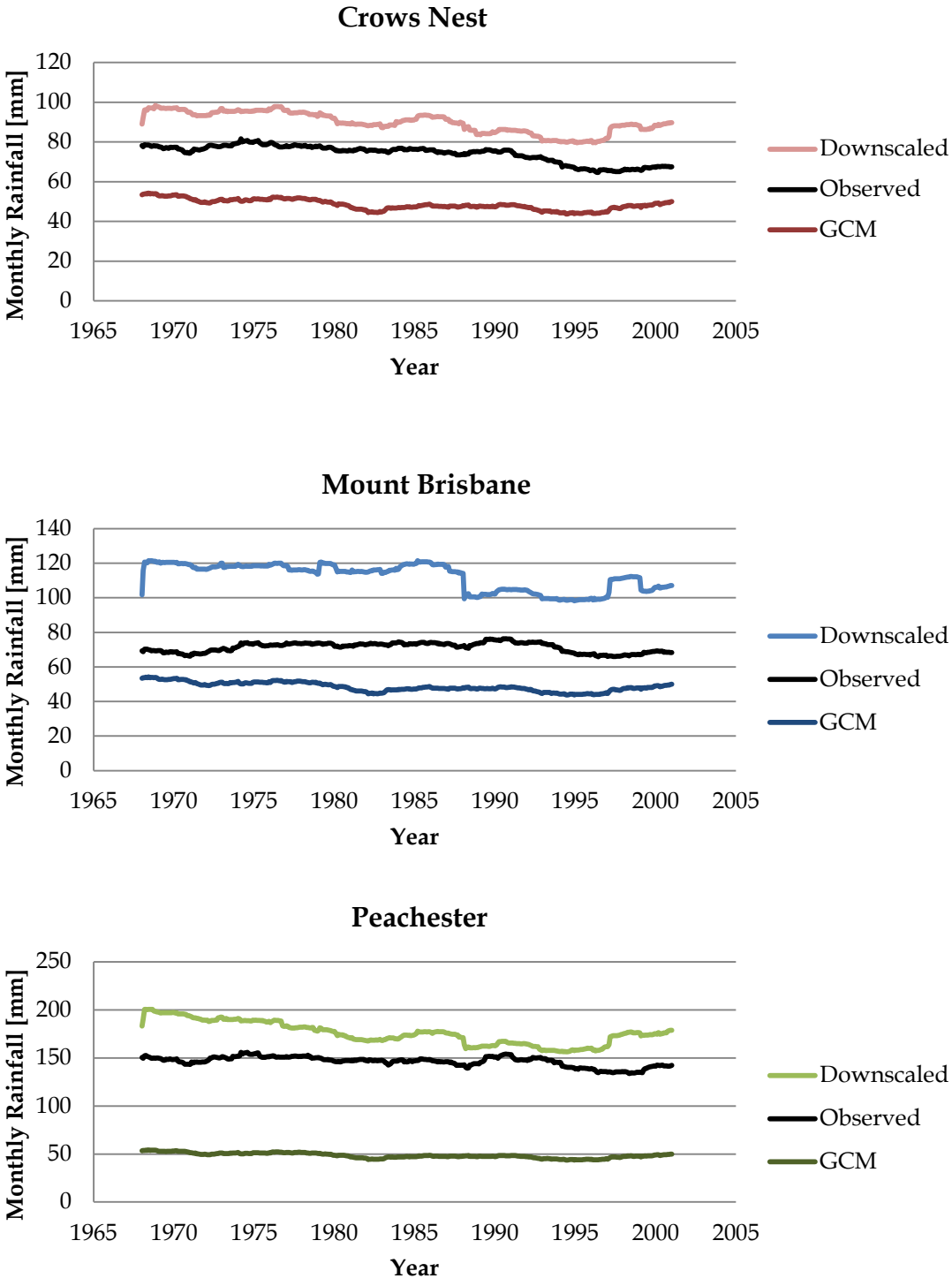

Figure 4.5: A comparison of GCM rainfall simulations at the nearest grid point and data obtained from downscaling GCM output with observed rainfall. The simulations are 20 year running means taken at Crow's Nest, Mount Brisbane and Peachester. The GCM used is the **GFDL – Mk2.1** model from the U.S.A.

The American GFDL – Mk 2.1 GCM in Figure 4.5 tended to underestimate the observed values, whereas the downscaled values were an overestimation. The downscaled values are a slight improvement for Peachester and Crow's Nest, but rainfall for Mount Brisbane is better tracked by the raw GCM data.

Observed rainfall totals for Crow's Nest are between 65 and 80mm/month and this is underestimated by the GCM rainfall data at the nearest grid point 20mm/month which vary from 40 to 55mm/month. The downscaled data overestimated the observed values by approximately the same amount with values ranging from 80 to 100mm/month. There is some improvement with the lower end of the range of the downscaling simulation providing values that match the upper value of the observed totals of 80mm/month.

Mount Brisbane also experienced long term rainfall total between 1970 and 2000 of between 65 and 80mm/month, which again are underestimated by the GCM by around 20mm/month. Though the GCM values are a better match for observed totals when compared to the downscaling models which range from 100 to 120mm/month. The discontinuities are created by high values for specific humidity and this will be discussed in Chapter 5.2.

Peachester rainfall averages from 140 to 150mm/month which is significantly above the GCM values of 40 to 55mm/month. As with the Crow's Nest rainfall values, the lower end of the statistically downscaled

model values matches the upper end of the observed totals. The simulated rainfall totals provided by the models gave values of 150 to 200mm/month.

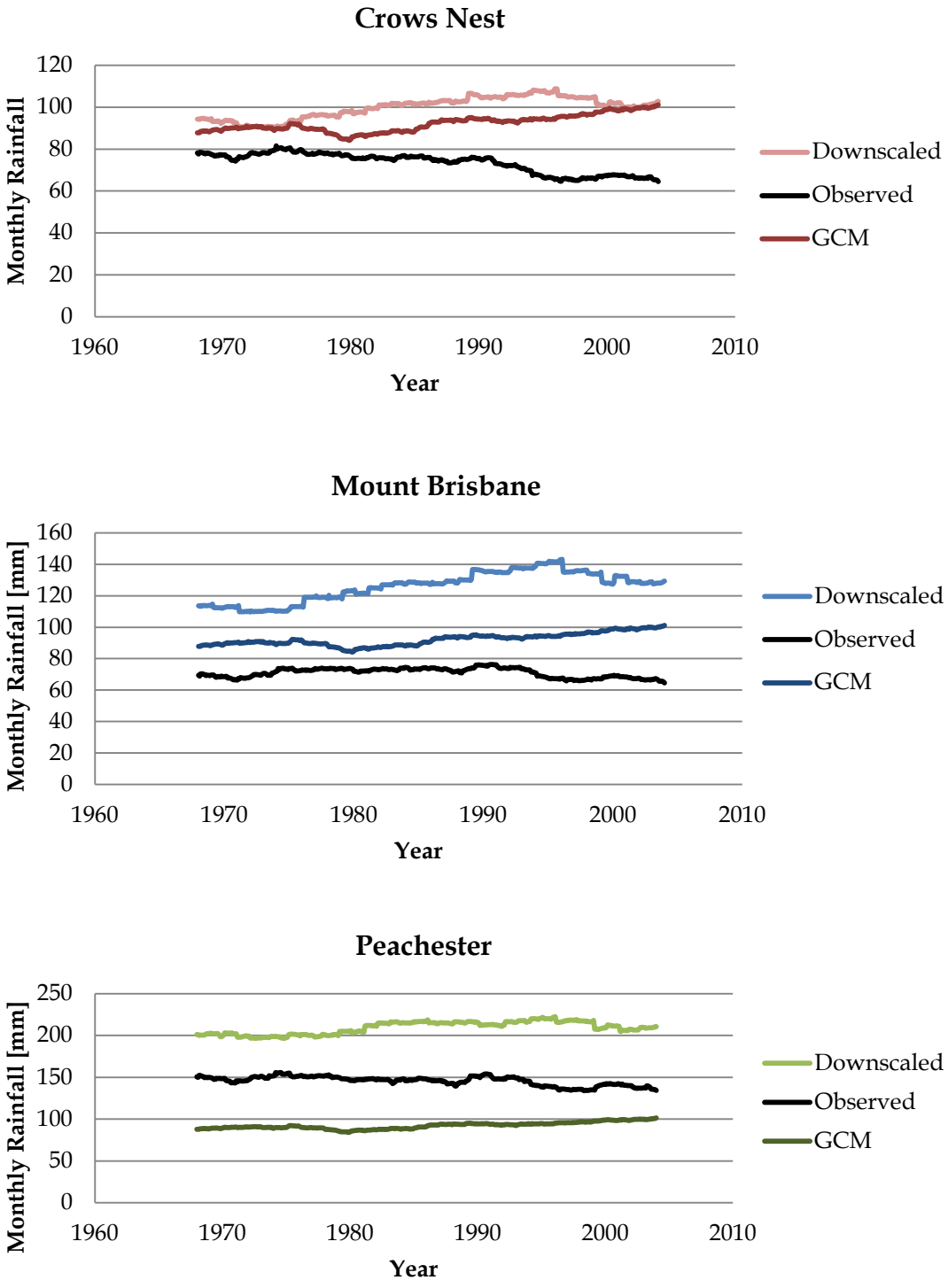

Figure 4.6: A comparison of GCM rainfall simulations at the nearest grid point and data obtained from downscaling GCM output with observed rainfall. The simulations are 20 year running means taken at Crow's Nest, Mount Brisbane and Peachester. The GCM used is the **GISS - ER** model from NASA.

Figure 4.6 shows rainfall values for Crow's Nest and Mount Brisbane were overestimated by both the GISS – ER model and the statistical downscaled models. No improvement is made by the statistical downscaled values over the values obtained by the raw GCM data at the nearest grid point.

Crow's Nest values are approximately the same for both GCM and downscaled simulations, 85 to 100mm/month for the GCM data and 90 to 110mm/month for the downscaled data. The observed long term values for the same period are 65 to 80 mm/month for both stations.

Mount Brisbane downscaled values between 110 and 140 mm/month are a larger overestimation compared to the raw GCM data at the nearest grid point.

Observed Peachester rainfall ranges from 140 to 150mm/month and these values split the two simulations down the middle with the raw data an underestimating by approximately 50mm/month. The downscaling data proved to be an overestimation with rainfall values ranging from 200 to 220mm/month, which again missed the observed totals by approximately 50mm/month.

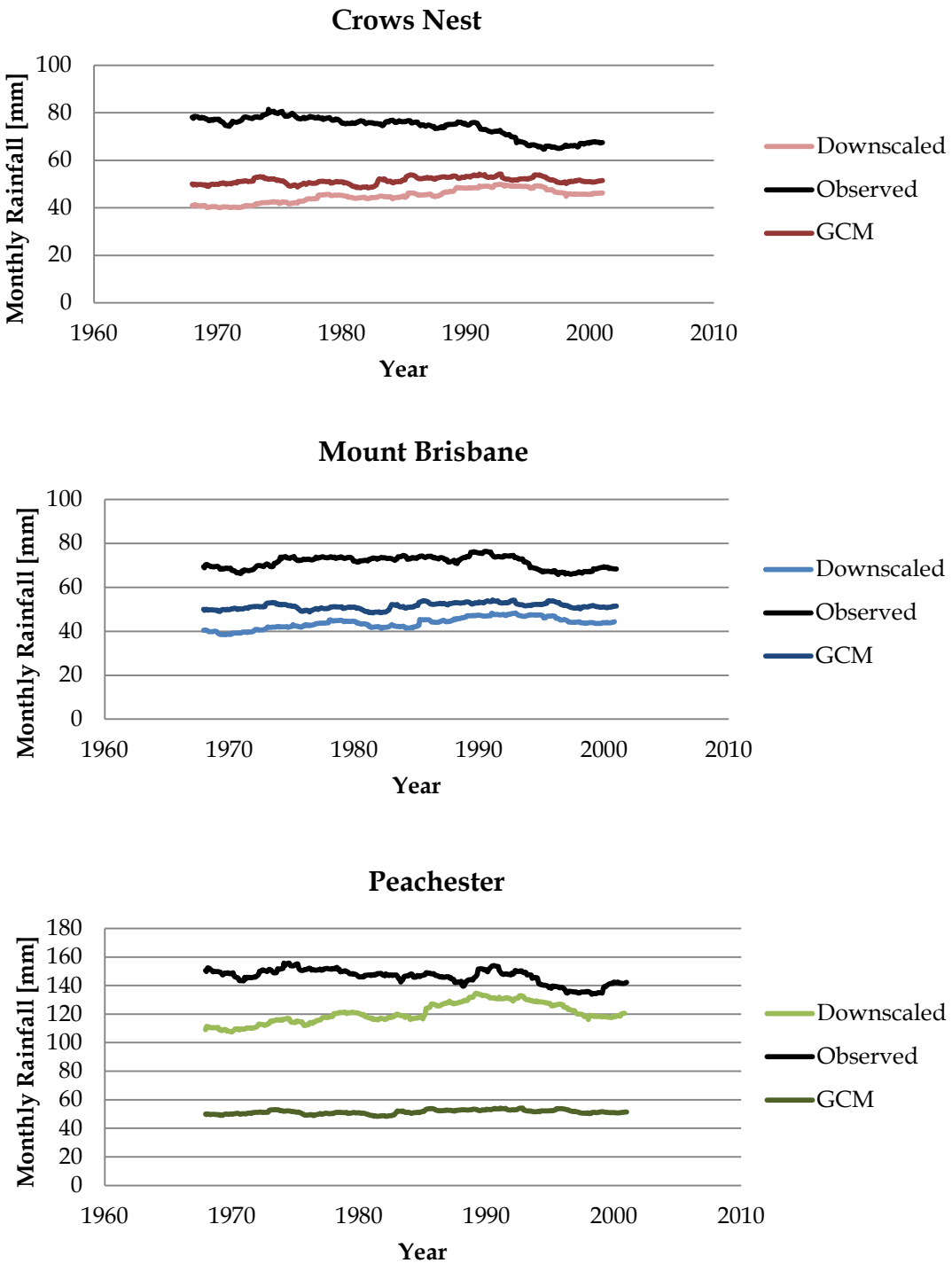

Figure 4.7: A comparison of GCM rainfall simulations at the nearest grid point and data obtained from downscaling GCM output with observed rainfall. The simulations are 20 year running means taken at Crow's Nest, Mount Brisbane and Peachester. The GCM used is the **CCCMA – CGCM t63** model from Canada.

The Canadian model CCCMA – CGCM t63 underestimated all three stations, with some improvement seen with the downscaled Peachester simulation over the raw GCM output (Figure 4.7). The downscaled simulations for the other two stations only increased the underestimation over the GCM output; however these two simulations closely track one another.

Crow's Nest observed rainfall totals between 65 and 80 mm/month are underestimated by the GCM rainfall data at the nearest grid point which give values of approximately 50mm/month. This underestimation is further extended with the values obtained from the statistical downscaling models of between 40 to 50mm/month.

The observed rainfall values at Mount Brisbane of 65 to 80mm/month are again underestimated by the GCM data by between 15 and 30mm/month. As with the Crow's Nest rainfall values, downscaling further exceeds this underestimation by 25 to 30mm/month.

The statistical model improved the rainfall simulation provided by the raw GCM data at Peachester. The model produced rainfall totals of between 110 and 135mm/month which is a significant improvement over the GCM total of approximately 50mm/month when compared to the observed rainfall values of 140 to 150mm/month.

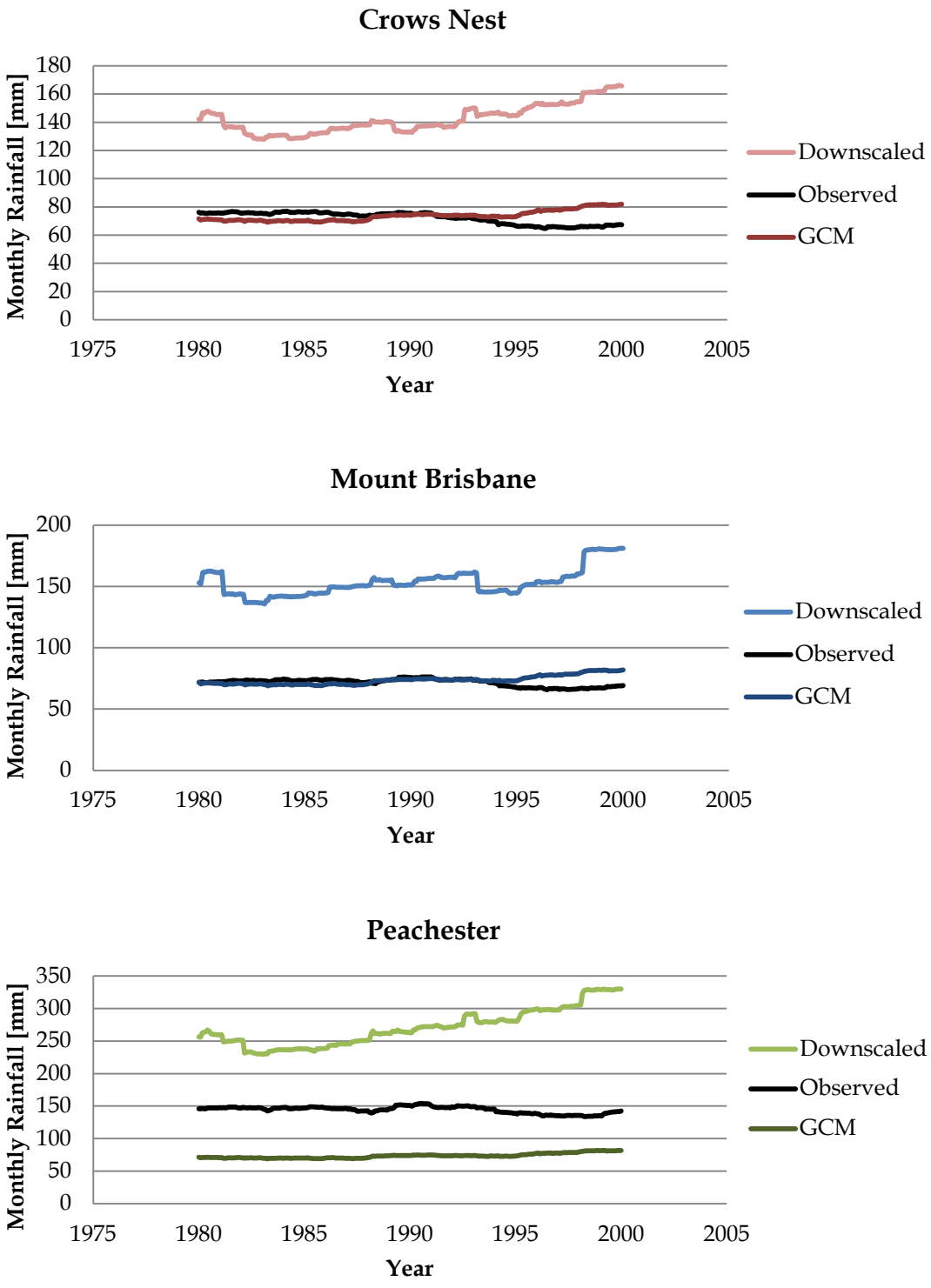

Figure 4.8: A comparison of GCM rainfall simulations at the nearest grid point and data obtained from downscaling GCM output with observed rainfall. The simulations are 20 year running means taken at Crow's Nest, Mount Brisbane and Peachester. The GCM used is the **CNRM – CM3** model from France.

The French model CNRM – CM3 shows a good ability to track observed long term mean rainfall for Crow's Nest and Mount Brisbane, but underestimated Peachester rainfall (Figure 4.8). The statistical downscaled data displays a large overestimation at all three stations and at no stage is a better representation of observed conditions.

Observed long term rainfall totals at Crow's Nest of 65 to 80mm/month are well simulated by the GCM rainfall at the nearest grid point which also ranges from 65 to 80mm/month. The statistical model provided totals of between 125 to 160mm/month which are a significant overestimation by 60 to 80mm/month.

This overestimation is further increased when comparing data from the statistical downscaling models with observed totals for Mount Brisbane of 65 to 80mm/month. The results from the models of 140 to 180mm/month is up to 100mm/month over what was experienced for the region and is far better expressed using the GCM rainfall totals at the nearest grid point, i.e. 65 to 80mm/month.

Despite the fact that the observed rainfall totals for Peachester are generally higher than those provide by the raw GCM data at the nearest grid point, the GCM data more closely matches the observed totals when compared to totals from the downscaling model. Observed totals for Peachester of between 140

and 150mm/month are around 80mm/month higher than the GCM data, but this is a closer match than the downscaling model values of between 230 and 330mm/month.

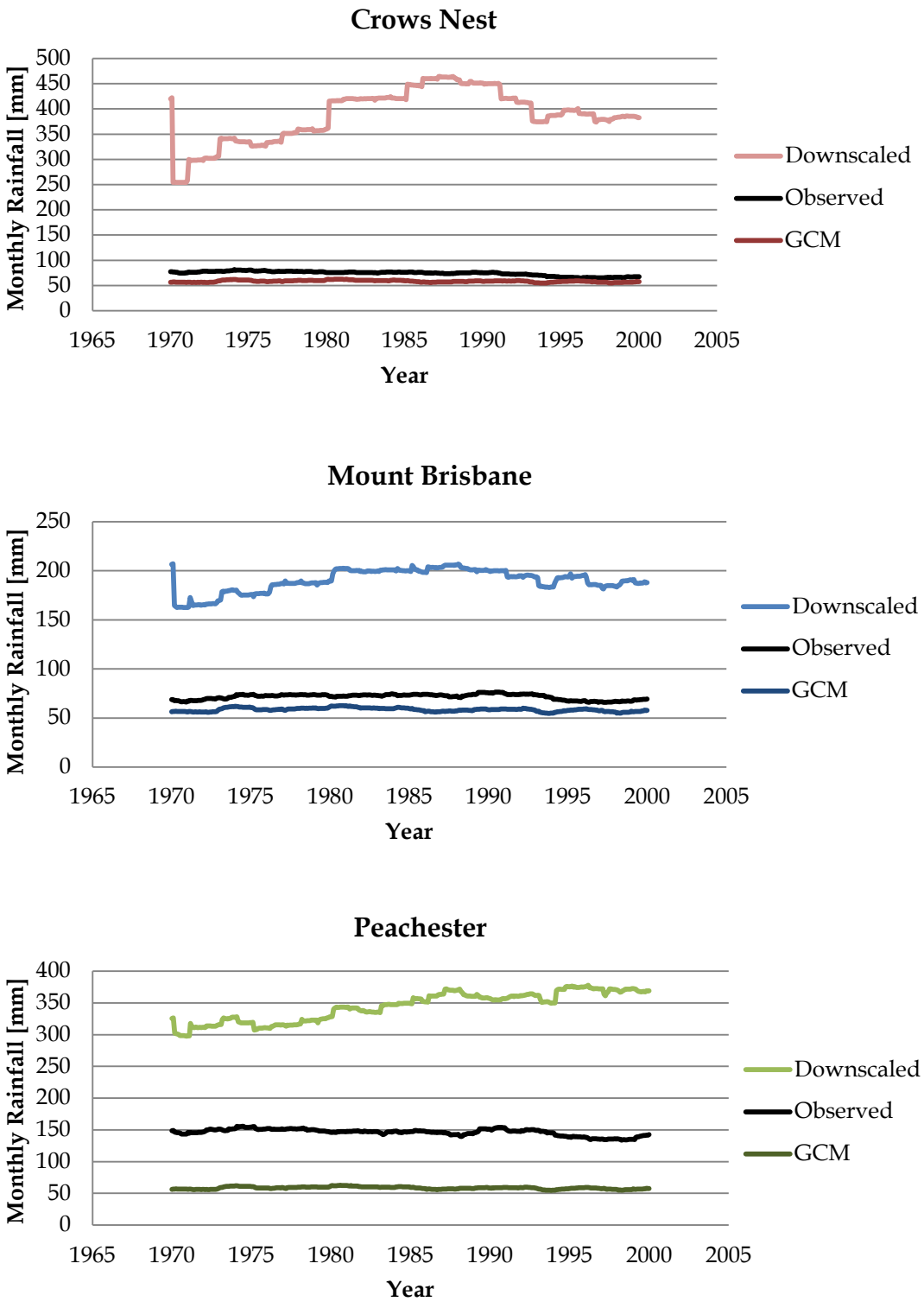

Figure 4.9: A comparison of GCM rainfall simulations at the nearest grid point and data obtained from downscaling GCM output with observed rainfall. The simulations are 20 year running means taken at Crow's Nest, Mount Brisbane and Peachester. The GCM used is the **CSIRO – Mk 3.5** model from Australia.

The CNRM results are somewhat replicated by the CSIRO Mk 3.5 GCM (Figure 4.9). Observed long term rainfall is well simulated by the raw GCM data at the nearest grid point, but the predictor variables provide a strong overestimation when used in the statistical downscaled models.

The observed values for Crow's Nest and Mount Brisbane of between 65 to 80mm/month are slightly underestimated by the GCM totals of 50 to 55mm/month. This is significantly better than the statistical downscaled values of 250 and 450mm/month for Crow's Nest and 160 to 200mm/month for Mount Brisbane.

As in Figure 4.8 the Peachester rainfall total of 140 to 150mm/month is underestimated by the GCM value at the nearest grid point of 50 to 55mm/month, but again this is closer than the values provided by the statistical model which is in the range of 300 to 375mm/month.

In summary the downscaling methods employed in this research only proved to be an improvement over the raw GCM data at the nearest grid point on a handful of occasions, in general they provided an overestimation of observed totals. The best match for the downscaling model was achieved at Peachester using predictor variables provided by the MIROC – medres

GCM. This example not only matched the observed range of values for that region but also tracks the rainfall trend experienced over the period 1970 to 2000. This fact highlights the ability of that particular GCM to recreate values for climate predictor variables over Southeast Queensland and the surrounding region. The climatic predictor variables are shown to be an effective means of simulating rainfall in section 4.2.1 and the following section will investigate how projected changes in these predictor variables (Appendix E) will influence regional rainfall over the coming decades.

4.3 Rainfall Projections

Rainfall projections are the core focus of this thesis and the following section will provide relevant graphics depicting the expected changes in monthly rainfall. As part of the investigation to see if the recent 40 year drying trend over the region will continue over the next decades, projected values for 21st Century predictor variables shown in Appendix E are used as input into the statistical models. The models are designed to apply the appropriate weight to each variable and calculate monthly rainfall for the next 30 years. Some consideration needs to be taken in account for the inability of these statistical models to reproduce legitimate monthly rainfall totals when projected values for predictor variables exceed those experienced in the past. Essentially the models have no precedent to make a rainfall simulation from so exact totals may not hold true, but general trends will be highlighted.

4.3.1 Rainfall Projections (2010 -2040)

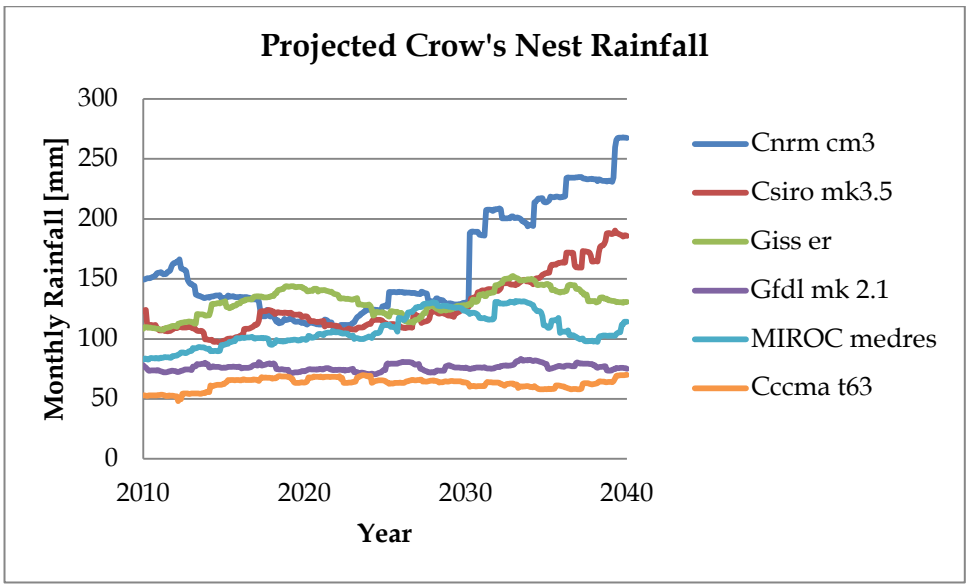

Figure 4.10: Rainfall projections for Crow's Nest using GCM data as input into statistical downscaled models. Monthly rainfall totals [mm] are provided as a 10 year running mean.

Figure 4.10 shows the projections from the downscaled models for Crow's Nest over the period of 2010 to 2040. Little trust can be put into these projections given that none of the downscaled models captured the long term mean for this location (Figures 4.4 to 4.9). However, downscaling the GFDL model did come closest to tracking the observed long term mean, though with an overestimation of just under 20mm/month (Figure 4.5). The projection in Figure 4.10 from downscaling this model suggests the average annual rainfall for the region will remain relatively constant at 75mm/month.

Downscaled values for the remaining models all project an increase in rainfall in the range of 20mm/month for the CCCMA – t63 GCM up to 120mm/month when the climate data is downscaled for the CNRM – cm3 GCM.

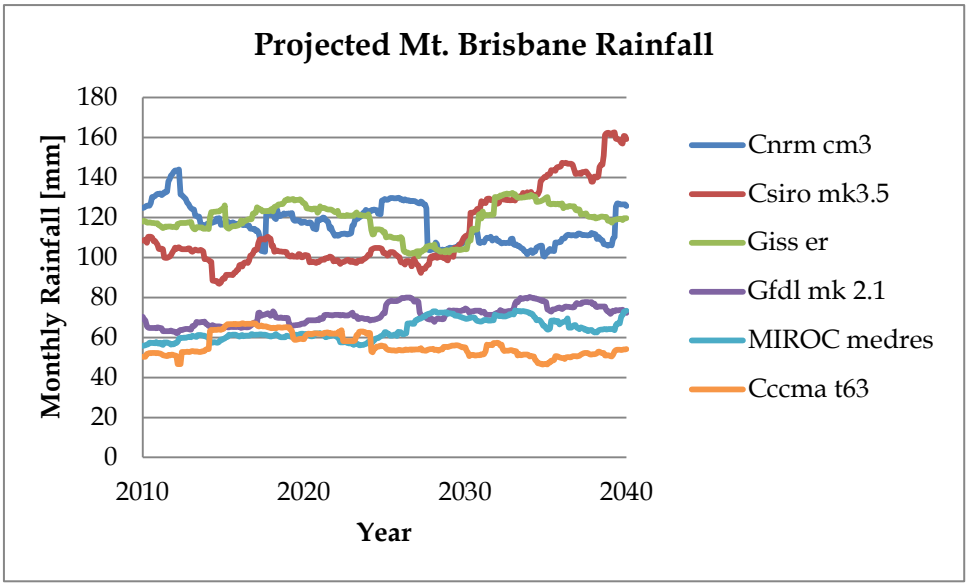

Figure 4.11: Rainfall projections for Mount Brisbane using GCM data as input into statistical downscaled models. Monthly rainfall totals [mm] are provided as a 10 year running mean.

Mount Brisbane long term rainfall was best captured by downscaling the MIROC – medres model (Figure 4.4), and this simulation goes on to suggest a slight increase in average annual rainfall for that location from just under 60mm/month up to 70mm/month (Figure 4.11).

Data from the downscaled CSIRO mk3.5 GCM projects an increase in rainfall for Mount Brisbane over the next 30 years from 110mm/month to 160mm/month. Though referring back to the 20th Century simulation values

provided by this model (Figure 4.9), this result can be considered to be a large overestimation. The remaining models all project little or no resultant change to average monthly rainfall between now and 2040.

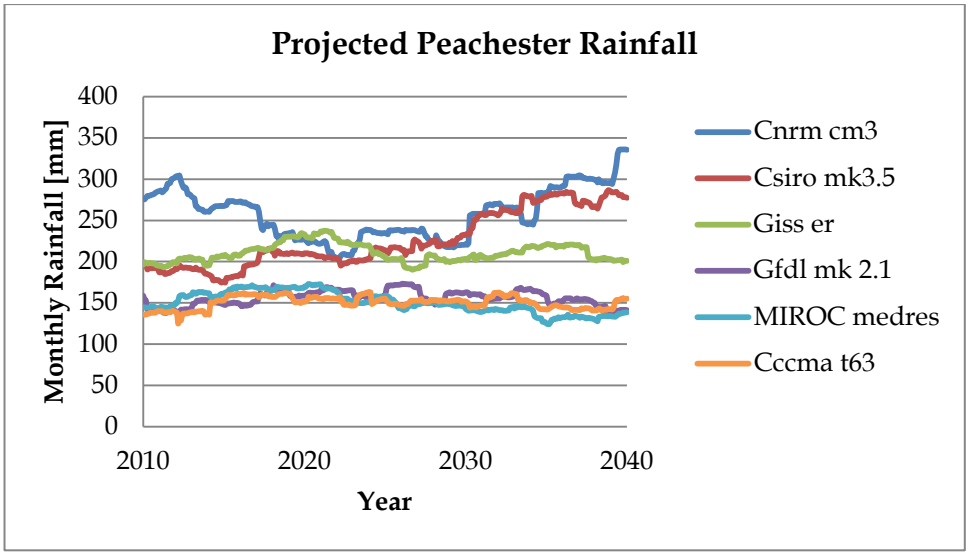

Figure 4.12: Rainfall projections for Peachester using GCM data as input into statistical downscaled models. Monthly rainfall totals [mm] are provided as a 10 year running mean.

Simulated rainfall at Peachester using the downscaling models was over and above the best simulation in the entire study. The MIROC – medres model provided data on predictor variables resulting in a far improved simulation of long term rainfall for the region over the raw GCM rainfall value at the nearest grid point (Figure 4.4).

The downscaled projections using the statistical model and the predictor variables from the MIROC – medres GCM show average annual rainfall for

the region is likely to remain relatively constant at around 150mm/month, if anything, a slight decrease to 145mm/month (Figure 4.12).

This scenario is backed up by the results from downscaling the GFDL model, which also showed improvements on simulating observed long term means for Mount Brisbane (Figure 4.5). This statistical model projects rainfall will remain constant over the next 30 years, again with values of 145 to 150mm/month.

Downscaling the GISS – er and CCCMA – t63 GCM's also produce results that project rainfall at Peachester will remain constant until the year 2040. The data produced from using predictor variables from the CSIRO mk3.5 and CNRM – cm3 in the statistical model for Peachester expect rainfall to increase for that region over the next three decades by 50 to 75mm/month.

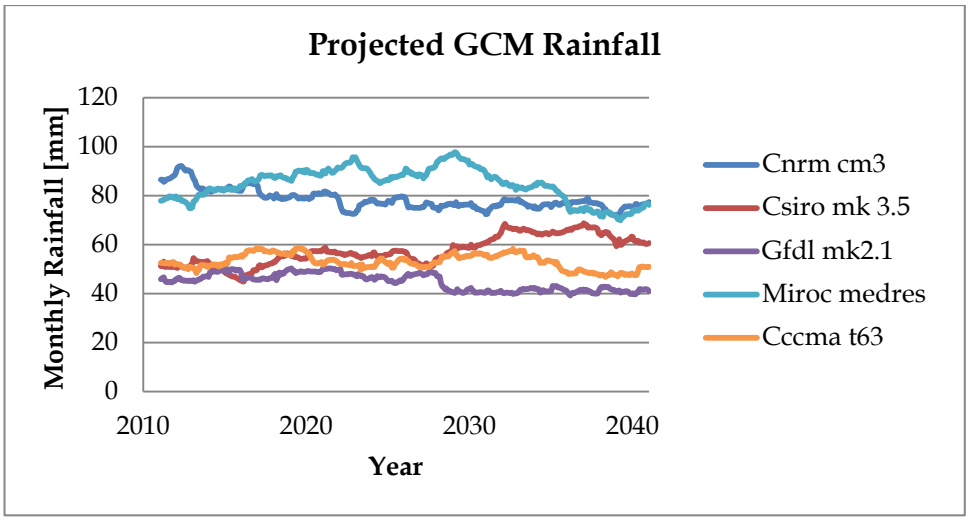

Figure 4.13: Rainfall projections from the GCM's at the nearest grid point. Monthly rainfall totals [mm] are provided as a 10 year running mean. Values for GISS – er are unavailable.

Figure 4.13 shows rainfall projections from the raw data provided by the GCM's at the nearest grid point. This has some bearing on the analysis of future rainfall projections as the simulations for Crow's Nest and Mount Brisbane using the raw data from the three of the GCM's output closely matched the observed long term means for those two stations. This allows some credit to be put into the projections made from these GCM's when it is shown to perform well at simulating 20th Century long term rainfall. Also, these projections can be used to validate or discredit the results obtained from the statistically downscaled models.

Long term Crow's Nest rainfall is well described by the raw output from the nearest grid point by the models CNRM – cm3, CSIRO mk3.5 and to a lesser extent GFDL mk2.1 (Figures 4.8, 4.9 and 4.5). The CNRM – cm3 model

projects a slight decrease of 5mm/month over the coming decades from 85 to 80mm/month. This reduction is also replicated by the GFDL mk2.1 GCM with monthly rainfall totals also reducing by 5mm/month from 45 to 40mm/month over the next 30 years. The CSIRO mk3.5 rainfall projections display a slight increase in average monthly rainfall of 10mm/month from 50 to 60mm/month.

Mount Brisbane long term rainfall was also simulated best by the GFDL and CNRM models (Figures 4.5 and 4.8). As with the Crow's Nest projections average annual rainfall will decrease slightly by about 5mm/month. These back up results obtained from the downscaled models with little or no change in average annual rainfall in the region, and show no indication of a continuation of the significant drying trend seen over the last 40 years.

4.3.2 Long Term Rainfall Projections

It can be argued that regional rainfall projections beyond 30 years enter the realm of uncertainty as the exact nature of how climate change will impact on the Earth's climate system in the long term is still not fully understood. Never the less, this section will provide snapshots of projected average monthly rainfall for the years 2010, 2040, 2070 and 2100. Rather than using all the models investigated in this research only the ones that were found to

perform the best in section 4.2.2 at each location will be employed to create these projected rainfall simulations.

Table 4.3: Projected average monthly rainfall [mm] for Crow's Nest over the Century taken from the three GCM's that were found to most closely match observed long term rainfall averages in section 4.2.2 for the second half of the 20th Century. Averages are taken from the previous 10 years leading up to the snapshot date.

Model	2010	2040	2070	2100
Observed	71.86			
CNRM – cm3 GCM	87.33	74.89	70.78	63.88
MIROC – medres GCM	75.73	73.62	89.24	103.99
CSIRO mk3.5 GCM	52.56	61.65	48.64	44.67

Table 4.3 lists projected monthly rainfall averages for Crow's Nest over the coming century with a snapshot at every 30 years. Each model has a different perception of what will transpire with CNRM – cm3 and CSIRO mk3.5 projecting decreases of 25mm/month and 8mm/month. Even within these two similar outcomes, the pattern of final decrease varies with the CNRM – cm3 GCM projecting a consistent decrease at each 30 year snapshot and the CSIRO mk3.5 first expecting an increase between 2010 and 2040 and then continuing on with decreases. The MIROC – medres GCM reverses the CSIRO mk3.5 scenario with initially a decrease between 2010 and 2040 and then a strong increase over the next 60 years of 30mm/month.

Table 4.4: Projected average monthly rainfall [mm] for Mount Brisbane over the 21st Century. Projection are taken from the two GCM's that were found to most closely match observed long term rainfall averages and one downscaled model in section 4.2.2 for the second half of the 20th Century. Averages are taken from the previous 10 years leading up to the snapshot date.

Model	2010	2040	2070	2100
Observed	69.86			
CNRM – cm3 GCM	87.33	74.89	70.78	63.88
MIROC – medres GCM	75.73	73.62	89.24	103.99
MIROC – medres Downscaled	55.77	73.35	90.14	150.79

Average monthly rainfall snapshots for the coming century at Mount Brisbane for the two selected GCM's are again inconsistent by the same amounts as with the Crow's Nest outlook. The projections from the downscaled data derived from the MIROC – medres GCM shows a very strong increase at each 30 year interval of 20, 20 and finally 60mm/month. The increases appear too large to be believed and are probably due to the inability of the statistical downscaling methods employed to incorporate climate predictor values outside of those included in the original regression analysis. The impact of other external climate forces not included in the statistical models but which affect rainfall totals also contribute to the results being larger than may occur in the real world.

Table 4.5: Projected average monthly rainfall [mm] for Peachester over the Century taken from the two downscaled models were found to most closely match observed long term rainfall averages in section 4.2.2 for the second half of the 20th Century. Averages are taken from the previous 10 years leading up to the snapshot date.

Model	2010	2040	2070	2100
Observed	142.84			
MIROC – medres Downscaled	144.71	138.42	181.22	251.17
GFDL mk2.1 Downscaled	158.63	141.20	144.43	129.87

Table 4.5 uses only downscaled models to make the rainfall projections from data obtained from the MIROC – medres and GFDL mk2.1 GCM's. Downscaling the MIROC – medres data for the 20th Century provided excellent results at simulating observed average monthly rainfall values. This model projects a decrease in monthly rainfall of around 6mm/month between 2010 and 2040, but then continues on to foresee very strong increase in rainfall for the second half of the 21st Century of 50mm/month between 2040 and 2070 finishing with a 70mm/month increase by the year 2100. As with downscaled MIROC – medres results for Mount Brisbane in the previous table, the results beyond the year 2040 seem to become erroneous.

The GFDL mk2.1 downscaled data shows first a decrease of 18mm/month by 2040, then an increase of 3mm/month at 2070 and a subsequent decrease at the year 2100 of 15mm/month. Despite the fact that the results from downscaling the GFDL mk2.1 GCM data are within the realm of possibility, the inconsistency across all models at the three different locations makes long

term rainfall projections difficult to rely on, especially for the projections made by the downscaling methods used in this research.

Chapter 5: Discussion and Conclusion

5.1 Introduction

The above results will be discussed in terms of current literature and in how they answered the original questions posed. Limitations on the work will be mentioned and what areas of further research are important in providing precipitation projections to best manage future water resources for Southeast Queensland.

5.2 Discussion

Section 4.2.1 validated the statistical downscaling models using the climate predictors from the NCEP climate data archive to replicate monthly rainfall totals from the second half of the 20th Century. The results tracked monthly variation in rainfall with a relatively high coefficient of determination (Figures 4.1, 4.2 and 4.3) when compared to results obtained directly from the GCM output (Appendix D). This is to be expected as the same NCEP data is used to calibrate the models. It shows that regional rainfall in the sub-tropics can be simulated through a regression between the rainfall and predictors on a monthly basis. The months where strong rainfall totals are missed by the statistical model simulations may be due to short but intense rainfall events. The associated changes in climate predictors during these events may be

hidden in the overall average value for the month, thus making the rainfall event undetectable to the downscaling models.

Comparing R^2 values in section 4.2.1 with values provided in Table 4.1 between monthly rainfall and GCM rainfall simulations shows a vast improvement in R^2 values using the statistical downscaled models in the order of 10. This also shows that recreating actual rainfall totals on a month to month basis in real time is above the capabilities of the GCM's. However, the GCM's are able to produce values for monthly rainfall with similar means and standard deviations to those observed in the real world (Table 4.2). This ability to reproduce the observed distribution of climate variables is utilised in the downscaling models by creating simulations of long term means.

The comparison of average monthly rainfall simulations for the second half of the 20th Century between the GCM's and the downscaled models in section 4.2.3 has mixed results. GCM's that did provide data for the statistical models resulting in a close match between observed and simulated monthly rainfall averages also performed well on their own without the aid of statistical downscaling. The only exception to this is the Peachester site which has consistently higher rainfall totals than those provided by all the GCM's tested at the nearest grid point. The surrounding topography and

proximity to the coastline provide that particular region with a higher than average rainfall than the rest of the catchments. As an example, the nearby location of Crohamhurst recorded Australia's highest 9am to 9am rainfall total, though this occurred in 1893 and as such, the exact total was not subject to quality control. Though high totals are not a one off for the locality which is geographically well placed and designed to enhance rainfall.

The rainfall projections of only six models in section 4.3.1 may not be enough to obtain a confident idea of future rainfall trends. This can be overcome by focusing on the models better able to simulate 20th Century observations in section 4.2.2, as more faith can be put in their projections. This seems to hold, with those models projecting small changes in average monthly rainfall, rather than extreme increases that are found using less reliable models. None of the simulations, good or bad, foresee a continuation of strong decreases in regional rainfall.

At no stage do the long term rainfall projections for projections for the next 90 years agree with one another, and this makes it difficult to know what can be expected in the long term. One can assume that extremely large increases in monthly rainfall are unreasonable. Looking at small changes, some up, some down and some stay the same. As mentioned in section 4.3.2, the long

term effects of climate change on regional rainfall is not fully understood, and this is reflected in regional precipitation projections over the long term.

Downscaling climate predictors from the CNRM – cm3 and CSIRO Mk 3.5 GCM's produced large variations and discontinuities between the simulated rainfall averages and observations. This is brought about by an over sensitivity in the statistical models to the values of specific humidity. The value of this variable from the GCM's has been transformed to fit the distribution of the same NCEP variable. The range in the specific humidity standardised values provided by the CNRM – cm3 and CSIRO Mk3.5 GCM's are both 0.00127 (0.00052 to 0.00179 and 0.00077 to 0.00212). Compare this with the range in specific humidity values from the MIROC – medres GCM of 0.00083 (0.00032 to 0.00115). The larger range in the first two GCM's creates a linear transformation equation that is sensitive to projected values outside of those used in the formation of the original statistical models. i.e. values for specific humidity do not need to change much for a large change in expected rainfall. This issue may have been overcome by using dewpoint depression which is more stable than specific humidity.

5.3 Conclusion

On average, projected annual precipitation changes have been quantified for Southeast Queensland by CSIRO BoM (2007), giving a value of a 3% to 5% decrease by the year 2050. This total matches values found in the best simulation from this study; Peachester rainfall provided by the MIROC - medres GCM output provides a decrease in monthly rainfall of around 4% by 2040.

Therefore monthly regression analysis of rainfall with climatic predictors can be used with some success in the sub-tropics provided values for the predictor variables obtained from GCM output is an accurate simulation of real world observations. This occurred with the Japanese MIROC – medres model which incorporates 10 additional climate forcing variables above atmosphere, ocean, sea ice and land use in its calculations which is at the upper end of GCM complexity (Table 3.1).

Using the MIROC – medres model to provide climate predictor data to simulate rainfall at Peachester proved an effective means of replicating long term rainfall averages. This example not only tracked long term rainfall closely but also was a clear improvement over the rainfall data obtained from the raw GCM output at the nearest grid point.

It can be argued that the long term rainfall mean at Peachester was simulated by the raw GCM data but with an underestimating bias, and this could be remedied by adjusting the data up to meet the observed long term average. However, this does not detract from the fact that the statistical models created using monthly regressions of rainfall and predictors are able to provide a simulation of rainfall averages for that location.

It can also be argued that the strong Peachester result was due to luck, as the rest of the statistical models gave both higher and lower rainfall total than those observed. However, the close match between observed average rainfall at Peachester and those provide by downscaling the MIROC – medres data continued on to 2010. This is shown in Table 4.5 with a 2mm/month variation between the two values.

5.3.1 How does the data answer the original research question?

The original question and motivation for this research was whether recent decreases in rainfall over southeast Queensland would continue into the future. Rainfall projections using the models that provided realistic simulations suggest little change in average annual rainfall for the region. This is in agreeance with the better performing GCM output of the ones

selected in this analysis and the 50th percentile of climate model projections from the IPCC assessment reports.

The significant dry period from 2001 to 2008 was of concern as water resources dipped to very low levels and it seemed to follow a significant drying trend that had been occurring over the last 40 years. This drying trend has recently started to balance out over the period 2008 to 2012 culminating in two consecutive wet summer periods of 2011 and 2012. The 2011 summer was marked by an extreme rainfall event causing loss of life, inundation of thousands of properties and many millions of dollars damage to local infrastructure.

Projections of little change in overall annual rainfall for the region may in fact be accurate given what has been experienced over the last decade. Despite long term annual averages not undergoing any significant changes, fewer wet days (CSIRO - BoM, 2007) means the manner in which the rainfall is delivered is becoming increasingly important.

5.4 Implications for policy or practice

Water resource managers can take some solace in that the recent strong drying trend over the last 40 years may be part of a natural cycle, but

managing dam levels through extended periods of drought, and when to release water during extreme rainfall events will rely on accurate estimations of the duration of dry periods and seasonal rainfall totals.

5.4.1 How does the data contribute to the field of study?

Simulating long term monthly rainfall totals in the Peachester region are improved by the implementing statistical downscaling techniques on data provide by the MIROC – medres and GFDL Mk 2.1 GCM's.

The poorly investigated drying trend experienced over Eastern Australia and Southeast Queensland may indeed be part of a multi-decadal natural variation in the climate. Current rainfall projections for the region say annual rainfall may only experience a slight decrease, projections which are backed up by the regression analysis of climate predictors undertaken in this thesis.

5.5 Limitations

The fact that only one month of the year had air pressure included in its statistical model (Appendix B) is of concern as this variable may become more influential in the future with a pole ward expansion Hadley cell and increased air pressure over sub-tropical regions (Meehl et al., 2007).

Average annual rainfall in the future will not change significantly but will be delivered on fewer days, meaning longer periods without rain and when it is received it will be in heavier falls (Christensen et al., 2007). This analysis is limited by its inability to detect extreme events such as long dry periods and heavy rainfall events. There is where using the weather generator statistical model may be more beneficial, as it has the ability to detect extreme events.

Also, the ability of regression analysis is limited under future climate change scenarios as atmospheric chemistry and physics may be altered the regression analysis is based on historical connections between predictors and rainfall.

5.6 Further research

Rather than choosing GCM's with the best ability at simulating rainfall, this research could be improved by determining which GCM is best able to simulate each climatic predictor for each month. By selecting GCM's with a superior ability at recreating NCEP values for predictor variables the accuracy of the input data into the statistical models would then improve and subsequently improve the simulations.

Further improvements in the simulations could also be made by taking into account the effect large scale climate drivers have on rainfall influences. The relative importance and impact of the climatic predictors on regional rainfall are altered depending on the state of the atmosphere. To allow for this, the ability of the models to track rainfall could be refined by calibrating the models with different regression analyses under various El Niña/La Niña and IPO scenarios. The impact these global scale climate variations have on influencing high intensity events in southeast Queensland would also improve the ability of this research to more accurately detect a larger proportion of the regions rainfall.

The standard outputs from the CMIP3 data has difficulty in finding any effects GHG's will have on rainfall over the coming decades and CMIP5 data may be better used, but was not available at the time of writing the thesis.

Despite being beyond the scope of this thesis, the use of Dynamical downscaling which would provide more meaningful projected rainfall totals for the entire region than the results derived from this thesis. By accounting for actual physical atmospheric processes, Dynamical downscaling does not rely on what has happened previously to describe what will happen in the future, and this may become more relevant with climate change producing weather events that are beyond what has been experienced.

Also beyond the scope of this thesis is determining the return periods of extreme rainfall events would be important information in managing the region's water resources. Also, the duration and likelihood of drought situations in the future will be helpful in setting realistic and sustainable water usage targets for the region.

References

Alexander, LV, Zhang, X, Peterson, TC, Caesar, J, Gleason, B, Klein Tank, AMG, Haylock, M, Collins, D, Trewin, B, Rahim, F, Tagipour, A, Kumar Kolli, R, Revadekar, JV, Griffiths, G, Vincent, L, Stephenson, DB, Burn, J, Aguilar, E, Brunet, M, Taylor, M, New, M, Zhai, P, Rusticucci, M & Luis Vazquez Aguirre, J 2006, Global observed changes in daily climate extremes of temperature and precipitation, *Journal of Geophysical Research – Atmospheres,* vol. 111.

Alexander, LV, Hope, P, Collins, D, Trewin, B, Lynch, A & Nicholls, N 2007, Trends in Australia's climate means and extremes: a global context, *Australian Meteorological Magazine*, vol. 56, pp. 1-18.

Allan, R, Lindesay, J & Parker, D 1996, *El niño Southern Oscillation and Climate Variability*. CSIRO Publishing, Melbourne, Australia.

Ashok, K, Tam, C & Lee, W 2009, ENSO Modoki impact on the Southern Hemisphere storm track activity during extended austral winter, *Geophysical Research Letters*, vol. 36.

Ashok, K and Yamagata, T 2009, The El Niño with a difference, *Nature*, vol. 461, no.7263, pp. 481-484.

Australian Bureau of Statistics, 2006, 'Population Projections, Australia 2004 to 2101', *ABS Statsite.* Viewed 20 July 2011, <http://www.abs.gov.au/AUSSTATS/abs@.nsf/Lookup/3222.0Main+Features12004%20to%202101?OpenDocument>

Australian Bureau of Statistics, 2010, 'Regional Population Growth, Australia, 2009-10', *ABS Statsite.* Viewed 20 July 2011,

<http://www.abs.gov.au/ausstats/abs@.nsf/Products/3218.0~2009-10~Main+Features~Queensland?OpenDocument>

ACIL Tasman 2006, *The impact of restricted water supply on South East Queensland: A short report on some of the social and economic impacts likely to arise if South East Queensland's current water situation is not addressed*. A report prepared for the Department of Natural Resources, Mines and Water.

Basist, A, Bell, GD & Meentemeyer, V 1994, Statistical Relationships between Topography and Precipitation Patterns, *Journal of Climate,* vol. 7, pp. 1305-1315.

BoM, 2011, Australian Bureau of Meteorology. <www.bom.gov.au> (last accessed 2/8/11)

BoM-QCCCE 2011, *Climate Change in Queensland – What the Science is Telling Us*. Queensland Climate Change Centre of Excellence. Department of Environment and Resource Management.

Cai, W, Cowen T & Sullivan, A 2009, Recent unprecedented skewness towards positive Indian Ocean Dipole occurrences and its impact on Australian rainfall, *Geophysical Research Letters,* vol. 36.

Charles, SP, Bates, BC, Smith, IN & Hughes, JP 2004, Statistical downscaling of daily precipitation from observed and modelled atmospheric fields, *Hydrological Processes* vol. 18 pp. 1373–1394.

Chiew, F and McMahon, T 2002, Modelling the impacts of climate change on Australian streamflow, *Hydrological Processes* vol.16 pp. 1235-1245.

Chiew, FHS and McMahon TA 2003, Australian rainfall and streamflow and El Niño/Southern Oscillation, *Australian Journal of Water Resources* vol. 6, no. 2, pp.115-129.

Chiew, FHS and Leahy, MJ 2003, *Inter-decadal Pacific Oscillation Modulation of the Impact of El Niño/Southern Oscillation on Australian Rainfall and Streamflow.* Cooperative Research Centre for Catchment Hydrology, Australia. Department of Civil and Environmental Engineering, University of Melbourne, Australia.

Christensen, J.H., B. Hewitson, A. Busuioc, A. Chen, X. Gao, I. Held, R. Jones, R.K. Kolli, W.-T. Kwon, R. Laprise, V. Magaña Rueda, L. Mearns, C.G. Menéndez, J. Räisänen, A. Rinke, A. Sarr and P. Whetton, 2007: Regional Climate Projections. In: *Climate Change 2007: The Physical Science Basis. Contribution of Working Group I to the Fourth Assessment Report of the Intergovernmental Panel on Climate Change* [Solomon, S., D. Qin, M. Manning, Z. Chen, M. Marquis, K.B. Averyt, M. Tignor and H.L. Miller (eds.)]. Cambridge University Press, Cambridge, United Kingdom and New York, NY, USA.

Coombes, P and Barry, M 2007, *Efficiency of Roof and Traditional Water Supply Catchments Subject to Climate Change*. 13th International Rainwater Catchment Systems Conference. 5th International Water Sensitive Urban Design Conference. Sydney, Australia.

CSIRO-BoM 2007, *Climate Change in Australia – Technical Report.* Commonwealth Scientific and Industrial Research Organisation, Bureau of Meteorology.

Diaz-Nieto, J and Wilby, RL 2005, A Comparison of Statistical Downscaling and Climate Change Factor Methods: Impacts on Lowflows in the River Thames, United Kingdom, *Climatic Change* vol.69 pp. 245-268.

DNRW 2007, *The Southeast Queensland Drought to 2007*. Department of Natural Resources and Water. Queensland State Government.

Donald, A, Meinke, H, Power, B, Maia, AHN, Wheeler, MC., White, N, Stone, RC & Ribbe, J 2006, Near-global impact of the Madden-Julian Oscillation on rainfall, *Geophysical Research Letters*, vol. 33.

Dowdy A, Mills G, & Timbal B 2011, *Large-scale indicators of Australian East Coast Lows and associated impacts.* CAWCR Technical report 37

Drosdowsky, W 2005, The latitude of the subtropical ridge over eastern Australia: The L index revisited, *International Journal of Climatology,* vol. 25, pp. 1291-1299.

E-Atlas Kalnay et al. 1996, The NCEP/NCAR 40-year reanalysis project, Bulletin of American Meteorological Society, vol. 77, pp. 437-470. *NCEP Reanalysis Derived data provided by the NOAA/OAR/ESRL PSD, Boulder, Colorado, USA, from their Web site at http://www.esrl.noaa.gov/psd/*

Fowler, HJ, Blenkinsopa, S, & Tebaldib, C 2007, Linking climate change modelling to impacts studies: recent advances in downscaling techniques for hydrological modelling, *International Journal of Climatology,* vol. 27, pp. 1547–1578.

Garnaut, R 2008, *The Garnaut Climate Change Review – Final Review*. Cambridge University Press. U.K.

Garnaut, Ross. 2011. *The Garnaut Climate Change Review – Update 2011 website*. <http://www.garnautreview.org.au/update-2011/update-papers.html> (accessed Dec 2011)

Gillet, NP, Kell, TD & Jones, PD 2006, Regional climate impacts of the Southern Annular Mode, *Geophysical Research Letters,* vol.33.

Gibson, T 1992, An Observed Poleward Shift of the Southern Hemisphere Subtropical wind Maximum – A Greenhouse Symptom? *International Journal of Climatology,* vol. 12, pp. 637-640.

Google Earth. 2011. < http://www.google.com/earth/index.html>

Held, I and Soden, B 2006, Robust Responses of the Hydrological Cycle to Global Warming, *Journal of Climate,* vol. 19, pp. 5686-5699.

Hendon, HH., Thompson, DWJ & Wheeler, MC 2007, Australian Rainfall and Surface Temperature Variations Associated with the Southern Hemisphere Annular Mode, *Journal of Climate,* vol. 20, pp. 2452-2467.

Hessami, M., Gachon, P, Ouarda, T & St-Hilaire, A 2008, Automated regression-based Statistical Downscaling Tool, *Environmental Modelling and Software,* vol. 23, pp. 813-834.

Hope, PK, Drosdowsky, W & Nicholls, N 2006, Shifts in the synoptic systems influencing southwest Western Australia, *Climate Dynamics* vol. 26, pp. 751-764.

Hope, PK, Timbal, B & Fawcett, R 2009, Associations between rainfall variability in the southwest and southeast of Australia and their evolution through time, *International Journal of Climatology,* vol. 30, no. 9, pp. 1360-1371.

Hopkins, LC and Holland, GJ 1997, Australian heavy-rain days and associated east coast cyclones: 1958-92, *Journal of Climate,* vol. 10, pp. 621-635.

Hunt, BG 2009, Multi-annual dry episodes in Australian climatic variability, *International Journal of Climatology,* vol. 29, pp. 1715–1730.

IPCC 2007, 'AR4 SYR Synthesis Report Summary for Policymakers', *IPCC Website.*<www.ipcc.ch/publications_and_data/ar4/syr/en/spm.html>, Intergovernmental Panel on Climate Change. (accessed 12 February 2009)

Kaspura, A 2007, *Water and Australian Cities*. Review of Urban Water Reform. Institution of Engineers Australia.

Kyriakidis, P, Kim, J & Miller, N 2001, Geostatistical Mapping of Precipitation from Rain Gauge Data Using Atmospheric and Terrain Characteristics, *Journal of Applied Meteorology,* vol. 40, no. 11, pp. 1855-1877.

Langford, S, Hendon, HH, & Lim, E-P 2011, *Assessment of POAMA's predictions of some climate indices for use as predictors of Australian rainfall.* CAWCR Technical Report **31**

Leung, RL, Qian, Y, Bian, X, Washington, WM, Han, J & Roads, JO 2004, Mid-Century Ensemble Regional Climate Change Scenarios for the Western United States, *Climatic Change,* vol.62, pp. 75-113.

Li, Y and Smith, I 2009, A Statistical Downscaling Model for Southern Australia Winter Rainfall, *Journal of Climate,* vol. 22, no. 5, pp. 1142-1158.

McAlister, T, Coombes, P. & Barry, M 2004, *Recent South East Queensland Developments in Intergrated Water Cycle Management – Going Beyond WSUD*

Meehl, G.A., T.F. Stocker, W.D. Collins, P. Friedlingstein, A.T. Gaye, J.M. Gregory, A. Kitoh, R. Knutti, J.M. Murphy, A. Noda, S.C.B. Raper, I.G. Watterson, A.J. Weaver and Z.-C. Zhao, 2007: Global Climate Projections. In: *Climate Change 2007: The Physical Science Basis. Contribution of Working Group I to the Fourth Assessment Report of the Intergovernmental Panel on Climate Change* [Solomon, S., D. Qin, M. Manning, Z. Chen, M. Marquis, K.B. Averyt, M.

Tignor and H.L. Miller (eds.)]. Cambridge University Press, Cambridge, United Kingdom and New York, NY, USA.

Meinke, H, DeVoil, P, Hammer, GL, Power, S, Allan, R, Stone, RC, Folland, C & Potgieter, A 2005, Rainfall variability at decadal and longer time scales: signal or noise? *Journal of Climate,* vol. 18, pp. 89-96.

Meneghini, B, Simmonds, I & Smith, I 2007, Association between Australian rainfall and the southern annular mode, *International Journal of Climatology,* vol. 27, no. 1, pp. 109–121.

Micevski, T, Franks, SW & Kuczera, G 2006, Multidecadal variability in coastal eastern Australian flood data, *Journal of Hydrology,* vol. 327, pp. 219–225.

Milly, P, Betancourt, J, Falkenmark. M, Hirsch, R, Kundzewicz, Z, Lettenmaier, D & Stouffer R 2008, Stationarity is Dead: Whither Water Management, *Science,* vol. 319, pp. 573-574.

Murphy, J 1999, An Evaluation of Statistical and Dynamical Techniques for Downscaling Local Climate, *Journal of Climate,* vol. 12, no. 8, pp. 2256-2284.

Murphy, AH and Epstein, ES 1989, Skill scores and correlation coefficients in model verification, *Monthly Weather Review,* vol. 117, pp. 572-581.

Murphy, BF & Timbal, B 2008, A review of recent climate variability and climate change in southeastern Australia, *International Journal of Climatology,* vol. 28, no. 7, pp. 859–80.

Nicholls, N 2004, The changing nature of Australian droughts, *Climatic Change,* vol 63, pp. 323–336.

Nicholls, N 2006, Detecting and attributing Australian climate change: a Review, *Australian Meteorological Magazine,* vol. 55, pp. 199-211.

Pacific Southwest Strategy Group. 2007. Northeast Business Park. Marina Demand Update.

Pittock, A.B 2009, *Climate Change. The Science, Impacts and Solutions,* 2nd ed, CSIRO Publishing, Melbourne, Australia.

Power S, Tseitkin F, Mehta V, Lavery B, Torok S & Holbrook N 1999a, Decadal climate variability in Australia during the twentieth century, *International Journal of Climatology,* vol. 19, pp. 169–184.

Power S, Casey T, Folland, C, Colman, A & Mehta, V 1999b, Interdecadal modulation of the impact of ENSO on Australia, *Climate Dynamics,* vol. 15, pp. 319–324.

Preston, B and Jones R 2006, *Climate Change Impacts on Australia and the Benefits of Early Action to Reduce Global Greenhouse Gas Emissions*. A consultancy report for the Australia Business Roundtable on Climate Change.

Qian B, Hayhoe H & Gameda S 2005, Evaluation of the stochastic weather generators LARS-WG and AAFC-WG for climate change impact studies, *Climate Research,* vol. 29, pp. 3–21.

Queensland Farmers Federation. 2008. *Communicating Climate Change – Fact Sheet.* An Initiative of the National Agriculture and Climate Change Action Plan.

R version 2.11.1 (2010-05-31) Copyright (C) 2010 The R Foundation for Statistical Computing

Raupach, M and Fraser, P 2011, 'Climate and Greenhouse Gases' in Cleugh, H, Smith, MS, Battaglia, M & Graham, P ed, *Climate Change: Science and Solutions for Australia,* pp. 15-34. CSIRO Publishing. Melbourne, Australia.

Riseby, JS, Pook, MJ, McIntosh, PC, Wheeler, MC & Hendon, HH 2009, On the Remote Drivers of Rainfall Variablility in Australia, *Monthly Weather Review,* vol. 137, pp. 3233-3253.

Ropelewski, CF and Halpert, MS 1987, Global and Regional Scale Precipitation Patterns Associated with the El Niño/Southern Oscillation *Monthly Weather Review,* vol. 115, pp. 1606-1626.

SEQWater, 2011, 'Latest Dam Levels', *SEQWater Website.* <www.seqwater.com.au> Southeast Queensland Water. (last accessed 4 March 2011)

South East Queensland Healthy Waterways. 2008. 'Fact Sheet: Catchments of South East Queensland' *Healthy Waterways Website.* <http://www.healthywaterways.org/HealthyWaterways/Resources/Factsheets.aspx> Healthy Waterways. (last accessed August 2008)

Speer, MS 2008, On the late twentieth century decrease in Australian east coast rainfall extremes, *Atmospheric Science Letters,* vol. 9, pp. 160–170.

Smith, I 2004, An Assessment of recent trends in Australian rainfall, *Australian Meteorological Magazine,* vol. 53, pp. 163-173.

Stern, Sir Nicholas, 2006, 'Stern Review final report', *The National Archives.* <http://webarchive.nationalarchives.gov.uk/+/http://www.hm-treasury.gov.uk/stern_review_report.htm>, HM Treasury (accessed 14 October 2009)

Stone, RC, Hammer, GL and Marcussen, T 1996, Prediction of global rainfall probabilities using phases of the Southern Oscillation Index, *Nature,* vol. 384, pp. 252-5.

Suppiah, R, Hennessy, KJ, Whetton, PH, McInnes, K, Macadam, I, Bathols, J Ricketts, J & Page, CM 2007. Australian climate change projections derived from simulations performed for the IPCC 4th Assessment Report, *Australian Meteorological Magazine,* vol. 56, pp.131-152.

Taschetto, AS and England, MH 2009, El Niño Modoki impacts on Australian rainfall, *Journal of Climatology,* vol. 22, pp. 3167-3174.

Thresher, RE 2002, Solar Correlates of Southern Hemisphere Mid-Latitude Climate Variability, *International Journal of Climatology,* vol. 22, no. 8, pp.901-915.

Timbal, B 2004, Southwest Australia past and future rainfall trends, *Climate Research,* vol. 26, pp. 233-249.

Timbal, B and Jones, D 2008, Future projections of winter rainfall in southeast Australia using a statistical downscaling technique, *Climate Change,* vol. 86, pp. 165-187.

Timbal, B, Hope, P & Charles, S 2008. Evaluating the Consistence between Statistically Downscaled and Global Dynamical Model Climate Change Projections, *Journal of Climate,* vol. 21, pp.6052-6059.

Walsh, K, Cai, W, Hennessy, K, Jones, R, McInnes, K, Nguyen, K, Page, C & Whetton, P 2004, *Climate Change in Queensland under Enhanced Greenhouse Conditions,* Report on research undertaken for Queensland Departments of State Development, Main Roads, Health, Transport, Mines and Energy, Treasury, Public Works, Primary Industries, and Natural Resources.

Wang, G and Hendon, HH 2007, Sensitivity of Australian rainfall to inter-El Nino variations, *Journal of Climate,* vol. 20, pp. 4211-4226.

WCRP – CMIP 2008. The World Climate Research Programme's (WCRP's) Coupled Model Intercomparison Project phase 3 (CMIP3) multi-model dataset.

Weitzman, ML 2009, On Modelling and Interpreting the Economics of Catastrophic Climate Change, *The Review of Economics and Statistics,* vol. 91, no. 1, pp. 1-19.

White WB, McKeon G, Syktus, J 2003, Australian drought: the interference of multi-spectral global standing modes and travelling waves, *International Journal of Climatology,* vol. 23, pp. 631–662.

Wilby, RL, Charles, SP, Zorita, E, Timbal, B, Whetton, P & Mearns, LO 2004, Guidelines for Use of Climate Scenarios Developed from Statistical Downscaling Methods.

Wilks, DS, 2006, *Statistical Methods in the Atmospheric Sciences*. 2nd ed. Academic Press, London.

Williams, AAJ and Stone, RC 2009, An assessment of the relationship between the Australian subtropical ridge, rainfall variability, and high-latitude circulation patterns, *International Journal of Climatology,* vol. 29, pp. 691-709.

Wilson, L, Manton, M & Siems, S 2010, Rainfall Climatology of South Eastern Queensland. Monash University Melbourne. Australian Meteorology and Oceanic Science Presentation

Zhang, X, Zwiers, F, Hegerl, G, Lambert, F, Gillett, P, Solomon, S, Stott, P & Nozawa, T 2007, Detection of human influence on twentieth-century precipitation trends, *Nature,* vol. 448, pp. 461-465.

Appendix A: Monthly Climatic Predictors

NCEP predictors are correlated with rainfall at the three stations for each month to improve the ability of the models to capture variations in rainfall drivers throughout the year. The values of the predictor variables are taken at 42 locations around the region and at 8 different height levels (see section 3.3.3). The predictors with the highest correlation values for each station and each month are used in the regression analysis and are included in the following tables. The abbreviations are: Prw (Precipitable Water), Rhum (Relative Humidity), Shum (Specific Humidity), Uwnd (Zonal Wind), Vwnd (Meridional Wind) and Zg (Geopotential Height). The altitude is provided after the variable abbreviation in millibars, and the latitude and longitude coordinates are also given.

Table A.1: NCEP predictor variables with highest correlation to rainfall for each month at the Crow's Nest Station at a 95% level of significance. q and RH: Specific and Relative Humidity, Prw: Precipitable Water, u and v: Zonal and Meridional Windspeed, Z: Geopotential Height. Altitude at which variable is taken follows the abbreviated variable as does the latitude and longitude coordinates. r values are in brackets.

Monthly Climatic NCEP Predictors and their Location for **Crow's Nest**. Predictors with Highest Correlation to Rainfall (1948 – 2000) are shown. Correlation Coefficient (r) included in brackets.				
January	RH850 @ 27.5°S 150°E (0.5707)			Z850 @ 25°S 145°E (-0.6680)
February	q400 @ 30°S 157.5°E (0.7682)	Prw @ 27.5°S 155°E (0.7317)	v600 @ 27.5°S 152.5°E (-0.7268)	
March	q850 @ 22.5°S 152.5°E (0.6945)	Prw@ 25°S 152.5°E (0.7059)		
April	q850 @ 30°S 157.5°E (0.7162)	Prw @ 27.5°S 155°E (0.6336)		
May	q600 @ 30°S 157.5°E (0.5268)	Prw @ 27.5°S 155°E (0.5129)	v400 @ 30°S 150°E (-0.5424)	
June	q600 @ 30°S 155°E (0.6335)	Prw @ 27.5°S 152.5°E (0.6583)	v600 @ 22.5°S 155°E (-0.5210)	
July	q850 @ 25°S 157.5°E (0.5958)		u850 @ 30°S 152.5°E (-0.4590)	
August	q850 @ 27.5°S 155°E (0.6783)	Prw @ 25°S 155°E (0.6822)	v600 @ 30°S 152.5°E (-0.5348)	
September	RH850 @ 30°S 150°E (0.6177)	Prw @ 25°S 152.5°E (0.6207)		
October	RH400 @ 30°S 160°E (0.6861)	Prw @ 27.5°S 152.5°E (0.5674)		
November	RH600 @ 27.5°S 155°E (0.6020)	Prw @ 25°S 155°E (0.5514)		
	q850 @	Prw @	v400 @	

December	22.5°S 160°E (0.4996)	25°S 160°E (0.4781)	32.5°S 155°E (-0.6625)	

Table A.2: NCEP predictor variables with highest correlation to rainfall for each month at the Mount Brisbane Station at a 95% level of significance. q and RH: Specific and Relative Humidity, Prw: Precipitable Water, u and v: Zonal and Meridional Windspeed, Z: Geopotential Height. Altitude at which variable is taken follows the abbreviated variable as does the latitude and longitude coordinates. r values are in brackets.

Monthly Climatic NCEP Predictors and their Location for **Mt. Brisbane**. Predictors with Highest Correlation to Rainfall (1948 – 2000) are shown. Correlation Coefficient (r) included in brackets.				
January	q400 @ 30°S 152.5°E (0.6305)		v600 @ 27.5°S 150°E (-0.4773)	Z850 @ 25°S 145°E (-0.6650)
February	q400 @ 30°S 157.5°E (0.7507)	Prw @ 27.5°S 155°E (0.7435)	v600 @ 30°S 152.5°E (-0.6821)	u250 @ 20°S 160°E (-0.6089)
March	RH850 @ 25°S 152.5°E (0.6170)		u850 @ 32.5°S 152.5°E (-0.6207)	Z850 @ 22.5°S 152.5°E (-0.5048)
April	q850 @ 30°S 155°E (0.6832)	Prw @ 30°S 155°E (0.6637)	v250 @ 32.5°S 150°E (-0.5386)	
May	q600 @ 30°S 157.5°E (0.6400)	Prw @ 27.5°S 157.5°E (0.6494)	v250 @ 32.5°S 152.5°E (-0.5533)	
June	q600 @ 30°S 155°E (0.5948)	Prw @ 27.5°S 157.5°E (0.6014)	v250 @ 30°S 152.5°E (-0.5032)	
July	q600 @ 25°S 160°E (0.5439)	Prw @ 25°S 157.5°E (0.5794)	u400 @ 30°S 152.5°E (-0.5054)	
August	q850 @ 27.5°S 155°E (0.6519)	Prw @ 27.5°S 155°E (0.6851)		
September	RH850 @ 27.5°S 150°E (0.5333)	Prw @ 25°S 152.5°E (0.4547)	v400 @ 30°S 150°E (-.4958)	
October	q850 @ 30°S 157.5°E (0.6537)	Prw @ 30°S 157.5°E (0.6513)		
November	RH600 @ 27.5°S 155°E (0.6020)	Prw @ 27.5°S 155°E (0.5173)		

December	q850 @ 30°S 160°E (0.5808)	Prw @ 30°S 160°E (0.5370)	v400 @ 32.5°S 155°E (-0.5473)	

Table A.3: NCEP predictor variables with highest correlation to rainfall for each month at the Peachester Station at a 95% level of significance. q and RH: Specific and Relative Humidity, Prw: Precipitable Water, u and v: Zonal and Meridional Windspeed, Z: Geopotential Height. Altitude at which variable is taken follows the abbreviated variable as does the latitude and longitude coordinates. r values are in brackets.

Monthly Climatic NCEP Predictors and their Location for **Peachester**. Predictors with Highest Correlation to Rainfall (1948 – 2000) are shown. Correlation Coefficient (r) included in brackets.				
January	q400 @ 32.5°S 150°E (0.5530)		v600 @ 32.5°S 155°E (-0.5227)	Z850 @ 25°S 145°E (-0.6838)
February	q400 @ 27.5°S 155°E (0.6745)	Prw @ 27.5°S 155°E (0.6937)	v600 @ 30°S 152.5°E (-0.7023)	
March	q850 @ 22.5°S 152.5°E (0.7411)	Prw @ 25°S 152.5°E (0.7637)	u850 @ 32.5°S 152.5°E (-0.7528)	
April	q850 @ 30°S 155°E (0.5782)	Prw @ 30°S 155°E (0.6272)	u850 @ 32.5°S 155°E (-0.5606)	
May	q600 @ 27.5°S 157.5°E (0.5372)	Prw @ 27.5°S 155°E (0.5927)	v250 @ 30°S 152.5°E (-0.5796)	
June	q600 @ 30°S 155°E (0.6183)	Prw @ 27.5°S 155°E (0.6705)	u850 @ 30°S 152.5°E (-0.565)	
July	q850 @ 25°S 157.5°E (0.6620)	Prw @ 25°S 157.5°E (0.6744)	u850 @ 30°S 152.5°E (-0.6117)	
August	q850 @ 22.5°S 155°E (0.5288)	Prw @ 27.5°S 155°E (0.6094)	u850 @ 32.5°S 157.5°E (-0.5705)	
September	RH850 @ 25°S 150°E (0.6723)	Prw @ 25°S 152.5°E (0.6735)	v400 @ 32.5°S 150°E (-0.4344)	
October	RH600 @ 25°S 155°E (0.6361)	Prw @ 30°S 157.5°E (0.5971)	v600 @ 30°S 157.5°E (-0.4775)	
November	RH600 @ 27.5°S 155°E (0.5844)	Prw @ 27.5°S 155°E (0.5436)		

December	RH400 @ 27.5°S 160°E (0.5593)	Prw @ 30°S 160°E (0.5150)	v400 @ 30°S 155°E (-0.6496)	

Appendix B: Statistical Models used to calculate Monthly rainfall

The following three tables provide the statistical models use to calculate rainfall for each month from the predictor variables at the selected stations. Abbreviations of predictor variables are as in Appendix A. The location where the predictor variable is taken at is not supplied but can be referenced from the Appendix A Tables.

Table B.1: Statistical models used to calculate the natural log of each months rainfall from predictor variables at **Crow's Nest**.

Month	Statistical Models used to calculate the natural log of monthly rainfall totals at **Crow's Nest**
January	28.33977 - 0.01758.Z850 + 0.04212.RH850
February	3.8352 + 1.355.q400 – 0.1918.v600
March	-0.8521 + 0.1523.Prw
April	-3.03321 + 0.09927.Prw + 0.76882.q850
May	1.8932 + 1.4848.q600 – 0.1452.v400
June	0.1497 + 0.1913.Prw – 0.2344.v600
July	-1.327 + 1.12.q850
August	-2.7341 + 0.3017.Prw
September	-4.53533 + 0.1452.Prw + 0.09041.RH850
October	-1.1061 + 0.1455.Prw + 0.0637.RH400
November	1.36708 + 0.08262.RH600
December	4.7138 – 0.1636.v400

Table B.2: Statistical models used to calculate the natural log of each months rainfall from predictor variables at **Mount Brisbane**.

Month	Statistical Models used to calculate the natural log of monthly rainfall totals at **Mt. Brisbane**
January	33.9251 – 0.02029.Z850 + 1.4228.q400
February	3.0016 + 2.0641.q400 – 0.1286.v600
March	-1.41128 – 0.15564.u850 + 0.08447.RH850
April	-2.16565 + 0.24051.Prw – 0.06495.v250
May	1.3454 + 1.7419.q600 – 0.1242.v250
June	3.1328 – 0.1782.v250
July	-3.6232 – 0.3387.Prw
August	-5.4947 + 0.4738.Prw
September	0.78437 + 0.05597.RH850 – 0.22864.v400
October	-2.6414 + 0.3015.Prw
November	0.83883 + 0.09399.RH600
December	2.38278 + 0.08068.Prw – 0.08806.v400

Table B.3: Statistical models used to calculate the natural log of each months rainfall from predictor variables at **Peachester**.

Month	Statistical Models used to calculate the natural log of monthly rainfall totals at **Peachester**
January	42.18188 – 0.02444.Z850 – 0.1133.v600
February	4.7202 + 1.2471.q400 – 0.2102.v600
March	2.8276 + 0.07304.Prw – 0.23682.u850
April	1.4429 + 0.1456.Prw – 0.138.u850
May	0.3147 + 0.18232.Prw – 0.07609.v250
June	-2.9042 + 0.3437.Prw
July	1.2367 + 0.8081.q850 – 0.227.u850
August	2.0745 + 0.5479.q850 – 0.1986.u850
September	-0.34809 + 0.08108.RH850 – 0.18512.v400
October	0.3671 + 0.0806.RH850
November	2.70141 + 0.05792.RH600
December	4.48261 + 0.02455.RH400 – 0.19171.v600

Appendix C: Shifts in Lat/Lon values from NCEP to GCM's

NCEP data is based on a 2.5° Latitude and Longitude grid and this does not necessarily transfer directly to the GCM's which have grid points distributed on different scales. The following tables list all the NCEP grid points for the predictor variables used and the corresponding GCM coordinates for each model.

Table C.1: NCEP Precipitable Water coordinates and the corresponding GCM coordinates.

NCEP	CCCMA-t63	CNRM-cm3	CSIRO mk3.5	GISS-er	GFDL mk2.1	MIROC-medres
155°E 30°S	154.7°E 29.3°S	154.7°E 29.3°S	155.6°E 30.8°S	152.5°E 30°S	153.8°E 29.3°S	154.7°E 29.3°S
157.5°E 30°S	157.5°E 29.3°S	157.5°E 29.3°S	157.5°E 30.8°S	157.5°E 30°S	156.2°E 29.3°S	157.5°E 29.3°S
160°E 30°S	160.3°E 29.3°S	160.3°E 29.3°S	159.4°E 30.8°S	157.5°E 30°S	158.8°E 29.3°S	160.3°E 29.3°S
152.5°E 25°S	151.9°E 23.7°S	151.9°E 23.7°S	151.9°E 25.2°S	152.5°E 26°S	151.2°E 25.3°S	151.9°E 23.7°S
155°E 25°S	154.7°E 23.7°S	154.7°E 23.7°S	155.6°E 25.2°S	152.5°E 26°S	153.8°E 25.3°S	154.7°E 23.7°S
157.5°E 25°S	157.5°E 23.7°S	157.5°E 23.7°S	157.5°E 25.2°S	157.5°E 26°S	156.2°E 25.3°S	157.5°E 23.7°S
152.5°E 27.5°S	151.9°E 26.5°S	151.9°E 26.5°S	151.9°E 27°S	152.5°E 26°S	151.2°E 27.3°S	151.9°E 26.5°S
155°E 27.5°S	154.7°E 26.5°S	154.7°E 26.5°S	155.6°E 27°S	152.5°E 26°S	153.8°E 27.3°S	154.7°E 26.5°S

Table C.2: NCEP Relative Humidity coordinates and the corresponding GCM coordinates.

NCEP	CCCMA-t63	CNRM-cm3	CSIRO mk3.5	GISS-er	GFDL mk2.1	MIROC-medres
157.5°E 27.5°S	157.5°E 26.5°S	157.5°E 26.5°S	157.5°E 27°S	155°E 28°S	156.2°E 27.3°S	157.5°E 26.5°S
160°E 27.5°S	160.3°E 26.5°S	160.3°E 26.5°S	159.4°E 27°S	160°E 28°S	158.8°E 27.3°S	160.3°E 26.5°S
150°E 30°S 5	149.1°E 29.3°S	149.1°E 29.3°S	150°E 30.8°S	150°E 32°S	148.8°E 29.3°S	149.1°E 29.3°S
160°E 30°S	160.3°E 29.3°S	160.3°E 29.3°S	159.4°E 30.8°S	160°E 32°S	158.8°E 29.3°S	160.3°E 29.3°S
150°E 25°S	149.1°E 23.7°S	149.1°E 23.7°S	150°E 25.2°S	150°E 24°S	148.8°E 25.3°S	149.1°E 23.7°S
152.5°E 25°S	151.9°E 23.7°S	151.9°E 23.7°S	151.9°E 25.2°S	150°E 24°S	151.2°E 25.3°S	151.9°E 23.7°S
155°E 25°S	154.7°E 23.7°S	154.7°E 23.7°S	155.6°E 25.2°S	155°E 24°S	153.8°E 25.3°S	154.7°E 23.7°S
150°E 27.5°S	149.1°E 26.5°S	149.1°E 26.5°S	150°E 27°S	150°E 28°S	148.8°E 27.3°S	149.1°E 26.5°S
155°E 27.5°S	154.7°E 26.5°S	154.7°E 26.5°S	155.6°E 27°S	155°E 28°S	153.8°E 27.3°S	154.7°E 26.5°S

Table C.3: NCEP Specific Humidity coordinates and the corresponding GCM coordinates.

NCEP	CCCMA-t63	CNRM-cm3	CSIRO mk3.5	GISS-er	GFDL mk2.1	MIROC-medres
152.5°E 30°S	151.9°E 29.3°S	151.9°E 29.3°S	151.9°E 30.8°S	150°E 32°S	151.2°E 29.3°S	151.9°E 29.3°S
157.5°E 30°S	157.5°E 29.3°S	157.5°E 29.3°S	157.5°E 30.8°S	155°E 32°S	156.2°E 29.3°S	157.5°E 29.3°S
155°E 22.5°S 5	154.7°E 23.7°S	154.7°E 23.7°S	155.6°E 23.3°S	155°E 24°S	153.8°E 23.3°S	154.7°E 23.7°S
157.5°E 25°S	157.5°E 23.7°S	157.5°E 23.7°S	157.5°E 25.2°S	155°E 24°S	156.2°E 25.3°S	157.5°E 23.7°S
155°E 27.5°S	154.7°E 26.5°S	154.7°E 26.5°S	155.6°E 27°S	155°E 28°S	153.8°E 27.3°S	154.7°E 26.5°S

Table C.4: NCEP Zonal Wind coordinates and the corresponding GCM coordinates.

NCEP	CCCMA-t63	CNRM-cm3	CSIRO mk3.5	GISS-er	GFDL mk2.1	MIROC-medres
152.5°E 30°S	151.9°E 29.3°S	151.9°E 29.3°S	151.9°E 30.8°S	150°E 32°S	151.2°E 29.3°S	151.9°E 29.3°S
152.5°E 32.5°S	151.9°E 32.1°S	151.9°E 32.1°S	151.9°E 32.6°S	150°E 32°S	151.2°E 33.4°S	151.9°E 32.1°S
155°E 32.5°S	154.7°E 32.1°S	154.7°E 32.1°S	155.6°E 32.6°S	155°E 32°S	153.8°E 33.4°S	154.7°E 32.1°S
157.5°E 32.5°S	157.5°E 32.1°S	157.5°E 32.1°S	157.5°E 32.6°S	155°E 32°S	156.2°E 33.4°S	157.5°E 32.1°S

Table C.5: NCEP Meridional Wind coordinates and the corresponding GCM coordinates.

NCEP	CCCMA-t63	CNRM-cm3	CSIRO mk3.5	GISS-er	GFDL mk2.1	MIROC-medres
150°E 30°S	149.1°E 29.3°S	149.1°E 29.3°S	150°E 30.8°S	150°E 32°S	148.8°E 29.3°S	149.1°E 29.3°S
152.5°E 30°S	151.9°E 29.3°S	151.9°E 29.3°S	151.9°E 30.8°S	150°E 32°S	151.2°E 29.3°S	151.9°E 29.3°S
155°E 30°S 5	154.7°E 29.3°S	154.7°E 29.3°S	155.6°E 30.8°S	155°E 32°S	153.8°E 29.3°S	154.7°E 29.3°S
150°E 32.5°S	149.1°E 32.1°S	149.1°E 32.1°S	150°E 32.6°S	150°E 32°S	148.8°E 33.4°S	149.1°E 32.1°S
152.5°E 32.5°S	151.9°E 32.1°S	151.9°E 32.1°S	151.9°E 32.6°S	150°E 32°S	151.2°E 33.4°S	151.9°E 32.1°S
155°E 32.5°S	154.7°E 32.1°S	154.7°E 32.1°S	155.6°E 32.6°S	155°E 32°S	153.8°E 33.4°S	154.7°E 32.1°S
155°E 22.5°S	154.7°E 23.7°S	154.7°E 23.7°S	155.6°E 23.3°S	155°E 24°S	153.8°E 23.3°S	154.7°E 23.7°S
150°E 27.5°S	149.1°E 26.5°S	149.1°E 26.5°S	150°E 27°S	150°E 28°S	148.8°E 27.3°S	149.1°E 26.5°S
152.5°E 27.5°S	151.9°E 26.5°S	151.9°E 26.5°S	151.9°E 27°S	150°E 28°S	151.2°E 27.3°S	151.9°E 26.5°S

Table C.6: NCEP Geopotential Height coordinates and the corresponding GCM coordinates.

NCEP	CCCMA-t63	CNRM-cm3	CSIRO mk3.5	GISS-er	GFDL mk2.1	MIROC-medres
145°E 25°S	146.2°E 23.7°S	146.2°E 23.7°S	144.4°E 25.2°S	145°E 24°S	143.8°E 25.3°S	146.2°E 23.7°S

Appendix D: 20th Century GCM Rainfall Simulations

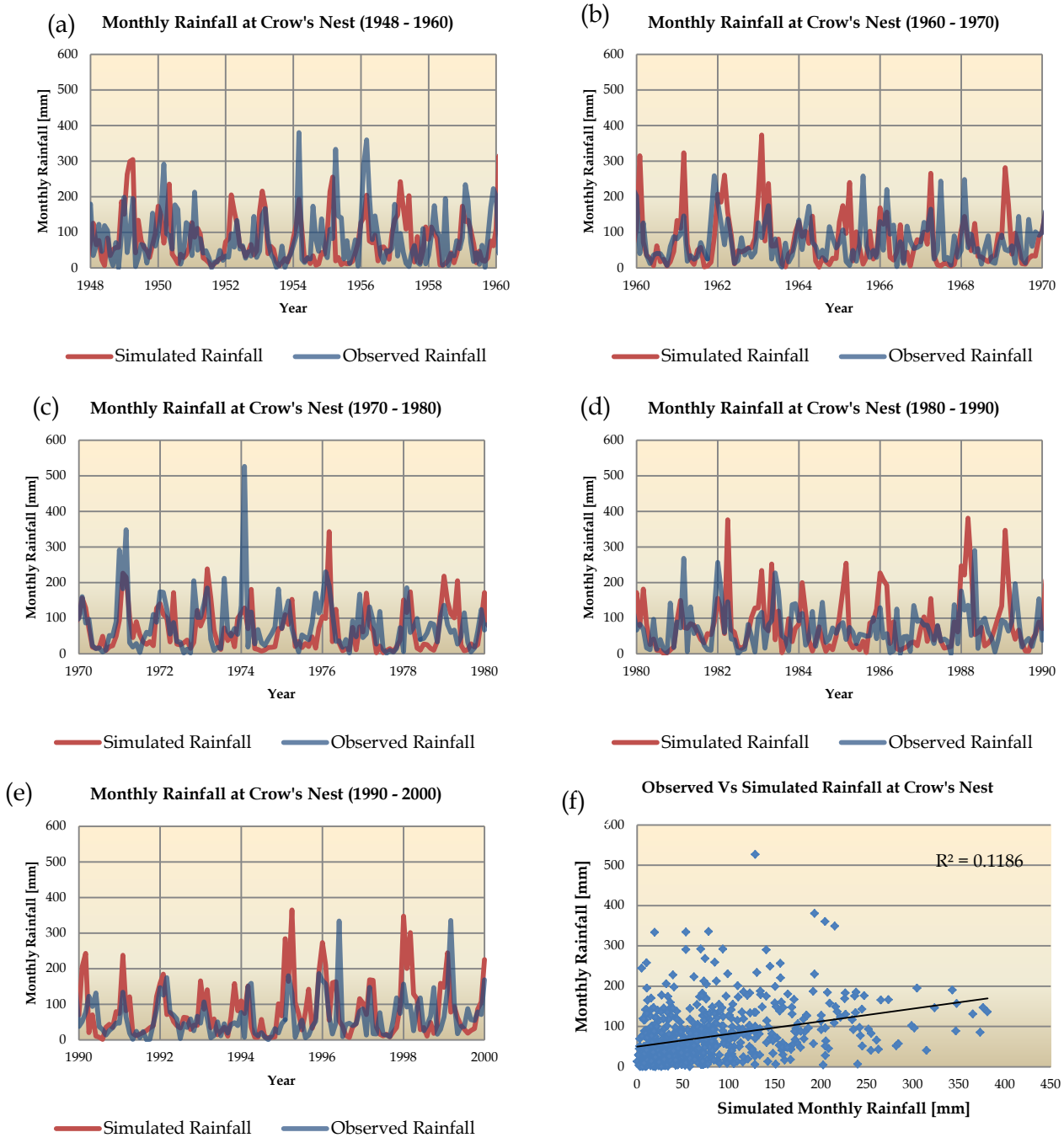

Figure D.1: Comparison of Observed rainfall [mm] [blue] at Crow's Nest for the periods (a) 1948 – 1960, (b) 1960 - 1970, (c) 1970 – 1980, (d) 1980 – 1990 and (e) 1990 – 2000 with data derived from the CNRM – cm3 GCM [red]. Coefficient of determination for the two sets of data from 1948 - 2000 provided in (f).

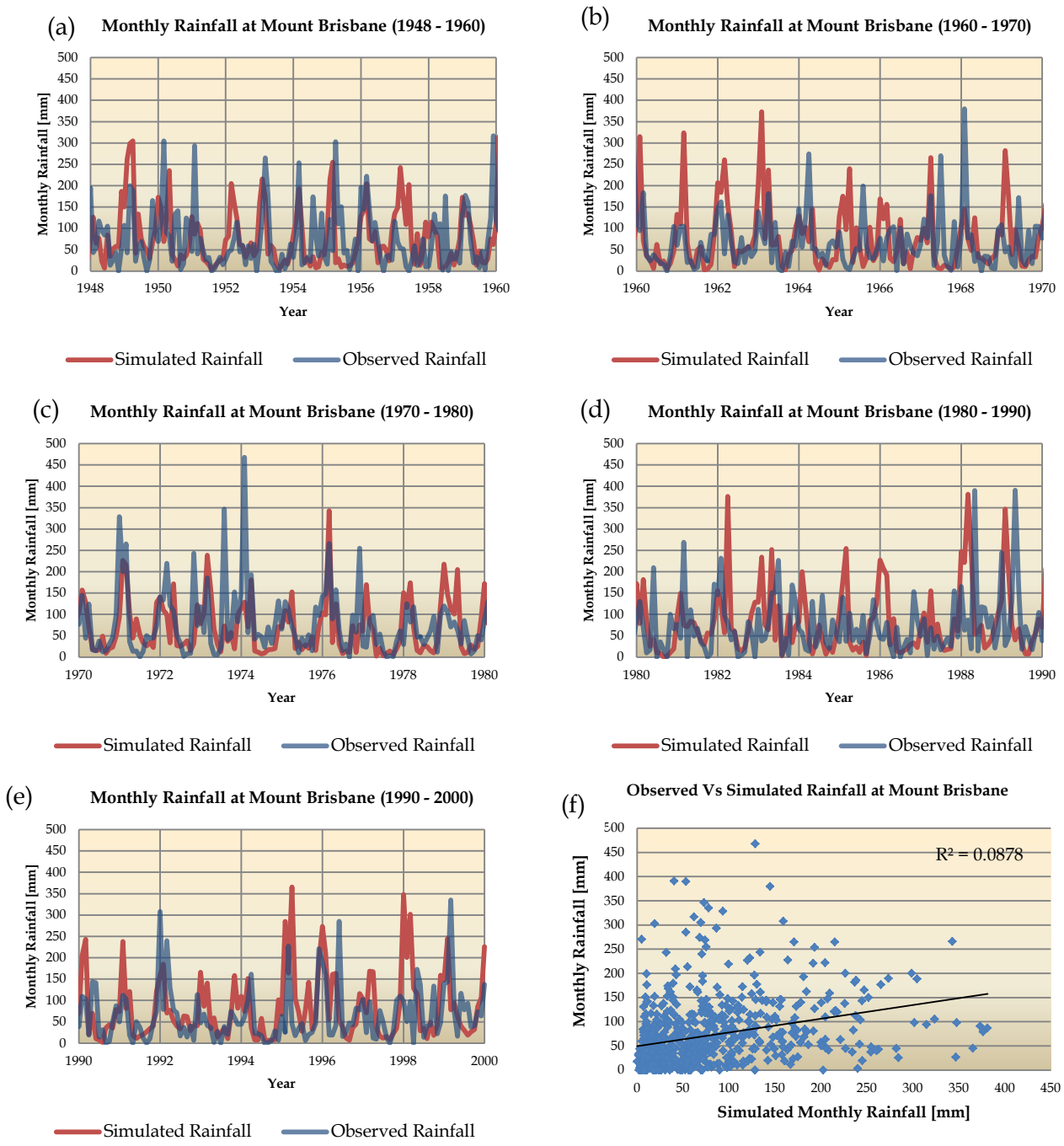

Figure D.2: Comparison of Observed rainfall [mm] [blue] at Mount Brisbane for the periods (a) 1948 – 1960, (b) 1960 - 1970, (c) 1970 – 1980, (d) 1980 – 1990 and (e) 1990 – 2000 with data derived from the CNRM – cm3 GCM [red]. Coefficient of determination for the two sets of data from 1948 - 2000 provided in (f).

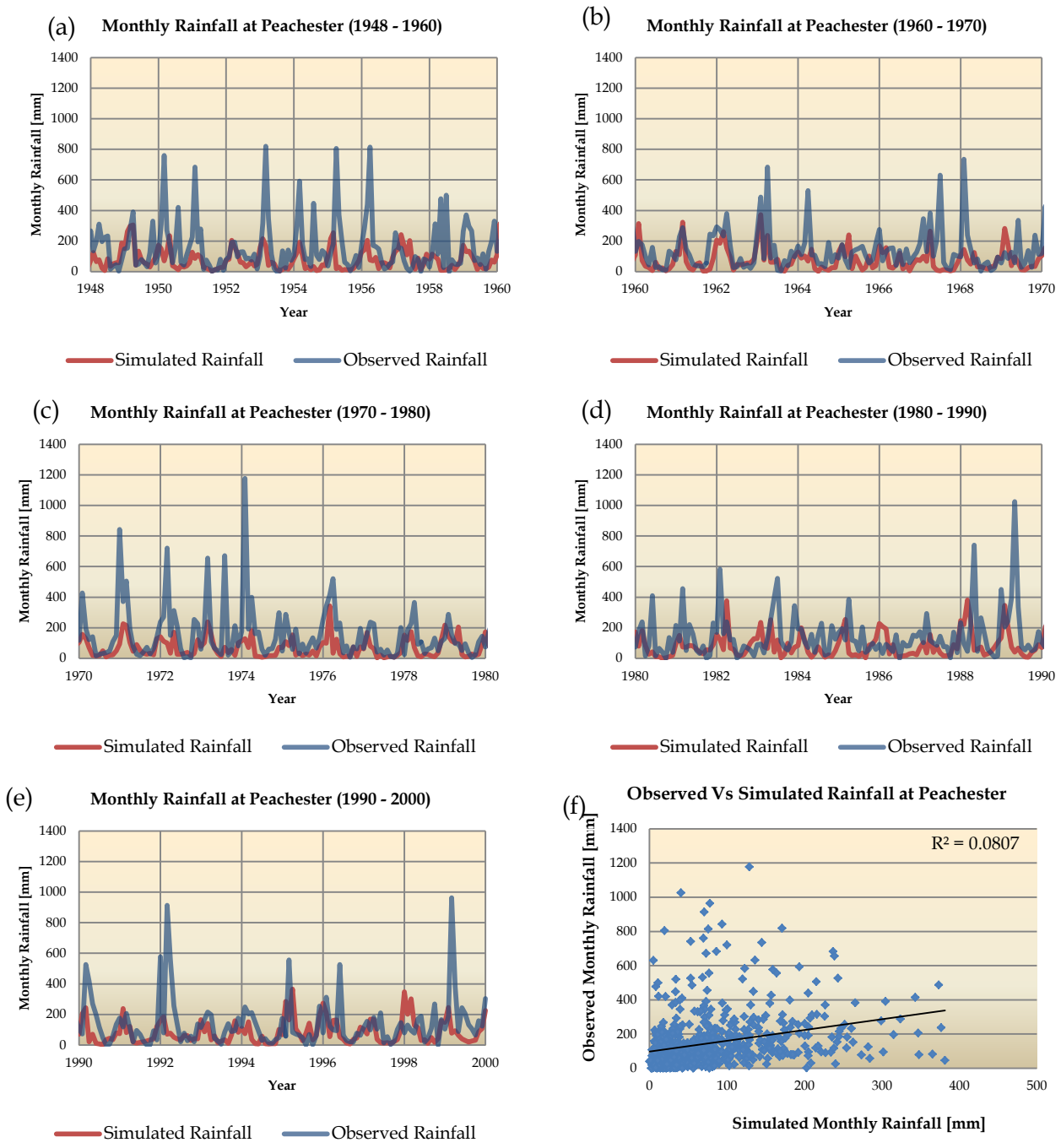

Figure D.3: Comparison of Observed rainfall [mm] [blue] at Peachester for the periods (a) 1948 – 1960, (b) 1960 - 1970, (c) 1970 – 1980, (d) 1980 – 1990 and (e) 1990 – 2000 with data derived from the CNRM – cm3 GCM [red]. Coefficient of determination for the two sets of data from 1948 - 2000 provided in (f).

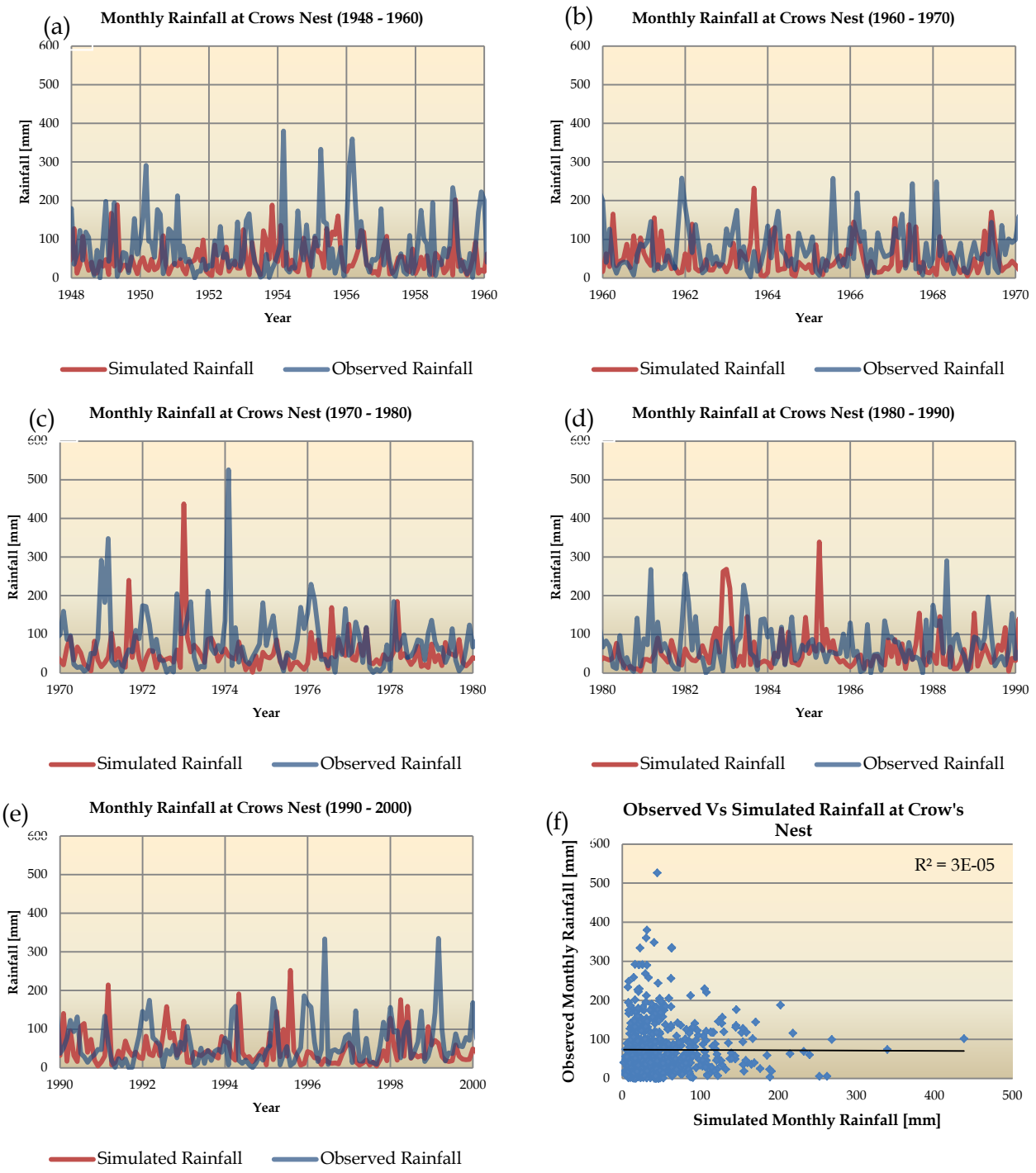

Figure D.4: Comparison of Observed rainfall [mm] [blue] at Crow's Nest for the periods (a) 1948 – 1960, (b) 1960 - 1970, (c) 1970 – 1980, (d) 1980 – 1990 and (e) 1990 – 2000 with data derived from the CCCMA – t63 GCM [red]. Coefficient of determination for the two sets of data from 1948 - 2000 provided in (f).

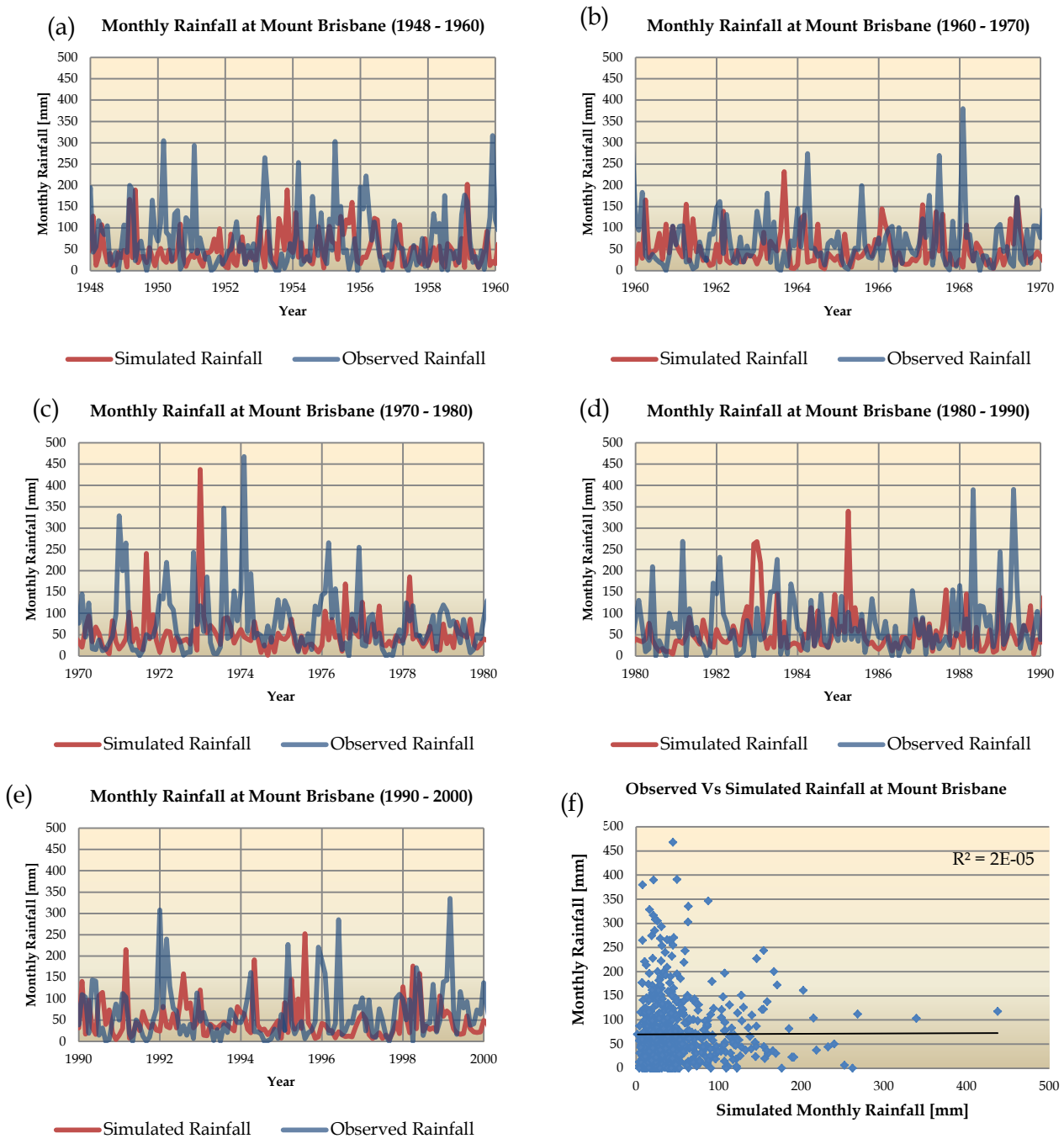

Figure D.5: Comparison of Observed rainfall [mm] [blue] at Mount Brisbane for the periods (a) 1948 – 1960, (b) 1960 - 1970, (c) 1970 – 1980, (d) 1980 – 1990 and (e) 1990 – 2000 with data derived from the CCCMA – t63 GCM [red]. Coefficient of determination for the two sets of data from 1948 - 2000 provided in (f).

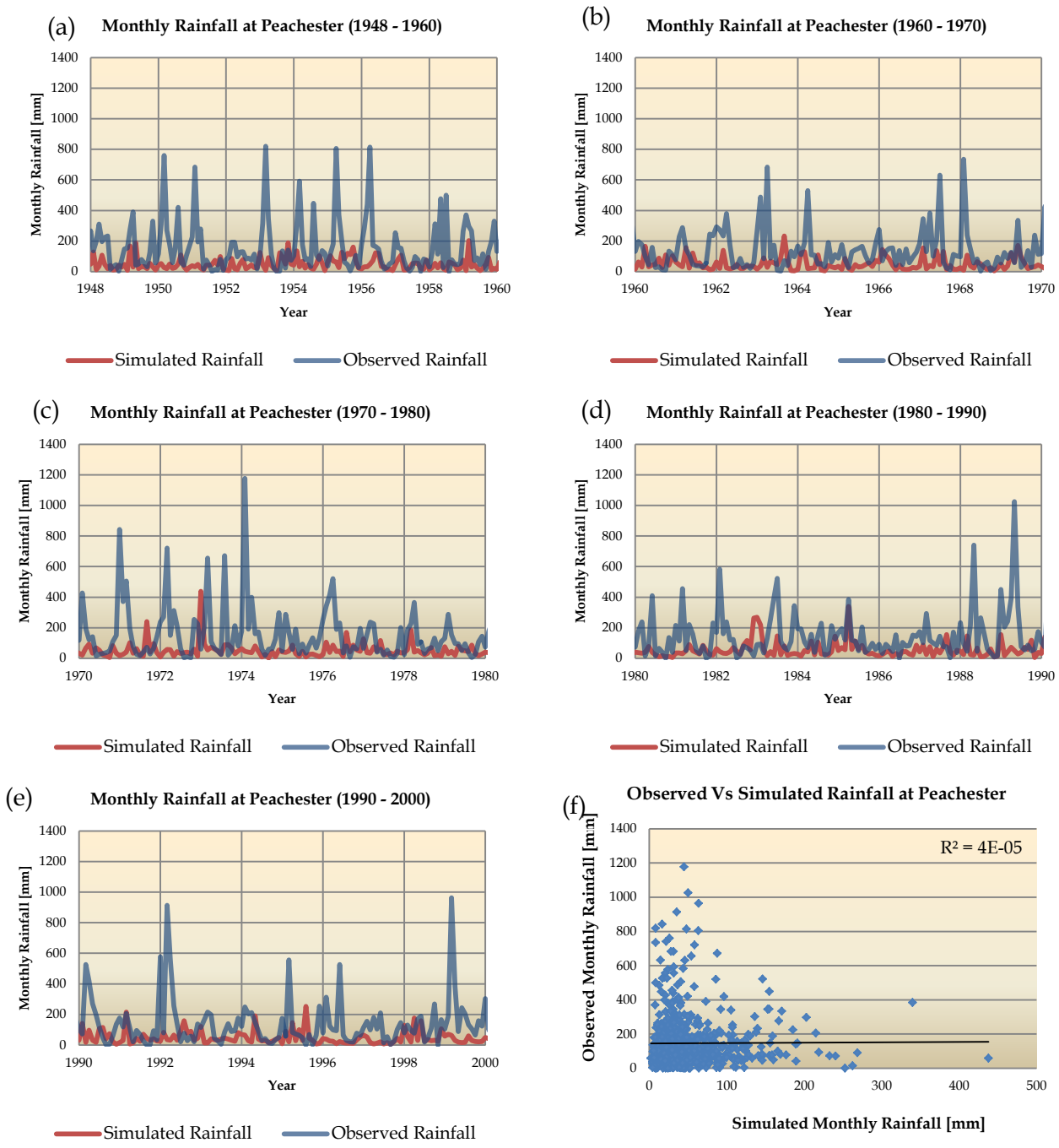

Figure D.6: Comparison of Observed rainfall [mm] [blue] at Peachester for the periods (a) 1948 – 1960, (b) 1960 - 1970, (c) 1970 – 1980, (d) 1980 – 1990 and (e) 1990 – 2000 with data derived from the CCCMA – t63 GCM [red]. Coefficient of determination for the two sets of data from 1948 - 2000 provided in (f).

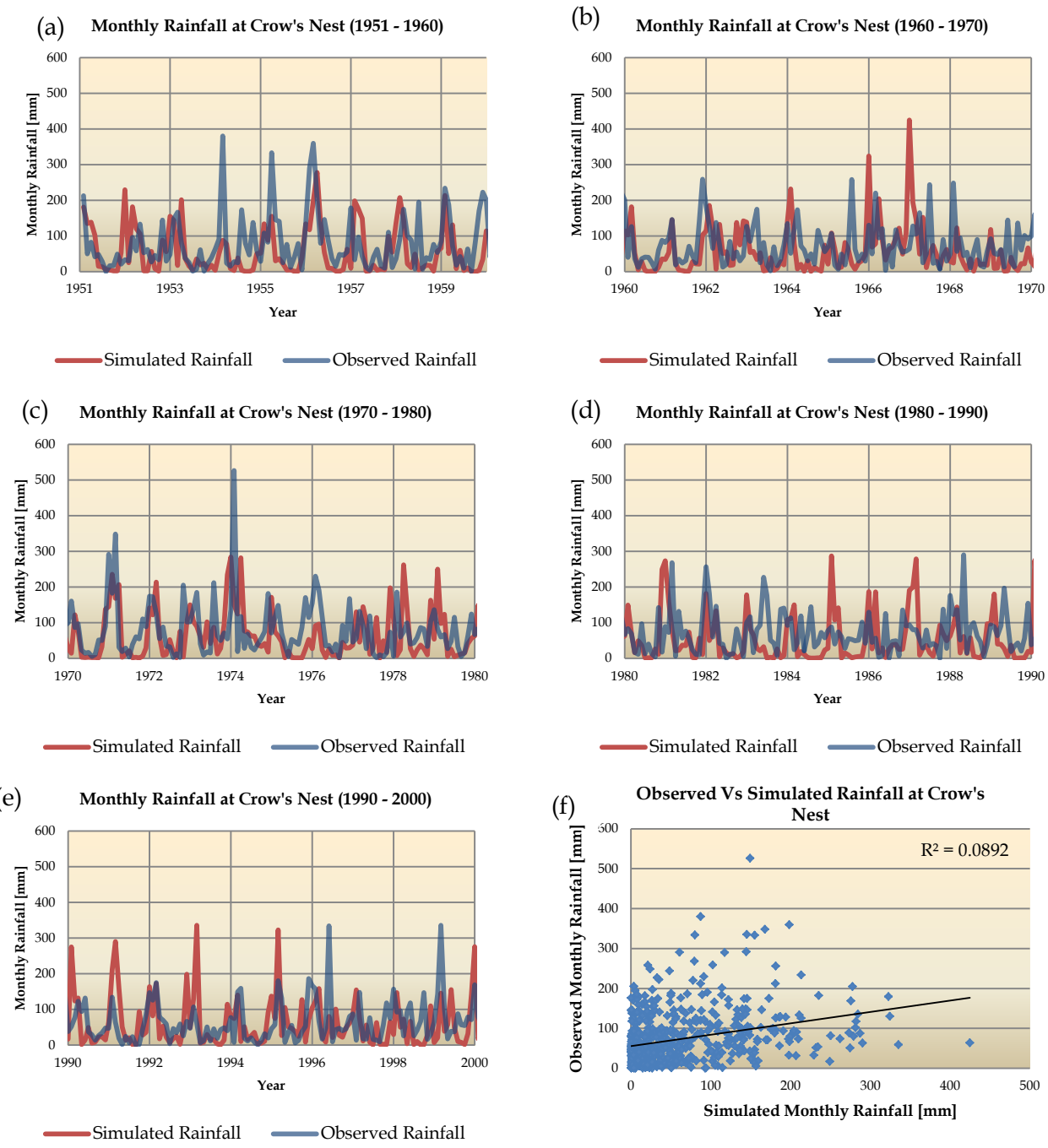

Figure D.7: Comparison of Observed rainfall [mm] [blue] at Crow's Nest for the periods (a) 1951 – 1960, (b) 1960 - 1970, (c) 1970 – 1980, (d) 1980 – 1990 and (e) 1990 – 2000 with data derived from the CSIRO Mk3.5 GCM [red]. Coefficient of determination for the two sets of data from 1948 - 2000 provided in (f).

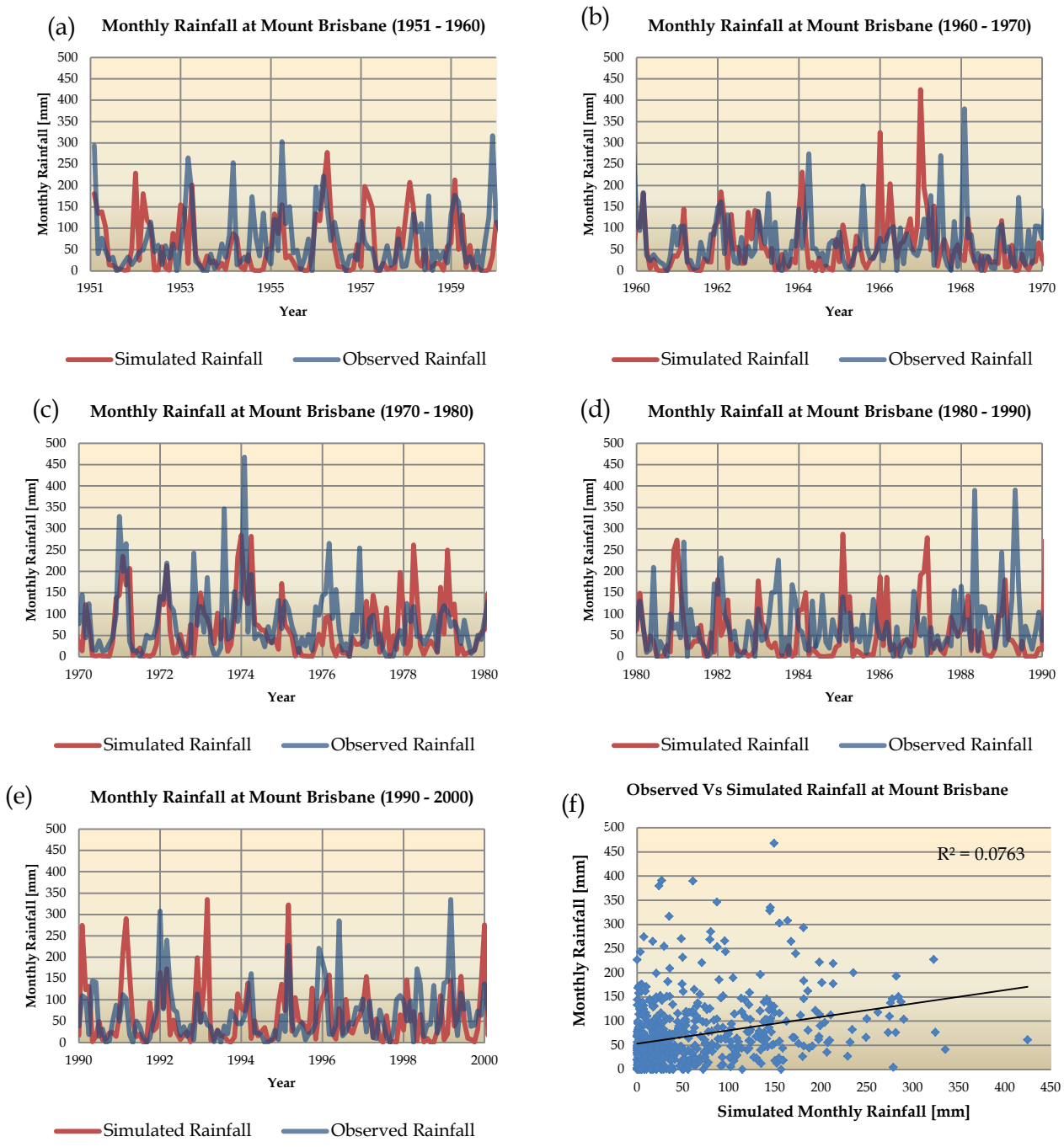

Figure D.8: Comparison of Observed rainfall [mm] [blue] at Mount Brisbane for the periods (a) 1951 – 1960, (b) 1960 - 1970, (c) 1970 – 1980, (d) 1980 – 1990 and (e) 1990 – 2000 with data derived from the CSIRO Mk3.5 GCM [red]. Coefficient of determination for the two sets of data from 1948 - 2000 provided in (f).

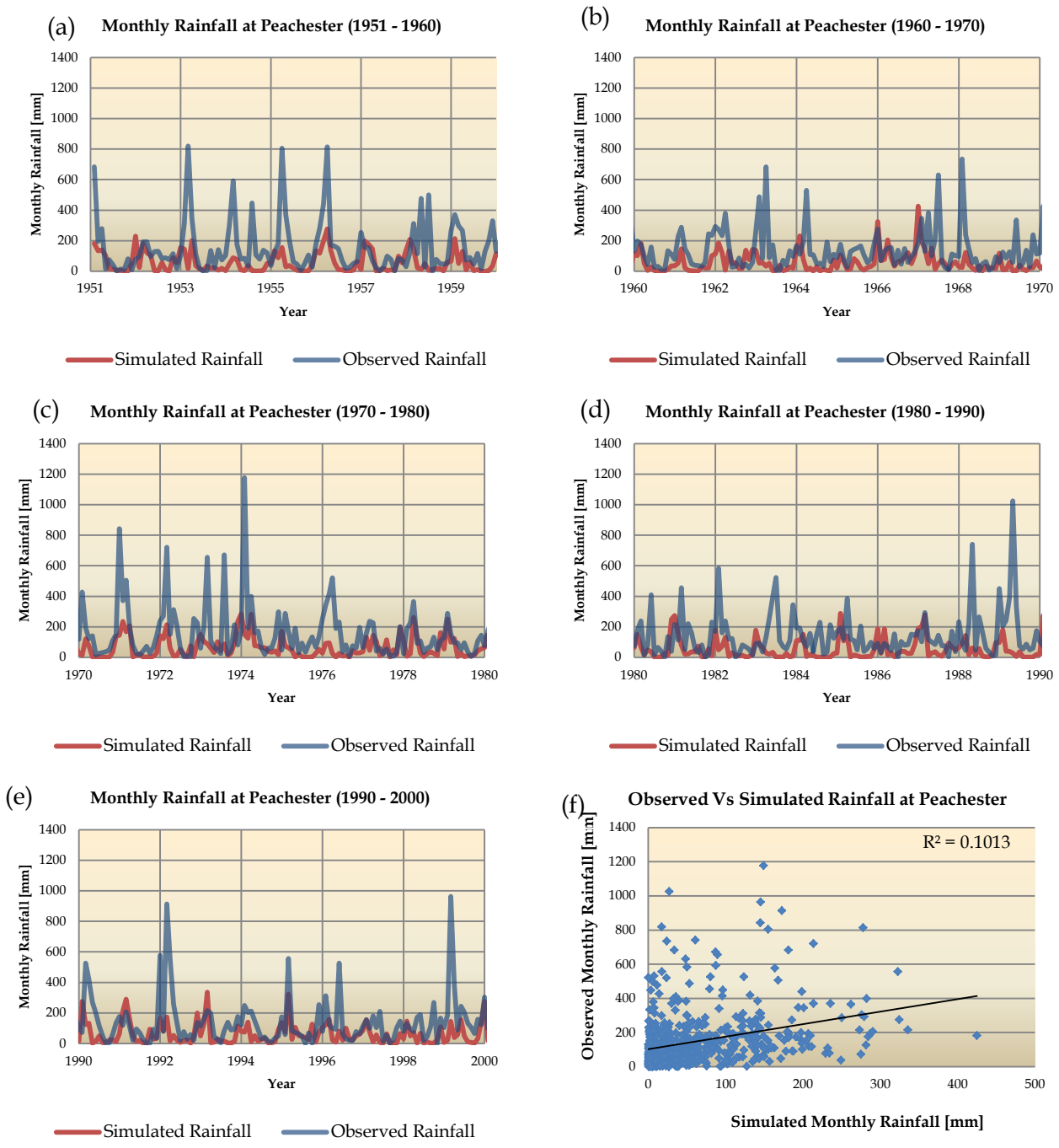

Figure D.9: Comparison of Observed rainfall [mm] [blue] at Peachester for the periods (a) 1951 – 1960, (b) 1960 - 1970, (c) 1970 – 1980, (d) 1980 – 1990 and (e) 1990 – 2000 with data derived from the CSIRO Mk3.5 GCM [red]. Coefficient of determination for the two sets of data from 1948 - 2000 provided in (f).

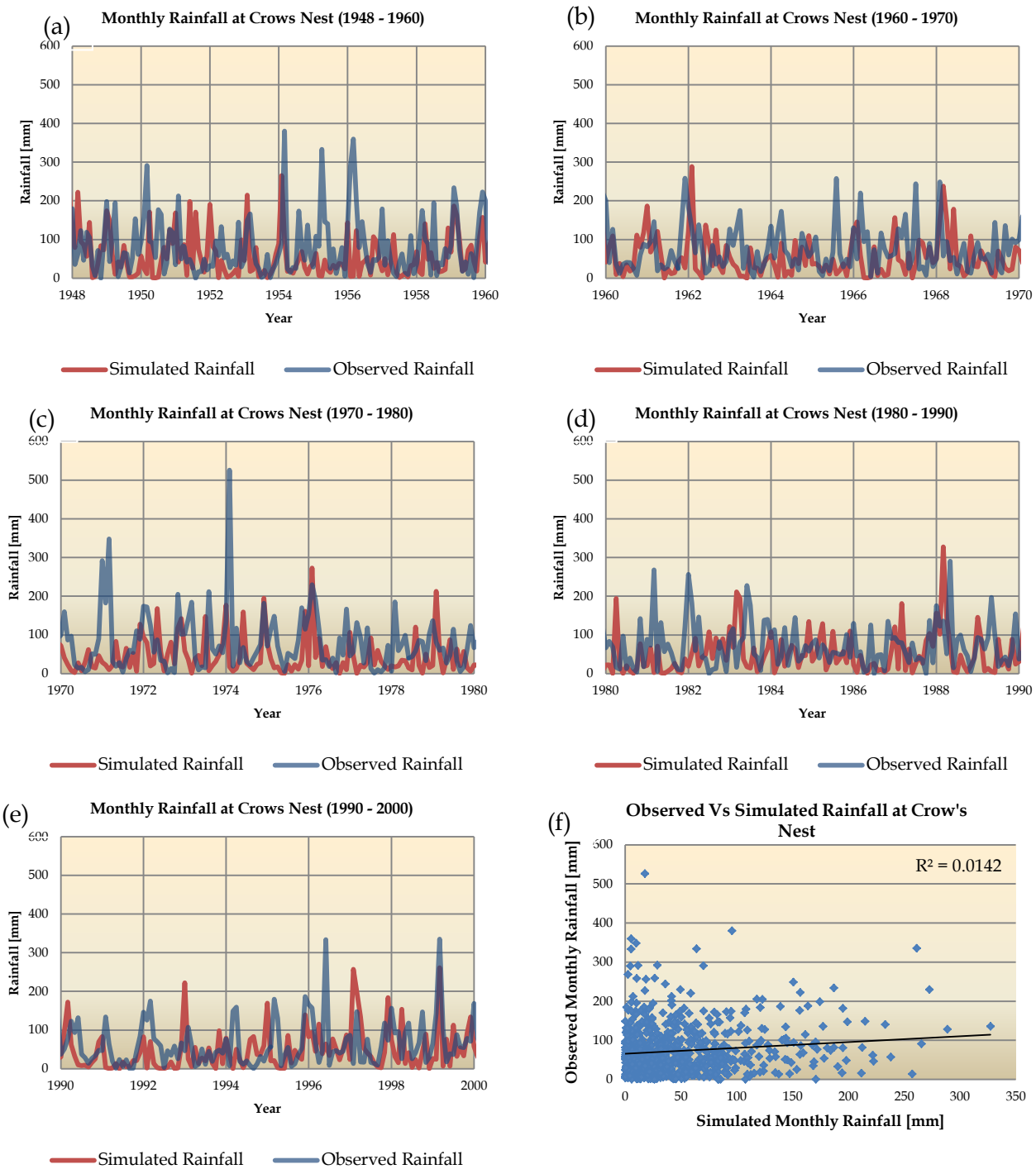

Figure D.10: Comparison of Observed rainfall [mm] [blue] at Crow's Nest for the periods (a) 1948 – 1960, (b) 1960 - 1970, (c) 1970 – 1980, (d) 1980 – 1990 and (e) 1990 – 2000 with data derived from the GFDL Mk2.1 GCM [red]. Coefficient of determination for the two sets of data from 1948 - 2000 provided in (f).

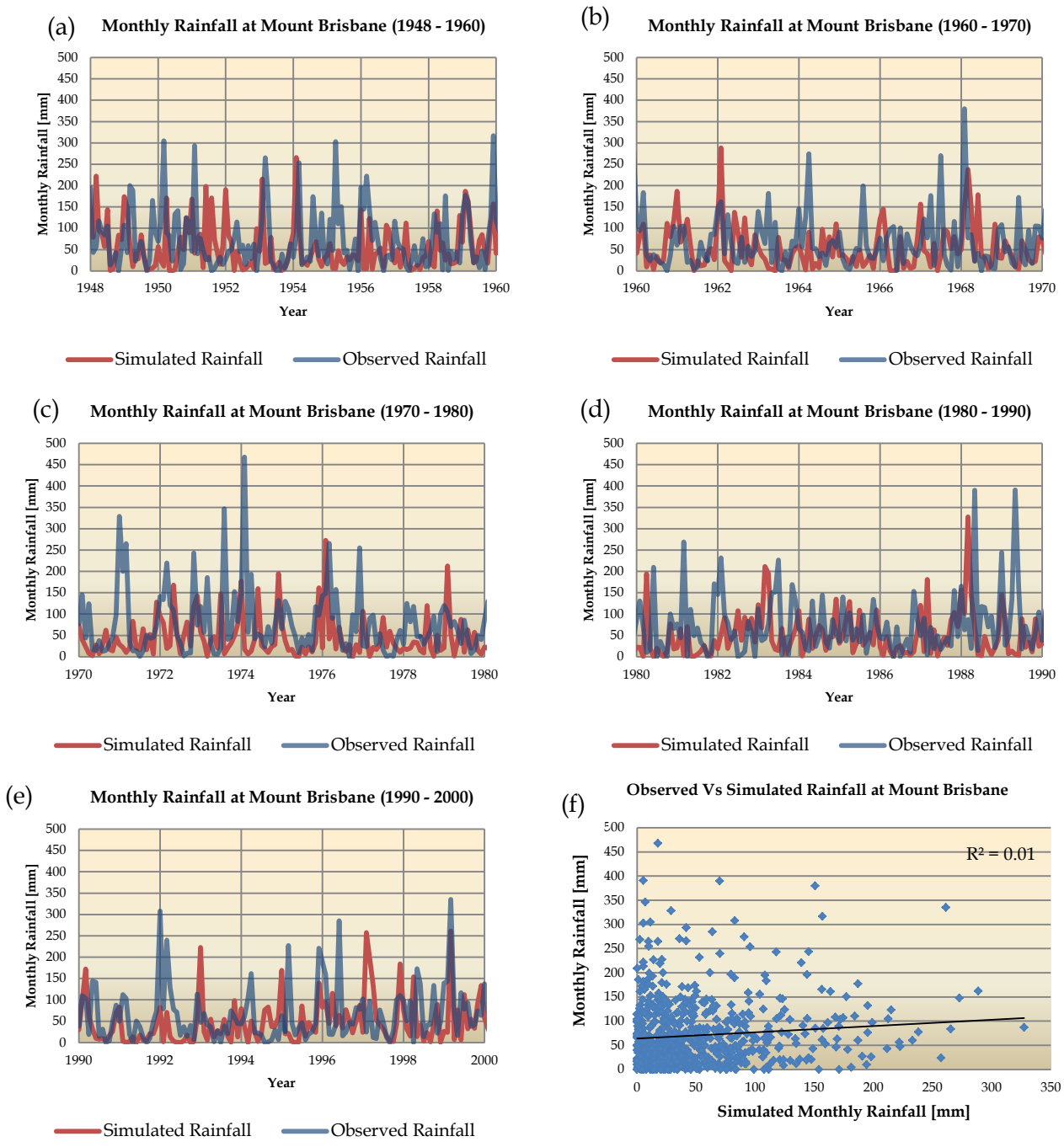

Figure D.11: Comparison of Observed rainfall [mm] [blue] at Mount Brisbane for the periods (a) 1948 – 1960, (b) 1960 - 1970, (c) 1970 – 1980, (d) 1980 – 1990 and (e) 1990 – 2000 with data derived from the GFDL Mk2.1 GCM [red]. Coefficient of determination for the two sets of data from 1948 - 2000 provided in (f).

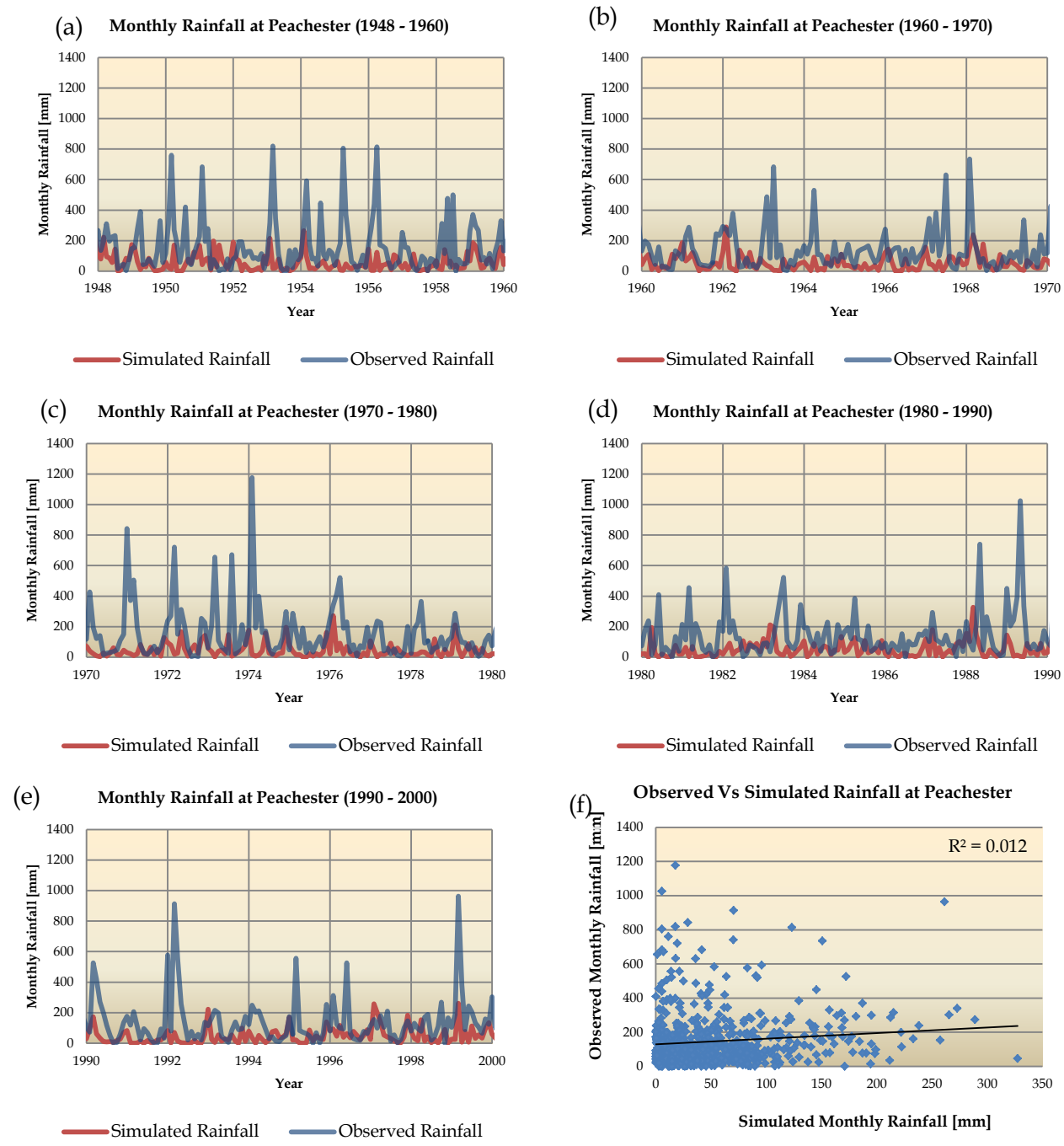

Figure D.12: Comparison of Observed rainfall [mm] [blue] at Peachester for the periods (a) 1948 – 1960, (b) 1960 - 1970, (c) 1970 – 1980, (d) 1980 – 1990 and (e) 1990 – 2000 with data derived from the GFDL Mk2.1 GCM [red]. Coefficient of determination for the two sets of data from 1948 - 2000 provided in (f).

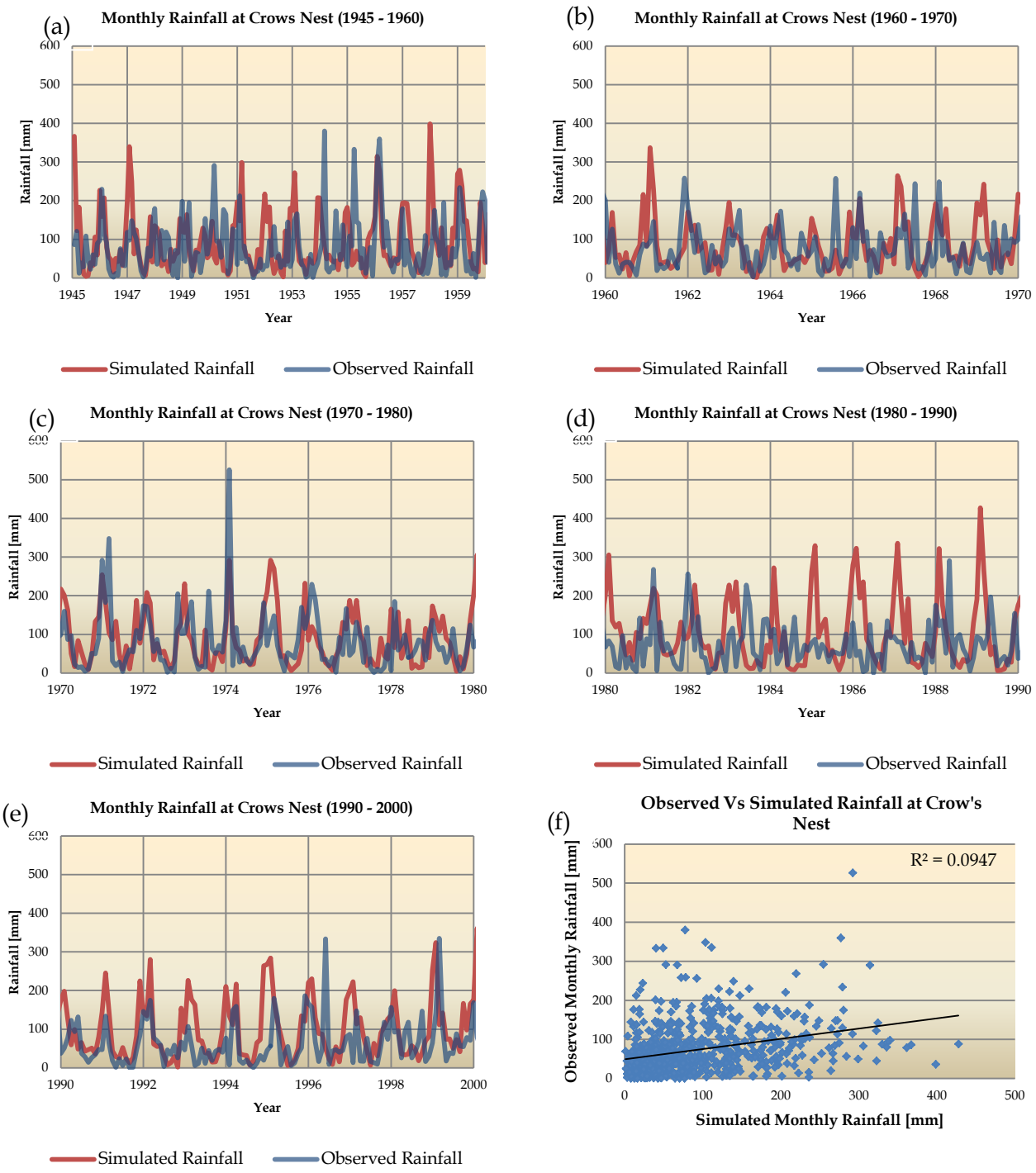

Figure D.13: Comparison of Observed rainfall [mm] [blue] at Crow's Nest for the periods (a) 1945 – 1960, (b) 1960 - 1970, (c) 1970 – 1980, (d) 1980 – 1990 and (e) 1990 – 2003 with data derived from the GISS - er GCM [red]. Coefficient of determination for the two sets of data from 1948 - 2000 provided in (f).

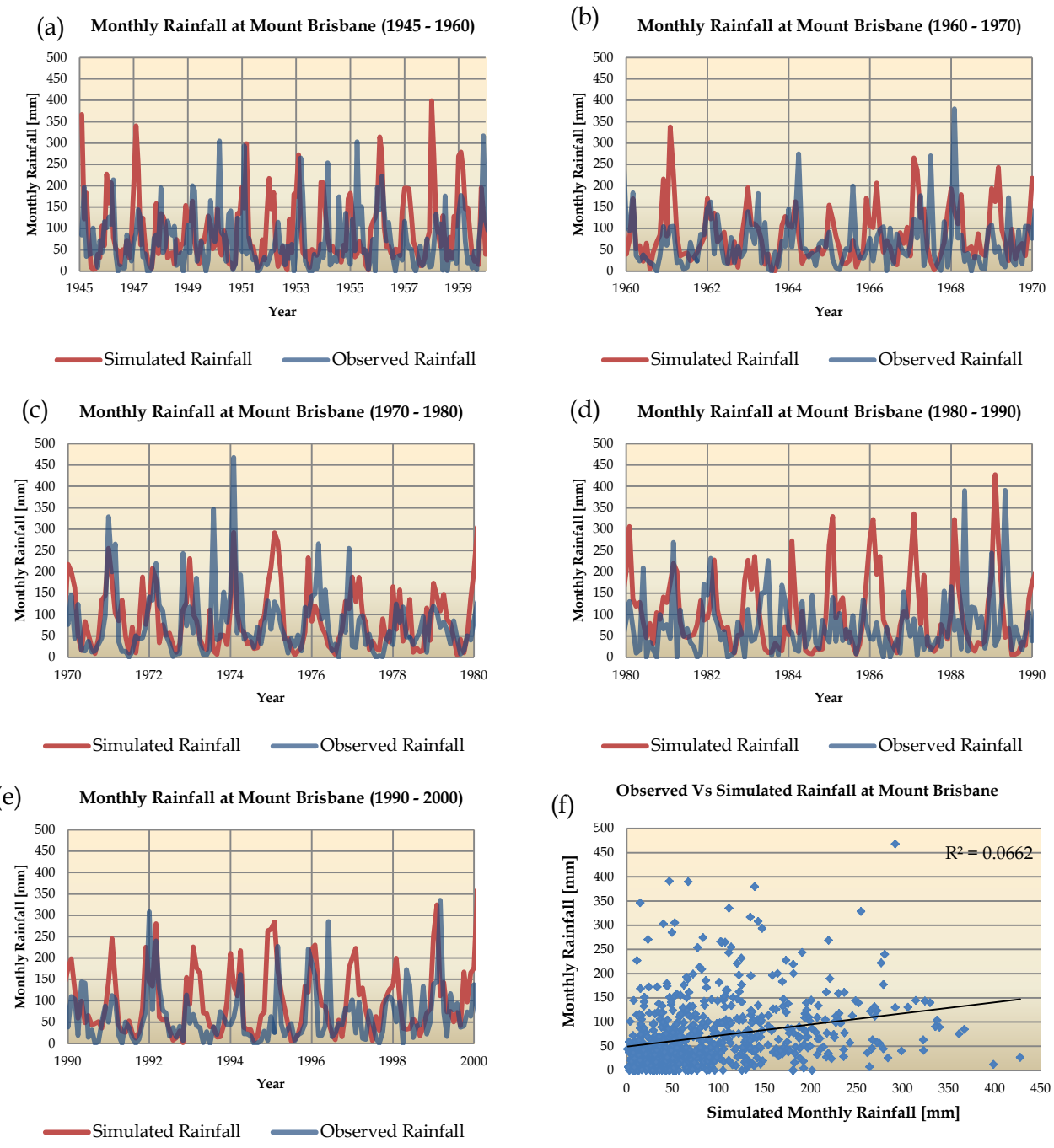

Figure D.14: Comparison of Observed rainfall [mm] [blue] at Mount Brisbane for the periods (a) 1945 – 1960, (b) 1960 - 1970, (c) 1970 – 1980, (d) 1980 – 1990 and (e) 1990 – 2003 with data derived from the GISS - er GCM [red]. Coefficient of determination for the two sets of data from 1948 - 2000 provided in (f).

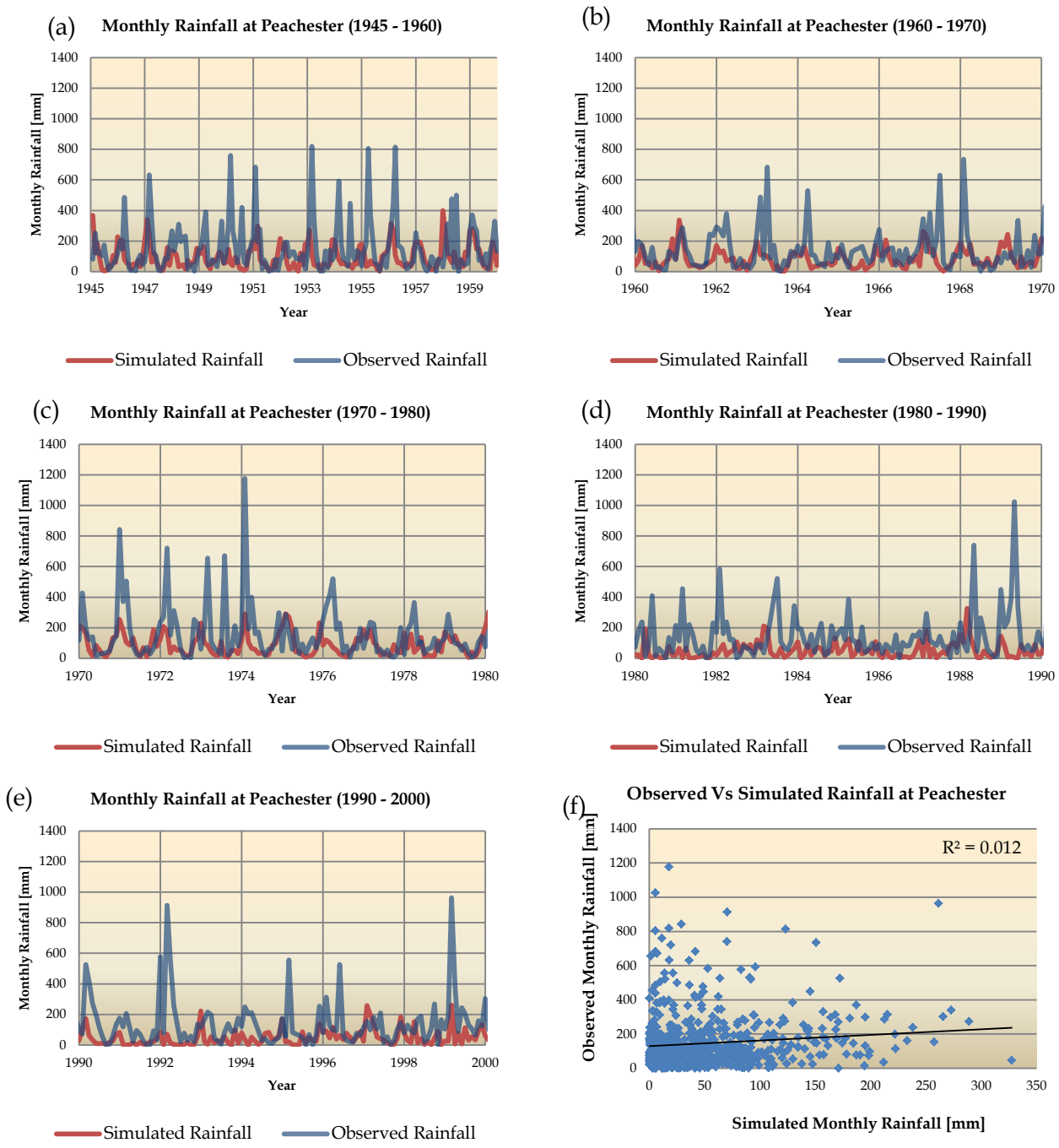

Figure D.15: Comparison of Observed rainfall [mm] [blue] at Peachester for the periods (a) 1945 – 1960, (b) 1960 - 1970, (c) 1970 – 1980, (d) 1980 – 1990 and (e) 1990 – 2003 with data derived from the GISS - er GCM [red]. Coefficient of determination for the two sets of data from 1948 - 2000 provided in (f).

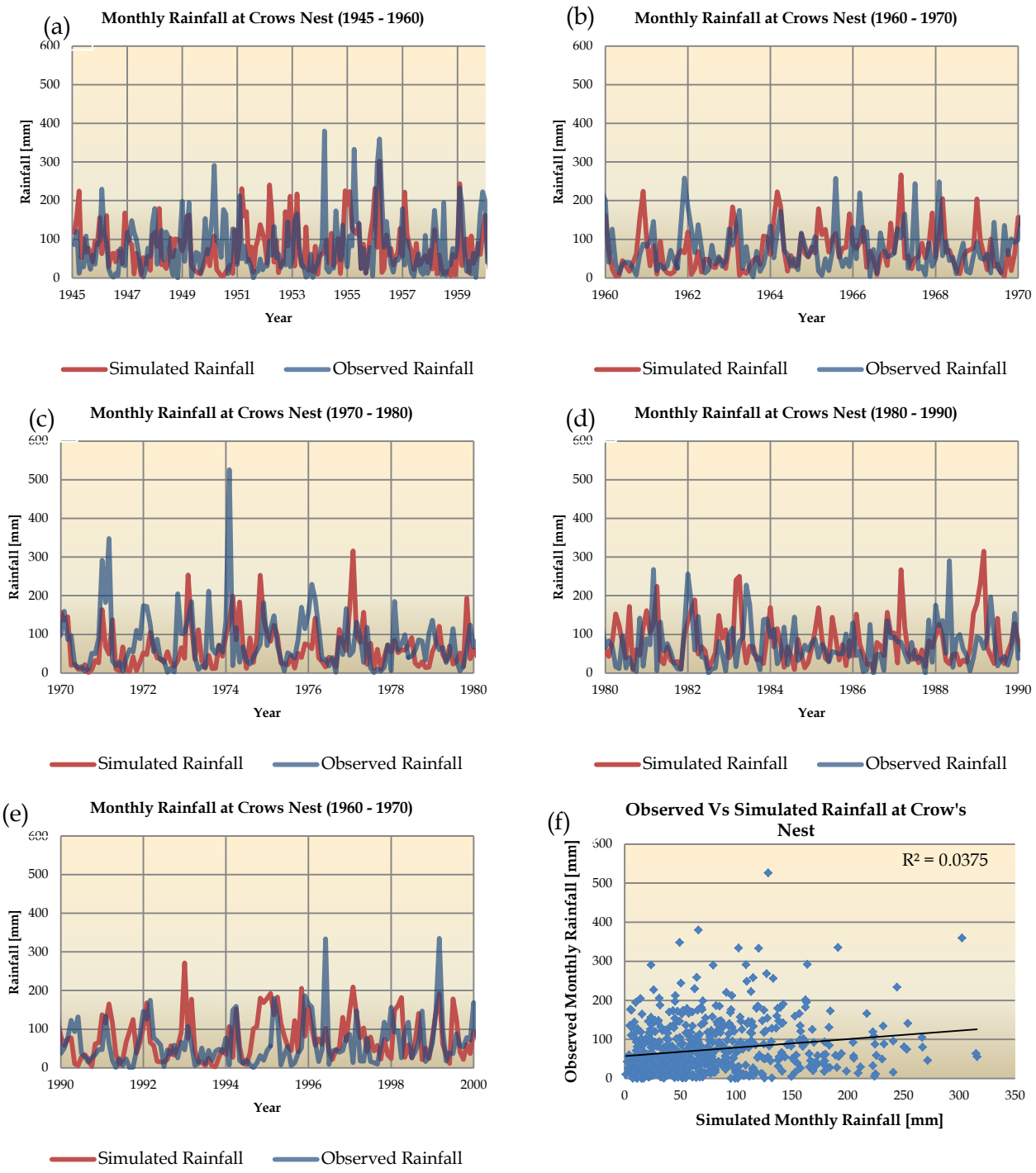

Figure D.16: Comparison of Observed rainfall [mm] [blue] at Crow's Nest for the periods (a) 1945 – 1960, (b) 1960 - 1970, (c) 1970 – 1980, (d) 1980 – 1990 and (e) 1990 – 2000 with data derived from the MIROC - medres GCM [red]. Coefficient of determination for the two sets of data from 1948 - 2000 provided in (f).

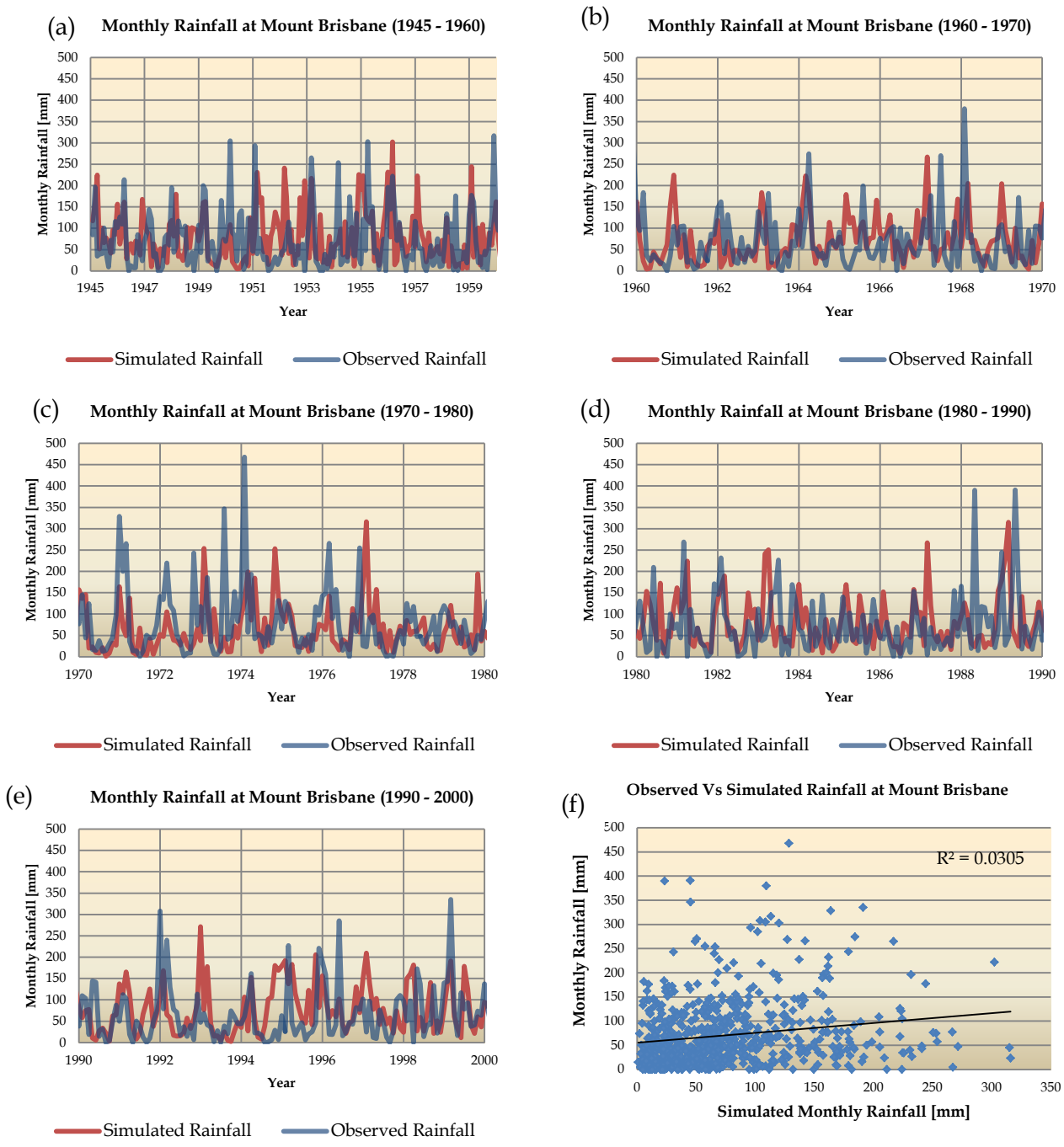

Figure D.17: Comparison of Observed rainfall [mm] [blue] at Mount Brisbane for the periods (a) 1945 – 1960, (b) 1960 - 1970, (c) 1970 – 1980, (d) 1980 – 1990 and (e) 1990 – 2000 with data derived from the MIROC - medres GCM [red]. Coefficient of determination for the two sets of data from 1948 - 2000 provided in (f).

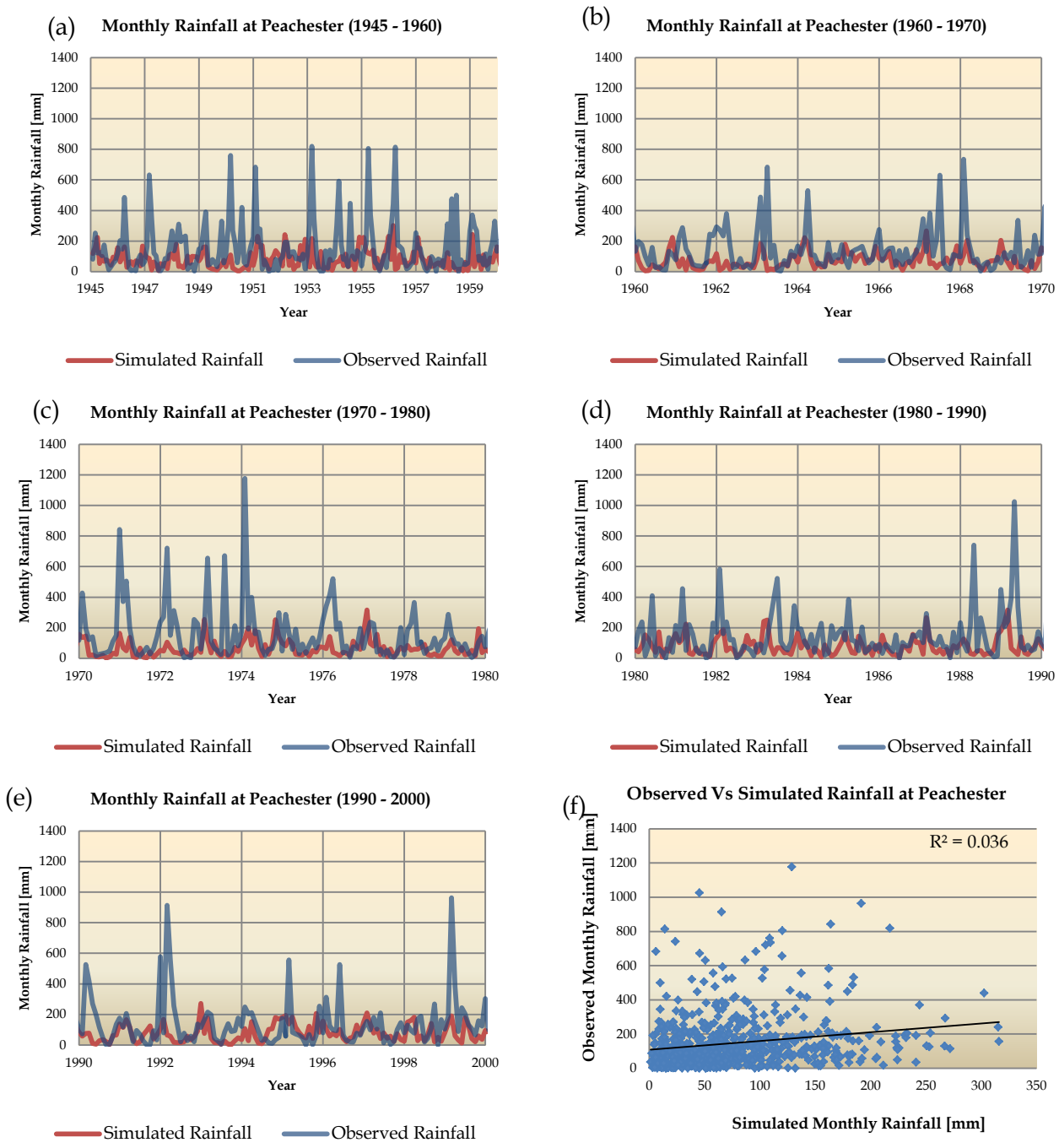

Figure D.18: Comparison of Observed rainfall [mm] [blue] at Peachester for the periods (a) 1945 – 1960, (b) 1960 - 1970, (c) 1970 – 1980, (d) 1980 – 1990 and (e) 1990 – 2000 with data derived from the MIROC - medres GCM [red]. Coefficient of determination for the two sets of data from 1948 - 2000 provided in (f).

Appendix E: Projected Changes in Climate Predictor Variables

The table below depicts projected changes in the selected predictor variables over the coming century. A thirty year average is taken at the nearest grid point from the GCM's used in this research. The MIROC – medres GCM title has been abbreviated to MIROC – med for the sake of keeping continuity of the cell size of the table. Predictor variables abbreviations are as above and the height of the variable is taken at 850mbar except for meridional wind speed (Vwnd) which had higher correlations at the 600mbar height (Appendix A).

Table E.1: Projected changes in climate predictors from 1980 to 2100 over region of interest. Values are a 30 year average taken at the nearest grid point to the region. Prw: Precipitable Water [kg/m²], Z850: Geopotential Height of 850mbar [m], RH and q: Relative and Specific Humidity at 850mbar[%][standardized value], u at 850mbar and v at 600mbar: Zonal and Meridional Wind speed [m/s].

Predictor	Model	1980-2010	2010-2040	2040-2070	2070-2100
Prw	CNRM – cm3	26.78	27.80	29.46	31.38
	GISS - er	25.86	27.41	28.92	30.58
	GFDL Mk2.1	22.03	23.15	23.55	24.58
	MIROC - med	23.82	25.79	28.08	30.74
	CCCMA - t63	20.05	21.17	23.08	25.07
	CSIRO Mk3.5	27.47	29.45	31.11	33.08
Z850	CNRM – cm3	1534.71	1543.58	1551.96	1556.31
	GISS - er	1512.97	1517.05	1521.63	1526.10
	GFDL Mk2.1	1520.95	1528.27	1537.19	1542.57
	MIROC - med	1529.23	1536.71	1545.00	1554.22
	CCCMA - t63	1539.53	1545.24	1552.38	1556.12
	CSIRO Mk3.5	1539.43	1544.30	1551.88	1558.18
RH	CNRM – cm3	64.50	63.02	62.27	62.88
	GISS - er	62.52	63.50	63.15	63.80
	GFDL Mk2.1	63.30	63.64	61.61	61.83
	MIROC - med	63.75	63.75	63.47	64.63
	CCCMA - t63	54.88	56.13	56.31	58.45
	CSIRO Mk3.5	60.71	61.00	58.75	58.74
q	CNRM – cm3	0.0076	0.0079	0.0082	0.0087
	GISS - er	0.0070	0.0083	0.0087	00.93
	GFDL Mk2.1	0.0064	0.0068	00.70	0.0073
	MIROC - med	0.0094	0.0067	0.0072	0.0078
	CCCMA - t63	0.0051	0.0056	0.0060	0.0065
	CSIRO Mk3.5	0.0063	0.0067	0.0071	0.0076
u	CNRM – cm3	-1.63	-1.89	-1.89	-1.97
	GISS - er	-1.13	-1.89	-2.00	-2.11
	GFDL Mk2.1	-1.92	-2.19	-2.00	-2.09
	MIROC - med	-0.61	-0.43	-0.34	-0.50
	CCCMA - t63	-2.12	-2.38	-2.57	-2.97
	CSIRO Mk3.5	2.24	2.18	2.32	2.20
v	CNRM – cm3	1.22	0.48	0.60	0.31
	GISS - er	-0.26	1.43	1.59	1.70
	GFDL Mk2.1	0.06	2.92	3.43	3.23
	MIROC - med	0.51	1.61	1.55	1.33
	CCCMA - t63	1.59	1.96	2.12	1.78
	CSIRO Mk3.5	1.83	1.50	1.86	2.13